Parametric Study on Seismic Behaviour of Dual-Concentrically Braced Steel Frames

Author: Slobodanka Jovašević

Supervisors: Prof. Carlos Alberto da Silva Rebelo

Prof. Luís Alberto Proença Simões da Silva

University: University of Coimbra

University: University of Coimbra

Date: 12.01.2015

ACKNOWLEDGEMENTS

I would like to express my gratitude to Prof. Carlos Rebelo and Prof. Luís Simões da Silva for useful comments, remarks and engagement through this thesis and for the opportunity to participate in the research project "EqualJoints" at University of Coimbra. I am highly indebted to them for their valuable thoughts and contribution towards development of my thesis.

Special thanks are also extended to my colleague, Filippo Gentili who was supporting me through the course of this research. His generosity and always there to help will not be forgotten.

My sincere thanks to Prof. František WALD, Prof Dan DUBINA, Prof.Luís Simões da Silva, Prof. Jean-Pierre JASPART, Prof. Raffaele LANDOLFO and Prof. Milan VELjKOVIĆ as coordinators of SUSCOS_M European Erasmus Mundus Master program (Sustainable Constructions under natural hazards and catastrophic events), for organizing this excellent master degree program and for their assistance and guidance in Liege, Timisoara and Coimbra. I am very proud that I had opportunity to participate in this course. Also I would like to acknowledge the Erasmus Mundus scholarship, as without this founding I would not have been able to participate in this program.

I would like to thank all SUSCOS colleagues for their spirit, passion and companionship during the last one and a half year. Their advices and from colleagues from first SUSCOS edition have been greatly appreciated.

Finally, I would like to thank my family for their endless support, encouragement and love.

ABSTRACT

The earthquake resistance design plays an essential role in the design of steel structures. Cyclic behaviour of beam-to-column in crucial in seismic behaviour of moment resisting steel frames. At the moment, the European design code in practice does not provide analytical tools to predict rotational capacity and cyclic performance of selected connection typology, but the code requires design supported by experimental testing or existing data on experimental tests performed on similar connections, what is unfeasible from designer's point of view. A European project has recently been started with the aim to develop design tool with typical beam-to-column connections used in European practice. In that way, designers will be able to directly use pre-qualified connection without performing experimental tests or literature reviews. One part of this European project is to estimate the seismic demand of the joints in typical D-CBF frames. In order to achieve these objectives seismic performance and dynamic response were estimated on basic of non-linear static analysis and non-linear time history analysis. Numerical models were create in order to perform non-linear static and dynamic analysis using OPENSEES software. Both analysis were performed in accordance with current European design code. The results of non-linear static analysis are presented in form of pushover curve and schematic illustration of formed plastic hinges. Dynamic response was estimated in term of i) maximum floor acceleration, ii) maximum interstorey drift ratio, iii) residual interstorey drift ratio and iv) maximum beam rotation ratio (at the exterior, one-side beam-column joints) at three performance levels: design (D), near collapse (NC) and twice near collapse (2xNC). As main conclusion, the analyses have showed that lateral resistance of D-CBFs is suddenly decrease when brace in compression buckles. This decrease is immediately followed by an increase of lateral stiffness. In seismic demand between selected parameters an important rule have hazard level and height of a structure.

Keywords: steel joints, D-CBFs, pushover analysis, incremental dynamic analysis (IDA)

TABLE OF CONTENTS

FIGURE INDEX

TABLE INDEX

NOTATIONS

A area of cross-section

A acceleration

A_d is the design peak ground acceleration

E elasticity modulus

F horizontal force

$\bar{F}$ force function or base excitation function

F_b design base shear force

I_b moment of inertia of the beam

K stiffness matrix

$\bar{L}$ coefficient vector

L_{eff} effective length

L_b length of the beam

M mass matrix

M_{Ed} design bending moment from the analysis

M_{pl} design value of bending moment

N_{Ed} design axial force from the analysis

N_{pl} design value of axial resistance

S soil factor

$S_d(T)$ design spectrum

$S_e(T)$ elastic response spectrum

T vibration period of a linear single-degree-of-freedom system

T_B lower limit of the period of the constant spectral acceleration branch

T_C upper limit of the period of the constant spectral acceleration branch

T_D value defining the beginning of the constant displacement response range of the spectrum

U	eigenvector
W_{el}	elastic section modulus
W_{pl}	plastic section modulus
a_g	design peak ground acceleration (PGA) on type A ground
a_{gR}	reference peak ground acceleration on type A ground
d_r	design interstorey drift obtained through seismic analysis and multiplied by displacement behaviour factor
f_y	expected yield strength of the material
h	reduction factor which takes into account importance class of the building
h	storey height
m	mass
m_{eff}	effective modal mass
$\hat{m}$	generalized mass matrix
q	behaviour factor
$\bar{r}$	influence vector
s	displacement of the mass
v	storey height
v_s	shear wave velocity
$v_{s,30}$	average value of propagation velocity of S waves in the upper 30m of the soil pfrofile at shear strain of 10^{-5} or less
$\bar{x}$	displacement vector
$\bar{\ddot{x}}$	acceleration vector
Γ	modal participation factor
Δ	relative horizontal displacement
β	lower bound factor for the horizontal design spectrum
γ_I	importance factor
γ_{ov}	material overstrength factor
η	damping correction factor with a reference value of $\eta = 1$ for 5% viscos damping
θ	rotation
θ_y	yield rotation

υ is the Poisson's ratio

λ correction factor

ϕ eigenvector matrix

ABBREVIATIONS

CBF	Concentrically Braced Frame
D	Design
DB	Displacement-Based
D-CBF	Dual-Concentrically Braced Frame
DCH	Ductility class high
D-EBF	Dual-Eccentrically Braced Frame
EBF	Eccentrically Braced Frame
EC	Eurocode
EN	European Norm
FB	Force-Based
HH	High Hazard
IDA	Incremental Dynamic Analysis
IM	Intensity Measure
MRF	Moment Resisting Frame
MH	Medium Hazard
NC	Near Collapse
OPENSEES	Open System for Earthquake Engineering Simulation
PBSD	Performance Based Seismic Design
PGA	Peak Ground Acceleration
PGV	Peak Ground Velocity
PSA	Peak Storey Acceleration
SF	Scale Factor
SUSCOS	Sustainable Constructions under natural hazard and catastrophic events

1. INTRODUCTION AND RESEARCH OBJECTIVES

1.1. Overview

The earthquake resistance design requires structures to safely sustain ground motion of a specified intensity that might occur during the lifetime of the structure. Cyclic behaviour of beam-to-column joints plays crucial role on seismic behaviour of moment resisting steel frames. At the moment, the European design code in practice, EN 1993-1-8 [1], contains a set of rules to compute the strength and the stiffness of connection but does not provide analytical tools to predict rotational capacity and cyclic performance of selected connection typology. On the other hand EN 1998-1 [2] requires design supported by experimental testing, which is an expensive and time-consuming approach and, for that fact, not practical to be used by designers. As an alternative for experimental testing the code prescribes finding existing data on experimental tests performed on similar connections what is also unfeasible from designer's point of view.

In contrast with current European design code, the design in other countries with high seismic hazard (e.g. US) is based on codified design tools and procedures. Following the Northridge and Kobe earthquake a number of researches were performed in order to improve understanding of the behaviour of steel connections subject to seismic loading. As a result, prequalified standard joints for seismic resistance were created. The same procedure was carried out in Japan. Unfortunately, US and Japanese design practice uses steel sections and steel grades different from European, making these prequalified standard joints for seismic resistance inapplicable in European design practice.

Following the previously mentioned approach, a European project has recently been started with the aim to develop a guide for the design of the connections subjected to cyclic loading

for European market, including design rules and detailing. Like in US practice the aim is to obtain a design tool with typical beam-to-column connections used in European practice. In that way, as long as connection design and detailing are covered by prequalification process, designers will be able to directly use pre-qualified connection without performing experimental tests or literature reviews.

1.2. Research objectives

This thesis emerged as part of the European project EqualJoints – European pre-qualified steel joints mentioned before.

The main objectives of this project are to provide codified seismic pre-qualification charts for a set of steel standard joints, to develop analytical and numerical models to predict behaviour of beam-to-column joints under cycling loading, on basic of experimental results and to define technological requirements for fabrication of the steel joint. In order to fulfil these objectives the research project is divided in several parts:

- Selection and design of joint typologies. Joints to be qualified will be selected and designed according to common European practice. Further on, seismic performance evaluation of selected joints will be carried out. Finally, specimens will be designed according to the seismic demand estimated from pushover analysis and time history non-linear dynamic analyses performed on a set of typical building frames.
- Analytical models: the aim is to characterize the behaviour of beam-to-column joints subjected to cyclic loading.
- Numerical tests: the objective is to provide the preliminary tools to design the experimental activity and to interpret experimental results as well.
- Experimental tests: tests on a set of typical steel joints selected and designed in the first part will be performed.
- Design tool: based on the results of previous work packages design guidelines will be defined [3].

1.3. Purpose and scope of this thesis

This thesis is focused on the part of the project which is devoted to estimate the seismic demand of the joints in typical frames, which are to be designed and tested in another part of the project for further prequalification. For this purpose joint configurations were selected in accordance with common European practice and also to be compatible with different structural systems (moment resistant frames (MRF), dual concentrically braced frames (D-CBF) and dual eccentrically braced frames (D-EBF). The focus of the thesis is the development of advanced seismic analyses of D-CBF designed in accordance with EN 1993 and EN 1998-1 in order to obtain a set of results that will allow the design of the test specimens and the definition of the loading protocol.

In order to achieve these objectives the seismic performance and dynamic response of the selected D-CBF is evaluated on the basis of non-linear static analysis and non-linear time-history analysis (incremental dynamic analysis).

Both static and dynamic analyses are performed using the software OPENSEES [4]. In detail, numerical models are created in order to perform both, nonlinear static and dynamic analysis, using force-based elements (FBE) with distributed plasticity along the elements. The distributed plasticity models allow yielding to occur at any location along the element. The cross-section is modelled using fibre approach that assigns uniaxial stress-strain relationship to each fibre.

Pushover analysis is performed in accordance with EN 1998-1, Section 4.3.3.4.2. The control displacement for the analysis is horizontal displacement of the last floor. Analysis was performed with uniform and modal distribution of lateral forces along the height of the building. The results are presented in form of pushover curve, as well as schematic illustration of formed plastic hinges.

Incremental dynamic analysis is performed using two set of seven accelerograms each, representing medium (MH) and high hazard (HH). Set of curves are constructed and plotted. Each curve corresponds to one ground motion record. Each curve is a plot of a stated variable

versus the number of the storey. Number of the storey is plotted on the vertical axis, while the performance variable is plotted on horizontal axis. As the sub-task of EQUALJOINTS project is to specify deformation demands on beam-column connection, the performance variables are defined as: (i) maximum interstorey drift ratio, (ii) residual interstorey drift ratio, (iii) maximum floor acceleration, and (iv) maximum beam rotation (at the exterior, one-side beam-column joints).

1.4. Overview of the thesis

This thesis is divided in eight chapters. In the following paragraphs the content of each chapter is presented.

Chapter 1 – Introduction and Research Objectives

Chapter 1 is introduction to the problem and the necessity to study the seismic behaviour of the structures. The motivation for this work as well as its main goals are presented in this chapter.

Chapter 2 – Seismic Design of Steel Buildings

Chapter 2 describes the seismic behaviour of three the most used structural systems. Also current approach of Performance Based Design is addressed in this chapter. Moreover, a brief description of current code is presented.

Chapter 3 – Selected Case Studies Typology

Chapter 3 is based on selection and description of building configuration, as well as description of parameters used for pre-design of the D-CBF. Also in this chapter are presented all the frames that are used in the analysis.

Chapter 4 – Finite Element Modeling in OpenSees

Chapter 4 is devoted to modelling parameters of chosen frame typologies. Also parameters used in modal, pushover and IDA are presented in this chapter.

Chapter 5 – Parametric study

In Chapter 5 are given results of modal, non-linear static and dynamic analysis for selected Dual-Concentrically Braced Frame typologies.

Chapter 6 – Conclusions and future works

Final remarks and future work are presented in this chapter.

2. SEISMIC DESIGN OF STEEL BUILDINGS

2.1. Steel structural systems in seismic areas

Buildings are designed to resist two types of loads: vertical load due to gravity and lateral load due to earthquake and wind. In order to efficiently transfer lateral load a number of structural systems have been developed. The aim of lateral load resisting systems is to absorb the energy by moving, or deformation, without collapse. The ability of structural system to dissipate the energy by deforming, without collapse, depends on its ductility. The most used steel lateral resisting systems are moment-resisting frames (MRFs), frames with concentric bracings (CBFs) and frames with eccentric bracings (EBFs).

Moment resisting frames – MRF

Moment resisting frames are lateral loads resisting systems in which lateral loads are resisted by bending of the members. The rigidity of MRF depends also on rigidity of connection between beams and columns. Dissipative zones should be located in plastic hinges in the beams or, under certain conditions defined in the codes in the beam-column joints.

Concentrically braced frames – CBF

Concentrically Braced Frames consist of diagonal brace members pinned to beam to column joints, ensuring that only axial force is developed in them. In CBF lateral load is resisted by members subjected to axial forces. A dissipative zone should be located in the diagonals in tension where energy is dissipated, through yielding cyclic behaviour. The ductility of CBF is lower than that of MRF.

Eccentrically braced frames – EBFs

An eccentrically Braced Frame (EBF) is a type of lateral load resisting system that includes beams, columns and braces. These members are arranged in a way that at least one end of each brace is connected to isolated segment of the beam called a link. An EBF can be considered as a hybrid between conventional Moment Resisting Frames (MRF) and Concentrically Braced Frames (CBF) because lateral load is resisted by members subjected to axial forces, but also by seismic links in beams. Seismic links should be designed to be active and able to absorb the energy, either by cyclic bending or cyclic shear.

Dual frames – D-CBF or D-EBF

The Dual typology is a system in which the two structural systems MRF and CBF or EBF contribute in dissipation of the energy. Bay composed of braced system absorbs the energy by yielding of the braces (CBF) or the links (EBF), while the other bay behaving as MRF absorbs the energy by bending of the beams [2].

2.2. Performance based design

In the recent major earthquakes at the end of the 20th century (e.g. 1994 Northridge earthquake and 1995 Kobe earthquake) it was noticed that damage, sometimes severe, can occur in buildings designed in accordance with the code. This damage of the buildings had high economic impact due to lose of building functionality and need for rehabilitation, which implies that changes in the code are required. It is believed that one of the best ways is Performance-Based Seismic Design (PBSD). This term has been widely used since 1994 Northridge Earthquake, perhaps the most expensive earthquake in US history, and other major earthquakes around the world that occurred at the end of the 20th century.

Performance-Base Seismic Design is a method based on the predicted performance of the structure during an earthquake. A general methodology was formulated in such a way to involve all the variables that may affect the performance of a structure. The structure

subjected to different seismic hazards should be designed in the way to meet specific performance objectives, such as seismic hazard, damage measures, collapse, financial losses or length of downtime due to damage, engineering demands such as floor accelerations, displacement, inter-storey drift, residual inter-storey drift, rotation, level of stresses.

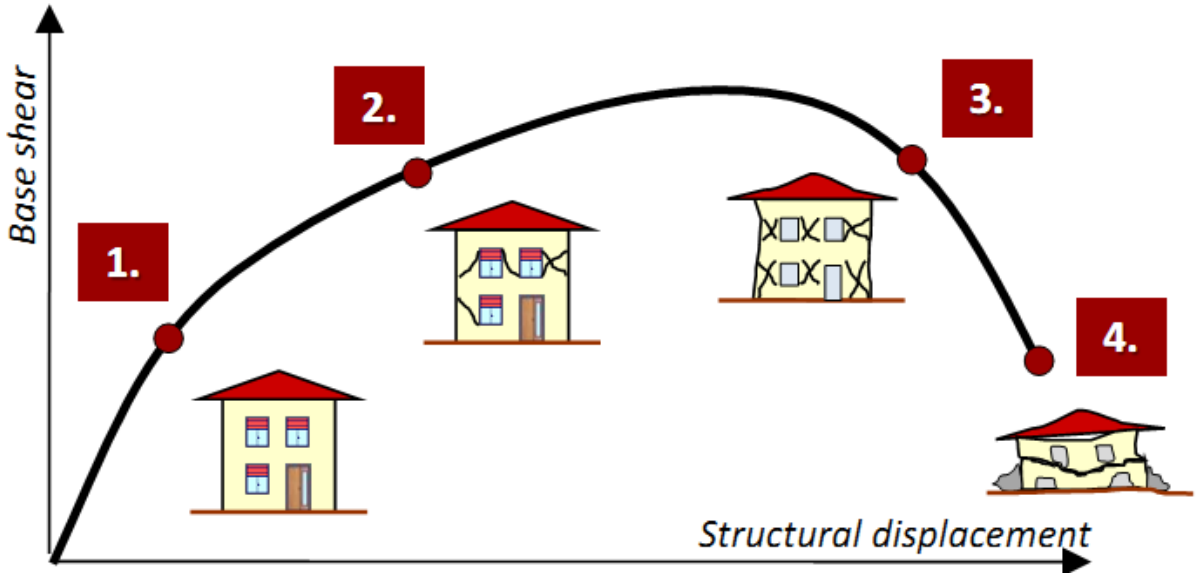

Figure 2.1 – Performance levels

The performance levels were generalized and described with overall damage states: (i) Fully operational (continuous service, negligible structural and non-structural damage). (ii) Operational (most operations and functions can resume immediately, structure is safe for occupancy, essential operations are protected while non-essential are disrupted, repair is required to restore some non-essential services, damage is light). (iii) Life safety (damage is moderated but structure remains stable, selected building systems, features or contents may be protected from damage, life safety is generally protected, building may be evacuated following earthquake, repair possible but maybe economically impractical). (iv) Near collapse (damage is severe but structural collapse is prevented, non-structural elements may fall, repair generally is not possible) [5].

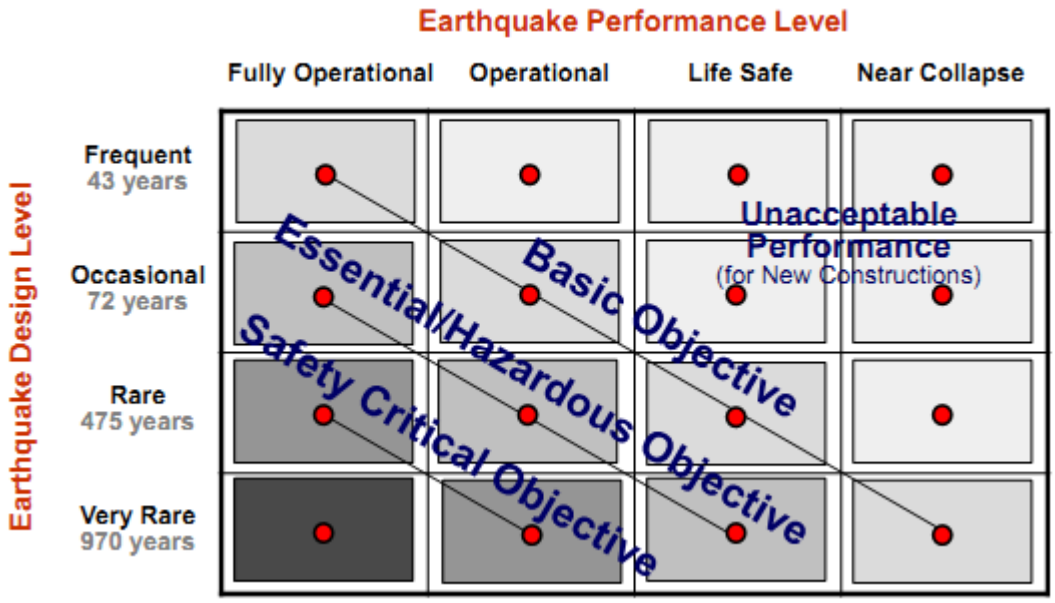

Figure 2.2 – Earthquake Performance Level

2.3. Seismic design according to European code

2.3.1. General

Seismic design in Europe is carried out according to EC 8 [2]. EC 8 requires two level seismic design: no-collapse requirement and damage limitation requirement.

No-collapse requirement

No-collapse requirement states that a structure should be designed and constructed to withstand the design seismic action without local and global collapse, ensuring people's safety. The design seismic action has return period of 475 years. According to EN1998-1 no-collapse requirement is met in the conditions regarding resistance, ductility, equilibrium, foundation stability and seismic joints are met.

Damage limitation requirement

Damage limitation requirement states that a structure should be designed and constructed to withstand a seismic action without damage and limitations of the use for which the costs would be disproportionally high, in comparison with cost of the structure itself. The seismic action that is taken into account for damage limitation requirement has a return period of 95 years. The damage limitation requirement is based on interstorey drifts and is limited, in case of brittle non-structural elements, by following expression:

$$d_r \cdot \nu = 0.005 \cdot h \tag{2.1}$$

where:

d_r is the design interstorey drift obtained through seismic analysis and multiplied by displacement behaviour factor

h is the storey height

ν is the reduction factor which takes into account importance class of the building

2.3.2. Elastic and Design spectra

The earthquake motion at a point on the surface is represented in the EC 8 by an elastic ground acceleration response spectrum called “elastic response spectrum”. The shape of an elastic response spectrum is the same for both of two levels of seismic design (no-collapse requirement and damage limitation requirement). Horizontal seismic action is defined by two independent orthogonal components and it is represented by the same response spectrum.

For the horizontal components of the seismic action, the elastic response spectrum $S_e(T)$ is defined by following expressions given in EN1998-1:

$$0 \le T \le T_B: \quad S_e(T) = a_g \cdot S \cdot \left[1 + \frac{T}{T_B} \cdot (\eta \cdot 2.5 - 1)\right] \tag{2.2}$$

$$T_B \le T \le T_C: \; S_e(T) = a_g \cdot S \cdot \eta \cdot 2.5 \tag{2.3}$$

$$T_C \leq T \leq T_D\colon\ S_e(T) = a_g \cdot S \cdot \eta \cdot 2.5 \cdot \frac{T_C}{T} \tag{2.4}$$

$$T_D \leq T \leq 4s\colon\ S_e(T) = a_g \cdot S \cdot \eta \cdot 2.5 \cdot \left[\frac{T_C \cdot T_D}{T^2}\right] \tag{2.5}$$

where:

$S_e(T)$	is the elastic response spectrum
T	is the vibration period of a linear single-degree-of-freedom system
a_g	is the design peak ground acceleration (PGA) on type A ground ($a_g = \gamma_I \cdot a_{gR}$)
T_B	is the lower limit of the period of the constant spectral acceleration branch
T_C	is the upper limit of the period of the constant spectral acceleration branch
T_D	is the value defining the beginning of the constant displacement response range of the spectrum
S	is the soil factor
η	is the damping correction factor with a reference value of $\eta = 1$ for 5% viscos damping

For ordinary residential buildings, since they belong to importance class II $\gamma_I = 1.0$, thus $a_g = a_{gR}$.

Allowing the structural system to resist seismic actions in non-linear range permits the design of the structure for seismic forces smaller than those corresponding to a linear elastic response. In order to avoid explicit inelastic structural analysis ductile behaviour of the structure and capacity to dissipate energy are taken into account by performing elastic analysis using reduced elastic response spectrum. This spectrum is called a “design spectrum”. The used reduction factor *q* (behaviour factor) is an approximation of the ratio of the seismic forces that the structure would experience if its response was completely elastic with 5% viscous damping, to the seismic forces that may be used in the design with conventional elastic analysis. The behaviour factor *q* depends on material, structural system and ductility class. For the horizontal components of the seismic action, the design spectrum $S_d(T)$ is defined by following expressions given in EN1998-1:

$$0 \le T \le T_B: \quad S_d(T) = a_g \cdot S \cdot \left[\frac{2}{3} + \frac{T}{T_B} \cdot \left(\frac{2.5}{q} - \frac{2}{3}\right)\right] \tag{2.6}$$

$$T_B \le T \le T_C: \; S_d(T) = a_g \cdot S \cdot \frac{2.5}{q} \tag{2.7}$$

$$T_C \le T \le T_D: \; S_d(T) \begin{cases} = a_g \cdot S \cdot \dfrac{2.5}{q} \cdot \left[\dfrac{T_C}{T}\right] \\ \ge \beta \cdot a_g \end{cases} \tag{2.8}$$

$$T_D \le T \le 4s: \; S_d(T) \begin{cases} = a_g \cdot S \cdot \dfrac{2.5}{q} \cdot \left[\dfrac{T_C \cdot T_D}{T^2}\right] \\ \ge \beta \cdot a_g \end{cases} \tag{2.9}$$

where:

$S_d(T)$	is the design spectrum
$a_g, S, T_B, T_C \; and \; T_D$	As previously defined
q	is the behaviour factor
β	is the lower bound factor for the horizontal design spectrum (recommended $\beta = 2$)

For the D-CBFs analysed in this work the maximum value of behaviour factor according to EN1998-1 is $q = 2.5$ corresponding to ductility class high (DCH). Frames are assumed to be on location of medium and high hazard where PGA a_g was assumed as 0.25g and 0.35g, respectively. For calculation of seismic loads Type 1 design spectra for Soil Type C was taken. In Table 2.1 are given parameters to define the elastic response spectrum and the design spectrum.

Table 2.1 – Characteristics of the elastic spectrum

a_g	S	T_B [s]	T_C [s]	T_D [s]	η	q	β
0.25g **0.35g**	1.15	0.2	0.6	2.0	1.0	2.5	0.2

Figure 2.3 illustrates Response spectra for CBFs, both elastic and deign spectra.

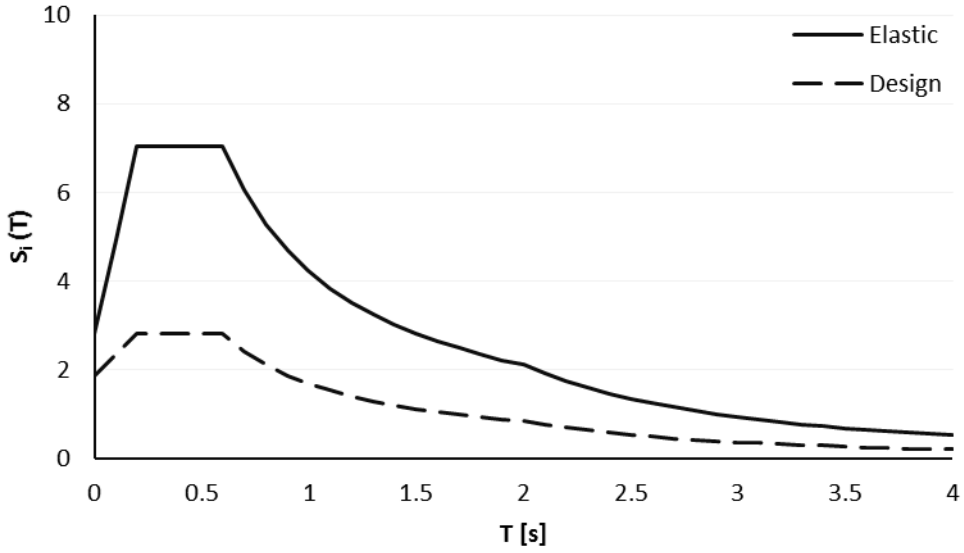

Figure 2.3 – Response Spectra

2.3.2.1. Design base shear force

The design base shear force for each of the frames is calculated in accordance to EN1998-1 using following expression:

$$F_b = S_d(T_1) \cdot m \cdot \lambda \tag{2.10}$$

where:

$S_e(T_1)$ is the ordinate of the design response spectrum at period T_1

T_1 is the fundamental period of vibration

m is the total mass of the building above the foundation or above the top of a rigid basement

λ is the correction factor

The correction factor λ takes into account the fact that the effective mass of the 1st mode of vibration is smaller than the total building mass.

Effective mass

The effective mass of the structure represents a “significance” of a vibration mode. Modes with relatively high effective masses are ones that can be excited by base excitation. Starting from equation of motion (2.10) eigenvalues and eigenvectors can be determined.

$$M\ddot{\bar{x}} + K\bar{x} = \bar{F} \tag{2.11}$$

where:

M is the mass matrix

K is the stiffness matrix

$\ddot{\bar{x}}$ is the acceleration vector

$\bar{x}$ is the displacement vector

$\bar{F}$ is the force function or base excitation function

For ϕ being the eigenvector matrix, the system's generalized mass matrix $\hat{m}$ is given by:

$$\hat{m} = \phi^T \cdot M \cdot \phi \tag{2.12}$$

The $\hat{m}_{ii} = 1$ for each index, eigenvectors are mass-orthogonal, if they have been normalized with respect to the mass matrix. In order to normalize eigenvector with respect to the mass matrix first generalized mass M_i was computed using following expression:

$$M_i = {U_i}^T \cdot M \cdot U_i \tag{2.13}$$

where U_i is unnormalized eigenvector. Generalized mass M_i must be positive under the assumption that mass matrix M is positively determined. Normalized eigenvector is obtained when eigenvector is divided by the positive square root of M_i.

The coefficient vector $\bar{L}$ is defined as:

$$\bar{L} = \phi^T \cdot M \cdot \bar{r} \tag{2.14}$$

where $\bar{r}$ is the influence vector which represents the displacement of the masses from static application of a unit ground displacement.

The modal participation factor matrix Γ_i for mode *i* is:

$$\Gamma_i = \frac{\bar{L}_i}{\hat{m}_{ii}} \tag{2.15}$$

The effective modal mass $m_{eff,i}$ for mode *i* is:

$$m_{eff,i} = \frac{\bar{L}_i^{\,2}}{\hat{m}_{ii}} \tag{2.16}$$

The correction factor λ, that shows how much of total mass is included in the 1st vibration mode, is given as ratio of effective modal mass and total mass of the structure [6].

2.3.3. Methods of analysis

Structural response assessment of the structures can be categorized as static or dynamic, linear or nonlinear. For seismic calculations according to EN1998-1 we can use both linear elastic structural analysis and non-linear analysis. In EN1998-1, Section 4.3.3.1 are given these methods as:

Two types of linear methods:

- "lateral force method of analysis"
- "modal response spectrum analysis"

Two types of non-linear methods:

- Non-linear static (pushover) analysis
- Non-linear time history (dynamic) analysis

2.3.4. Non-linear static (pushover) analysis

The nonlinear static analysis or pushover analysis is a standard procedure in current structural engineering practice to assess the inelastic behaviour of the structure. Incremental static load is applied to the structure. A certain lateral load pattern is selected and the intensity of load is monotonically increasing. The sequence of plastic hinge formation and component by component failure is observed until either target displacement is exceeded or the building collapses.

In order to perform pushover analysis, by EC 8 [2], at least two vertical distributions of lateral loads should be considered: a "uniform" distribution and a "modal" distribution. In case of "uniform" distribution lateral forces are proportional to the mass regardless of elevation while for "modal" pattern lateral forces are consistent with lateral force distribution determined in elastic analysis:

$$F_i = \frac{s_i \cdot m_i}{\sum s_j \cdot m_j} \tag{2.17}$$

where:

F_i horizontal force acting on storey *i*

s_i, s_j the displacement of masses m_i, m_j in the fundamental mode shape

m_i, m_j the storey masses

In both cases lateral loads are applied at the location of the masses in the model, at the floor level.

An important variable in pushover analysis is the target displacement, an estimate of the global displacement of the structure expected to experience during a design earthquake. The target displacement is usually measured by roof displacement at the centre of the mass of the structure.

The relation between base shear force and the control displacement is given in form of capacity pushover curve. It should be determined by pushover analysis for a range of values of the control displacement between zero and 150% of the target displacement.

2.3.5. Non-linear time history (dynamic) analysis

With the increase of the computer processing power complex time history analysis methods such as Incremental Dynamic Analysis (IDA) have been more used in the last decade. IDA is a parametric analysis used to estimate structural performance under seismic loading. Accelerograms with increasing amplitudes are applied to the structure until it reaches dynamic instability. IDA was specifically developed for seismic assessment as the dynamic load is earthquake ground motion usually scaled from lower to higher intensity. The scale factor (SF) of scaled accelerogram is non-negative scalar that produced scaled accelerogram when multiplies an unscaled (natural) accelerogram time-history. An intensity measure (IM) of a scaled ground motion is a non-negative scalar that depends on the unscaled acclerogram and is monotonically increasing with scale factor. Common examples of scalable IM are the Peak Ground Acceleration (PGA), Peak Ground Velocity, the 5% damped Spectral Acceleration at the structure's first-mode period and the normalized factor $R = \lambda/\lambda_{yield}$. When the structure

is subjected to desired input its response to the seismic load is monitored. A variable that characterizes the response of structural model due to seismic loading is damage measure (DM). Possible choices to observe DM could be maximum base shear, node rotation, damage indicators such as peak interstorey drift, peak roof drift and peak floor acceleration. If the damage of non-structural elements needs to be assessed DM could be peak floor acceleration [7].

2.3.5.1. Performance levels and criteria

In the case studies analysed in this work two sets of seven ground motions are applied to the structure in order to obtain statistics about the structure's performance at three limit states. In particular, performance at "design" (D) performance level, "near collapse" (NC) performance level (approximately 175%) and twice NC performance level (approximately 350%) is presented in terms of peak floor acceleration, interstorey drift ratio, residual interstorey drift ratio and beam rotation to yield beam rotation is presented.

Peak floor acceleration is given as relative acceleration of the floor in horizontal direction

Interstorey drift ratio $\boldsymbol{\Delta_i/h_i}$ is the ratio of relative horizontal displacement between two adjacent floors to storey height

Residual interstorey drift is the interstorey drift ratio at the moment of 20s after end of a ground motion that the structure was subjected to.

Beam rotation ratio $\boldsymbol{\theta/\theta_y}$ is the ratio of the node to yield rotation of the beam in the node, where yield rotation of the beam is calculated according to FEAM 356 using following expression [8]:

$$\theta_y = \frac{W_{pl} \cdot f_y \cdot L_b}{6 \cdot E \cdot I_b} \tag{2.18}$$

where:

W_{pl}	is the plastic section modulus
f_y	is expected yield strength of the material
L_b	is the length of the beam
E	is the elasticity modulus
I_b	is the moment of inertia of the beam

2.3.5.2. Selected ground motion records

Two sets of seven acceleration records were considered, representing the medium- and high-hazard cases. Acceleration records were selected from PEER NGA database, from European and Middle East events.

The first set of 7 records represents a medium seismic hazard (MH) selected from database using the following criteria: magnitude M from 5.0 to 6.5, distance from fault 10 km to 100 km, shear wave velocity Vs from 180 m/s to 800 m/s, EN1998-1 Type 1 Soil C target spectrum with PGA0 = 0.25 g and minimization of DRMS over a period range from 0.2 s to 2.0 s. The acceleration response spectra of the 7 records for the MH are presented in Figure 2.4, with the mean spectrum and the EC8 target spectrum. Basic descriptive and seismologic data are presented in Table 2.2.

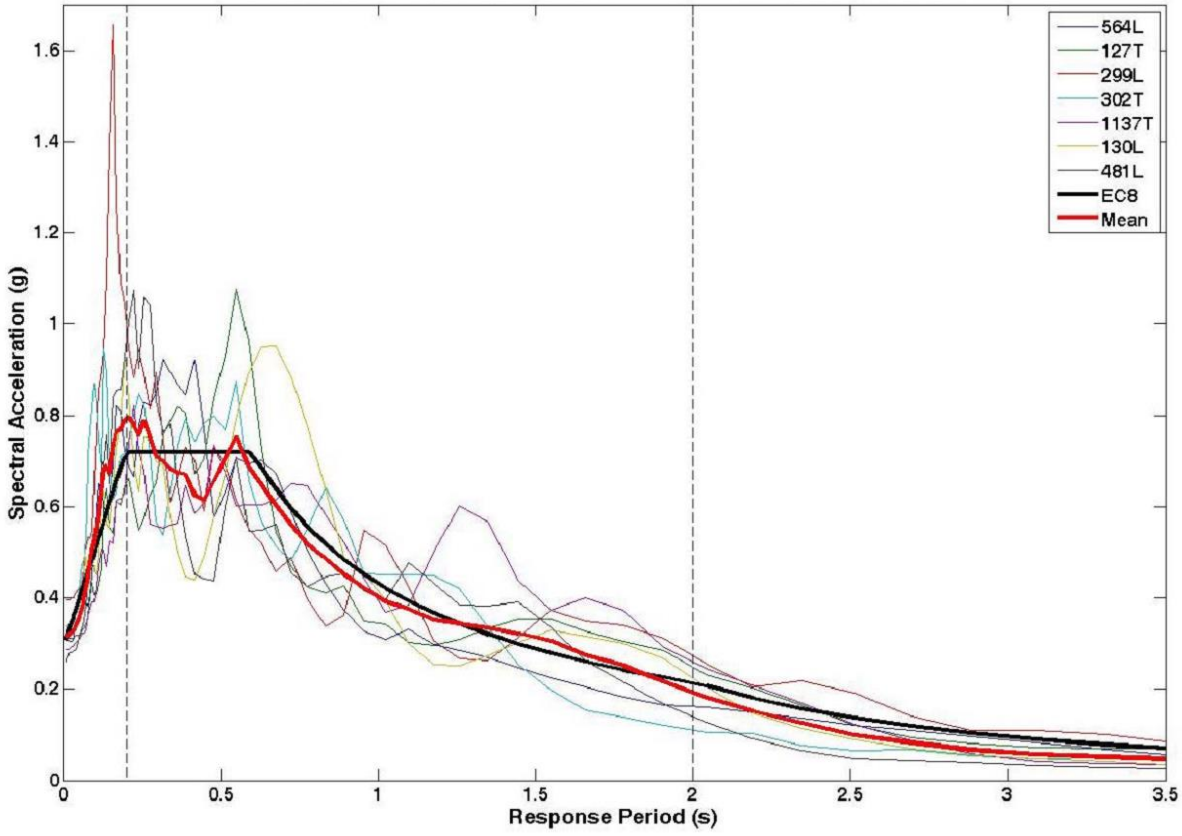

Figure 2.4 – Comparison of the scaled acceleration response spectra of the 7-record MH set with the 5% damped Type1, Soil C design spectrum of EN1998-1 with PGA = 0.25 g.

Table 2.2 – Seismological and scaling data for the 7-record MH set

NGA Record No.	Earthquake Name	Year	Magni-tude	Distance to Fault [km]	V_s30 [m/s]	PGA [g]	PGV [cm/s]	Scale Factor	D_{RMS}
00564L	Kalamata, Greece	1986	6.2	11.2	339	0.26	27.18	1.23	0.188
00127T	Friuli, Italy	1976	5.5	15.1	339	0.05	4.86	7.55	0.197
00299L	Irpinia, Italy	1980	6.2	41.7	500	0.04	3.45	9.83	0.226
00302T	Irpinia, Italy	1980	6.2	22.7	530	0.11	11.56	3.49	0.230
01137T	Dinar, Turkey	1995	6.4	35.6	339	0.04	4.65	7.16	0.245
00130L	Friuli, Italy	1976	5.9	14.3	339	0.11	11.37	3.03	0.246
00481L	Lazio-Abruzzo, Italy	1984	5.8	45.5	339	0.04	3.55	9.25	0.254

The second set of 7 records represents a high seismic hazard (HH) selected from database using the following criteria: magnitude *M* higher than 6.5, distance from fault 20 km to 100 km, shear wave velocity V_s from 180 m/s to 800 m/s, EN1998-1 Type 1 Soil C target spectrum with PGA_0 = 0.35 g and minimization of D_{RMS} over a period range from 0.2 s to 2.0 s. The acceleration response spectra of the 7 records for the MH are presented in Figure 2.5, with the mean spectrum and the EC8 target spectrum. Basic descriptive and seismologic data are presented in Table 2.3.

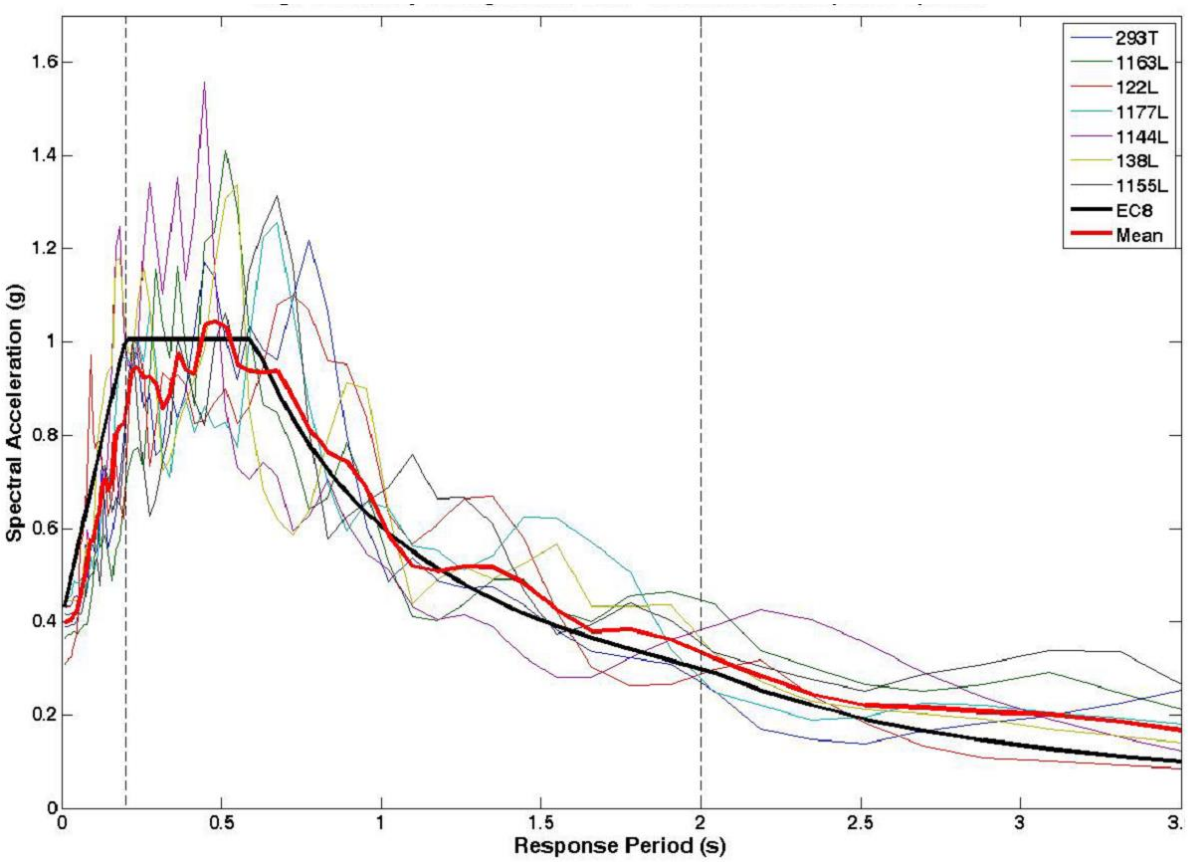

Figure 2.5 – Comparison of the scaled acceleration response spectra of the 7-record HH set with the 5% damped Type1, Soil C design spectrum of EN1998-1 with PGA = 0.35 g.

Table 2.3 – Seismological and scaling data for the 7-record HH set

NGA Record No.	Earthquake Name	Year	Magni-tude	Distance to Fault [km]	V_s30 [m/s]	PGA [g]	PGV [cm/s]	Scale Factor	D_{RMS}
00293T	Irpinia, Italy	1980	6.9	59.6	660	0.05	7.89	9.65	0.159
01163L	Kocaeli, Turky	1999	7.5	58.3	425	0.09	20.27	4.12	0.192
00122L	Friuli, Italy	1976	6.5	33.3	275	0.08	9.60	5.11	0.208
01177L	Kocaeli, Turky	1999	7.5	52.0	275	0.11	16.81	4.16	0.218
01144L	Gulf of Aqaba	1995	7.2	43.3	355	0.10	11.49	4.48	0.218
00138L	Tabas, Iran	1978	7.4	24.1	339	0.11	19.61	4.17	0.220
01155L	Kocaeli, Turky	1999	7.5	60.45	275	0.10	18.86	4.00	0.227

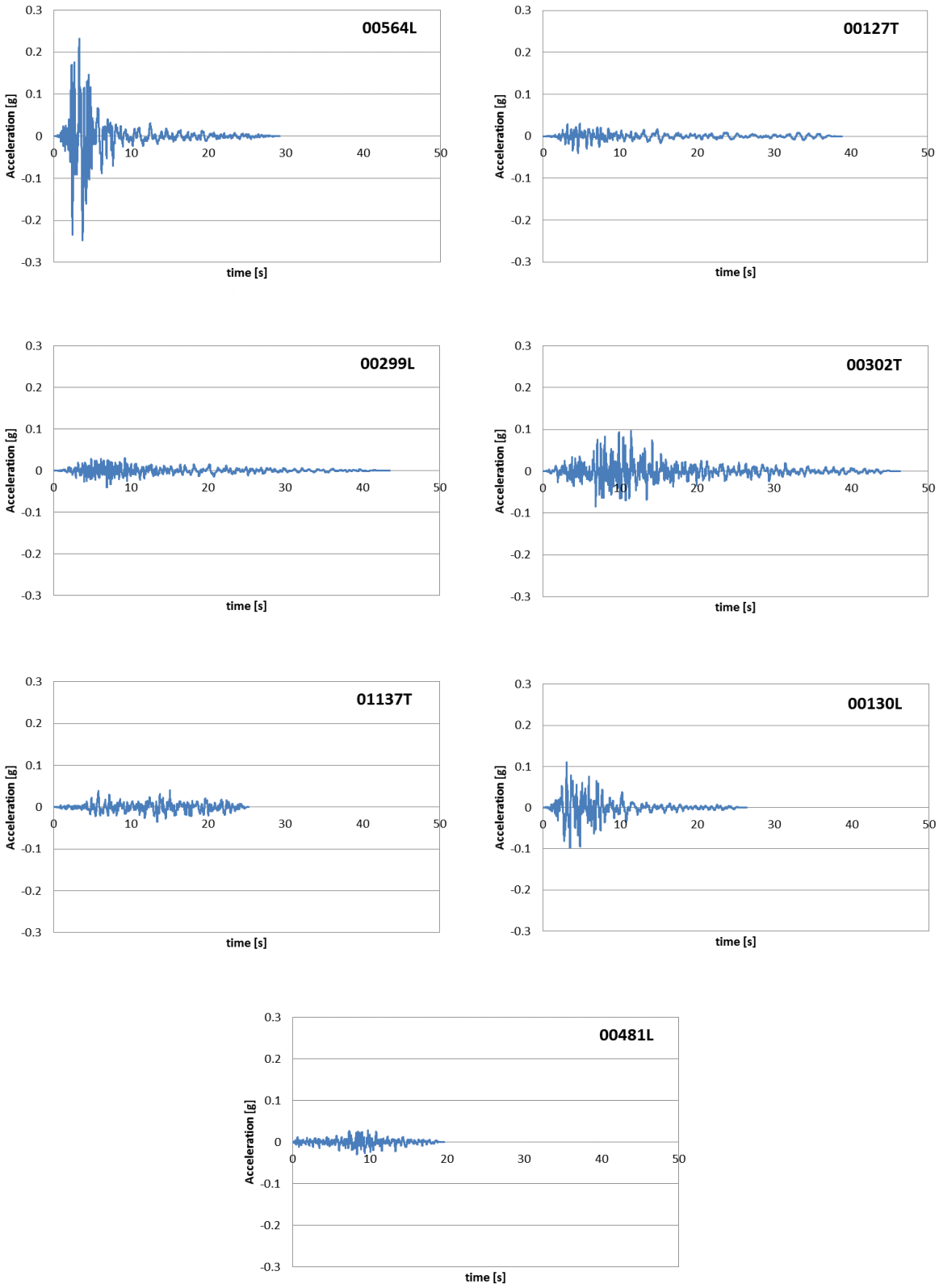

Figure 2.6 – Unscaled earthquake records for MH

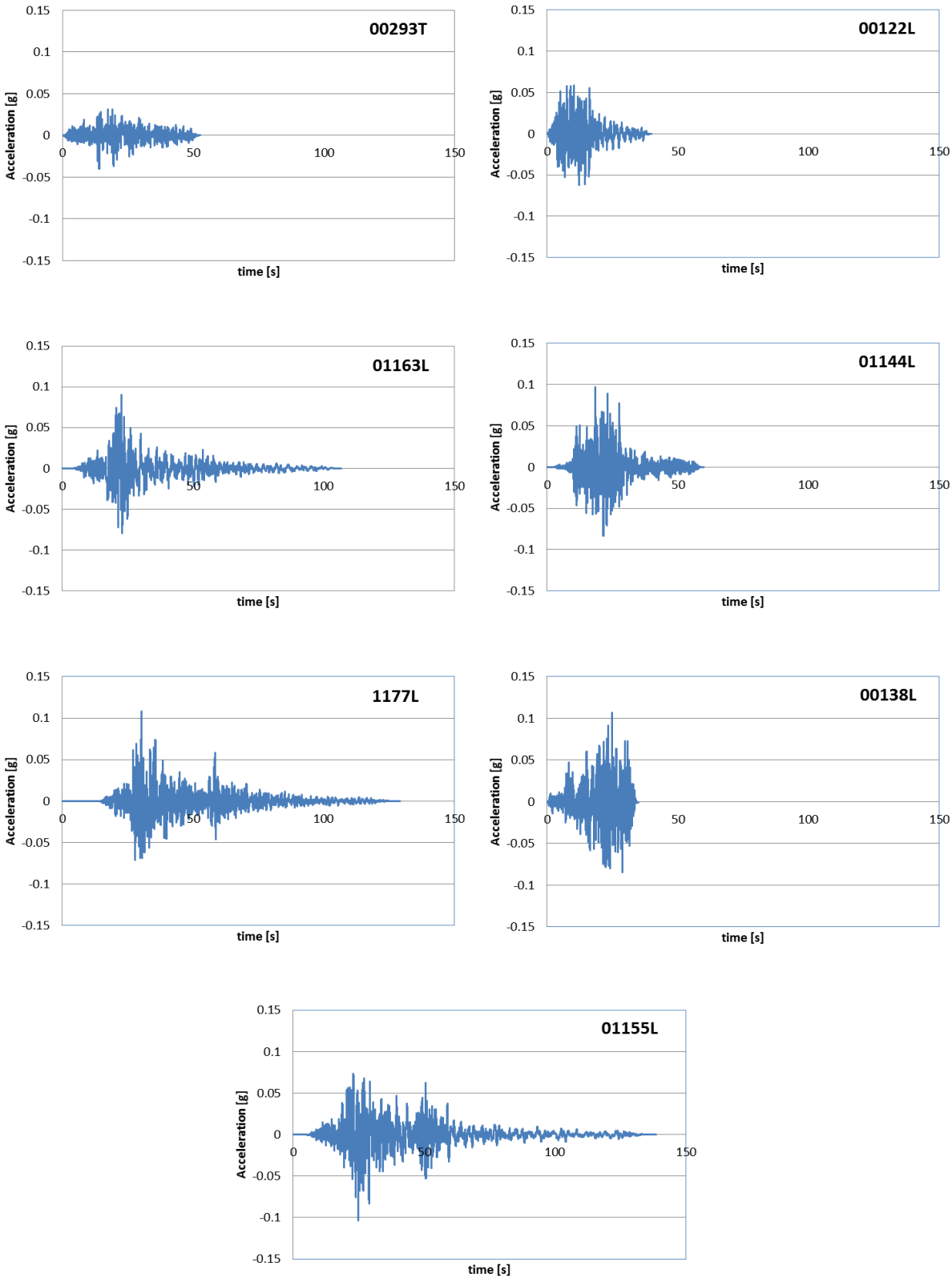

Figure 2.7 – Unscaled earthquake records for HH

3. SELECTED CASE STUDIES TYPOLOGY

A parametric study was carried out on order to evaluate seismic performance of dual-concentrically braced frames (D-CBF). In total 10 frames have been evaluated. Selected frames WERE previously designed in accordance with EN1993-1-1 and EN1998-1. Geometrical parameters that are varied are number of bays, span length and number of stories.

3.1. Description of building configuration

The considered building configuration is dual concentrically braced frame (D-CBF). Selected frames have 6 or 12 storeys with 3 (mainly) or 5 (in a few cases for comparison) bays. The span length is either 6m or 8m. The story height is the same for all the frames and it is 4.5m for ground storey and 3.5 for upper storeys. The storey plan is square in case of 3-bay frames and rectangular (5 by 3 bays) in case of 5-bay frames. The lateral resisting frames are placed at the perimeter of the plan of the building while interior frames are assumed to be gravity frames. Two-dimensional frame models were used for design. Typical building plan for the case of 3-bay frames is presented in Figure 3.1 and typical frame typologies in Figure 3.2 [9].

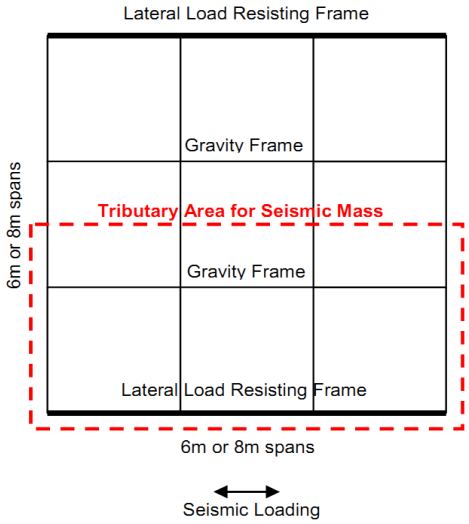

Figure 3.1 – Typical plan layout of the buildings

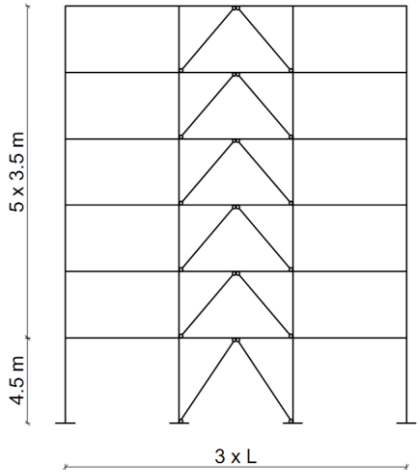

6-storey, 3-bay frame

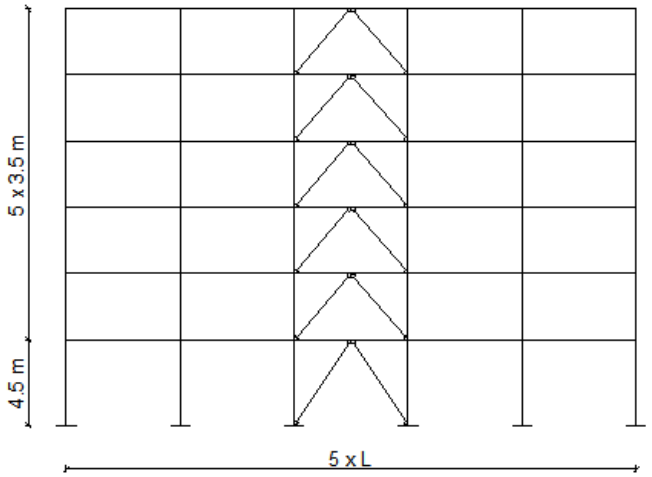

6-storey, 5-bay frame

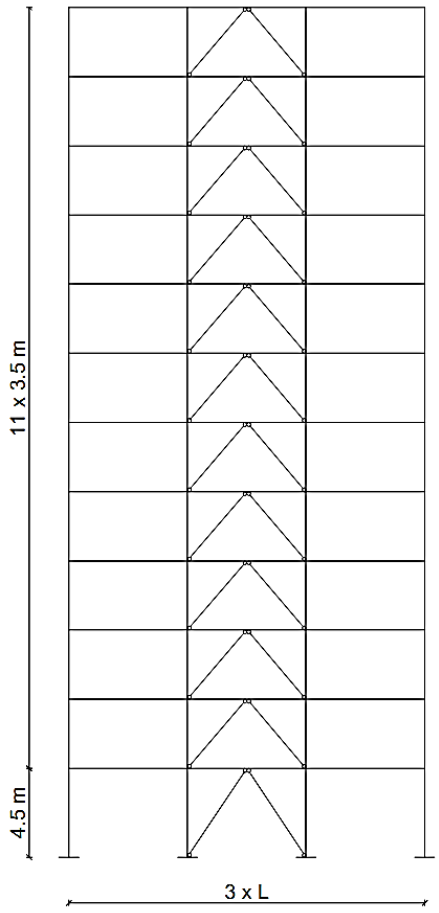

12-storey, 3-bay frames

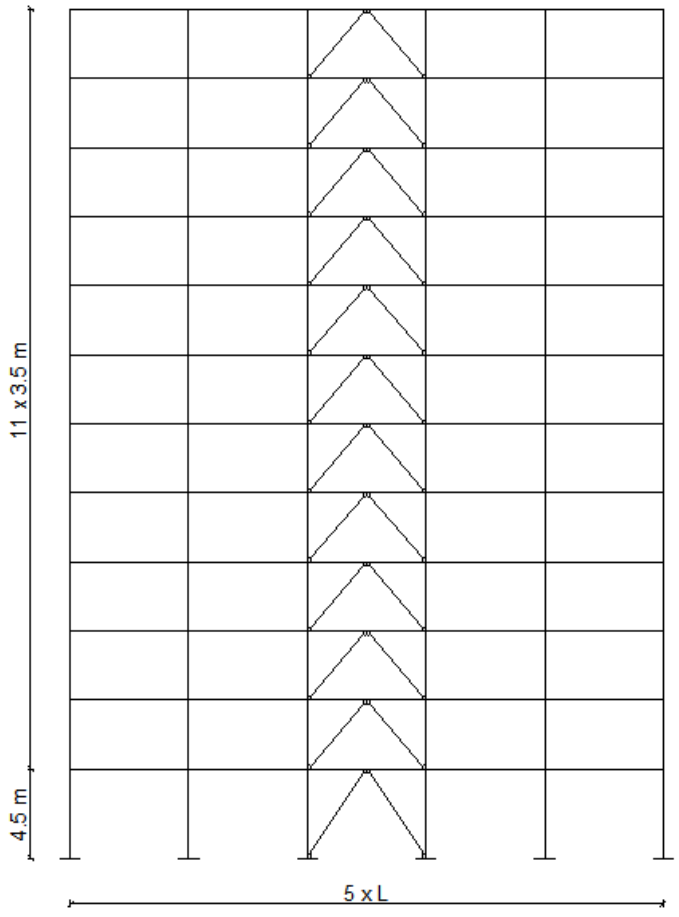

12-storeys, 5-bay frame

Figure 3.2 – Typology of D-CBFa

The columns of the frames are fixed at their bases. All the beams are fully restrained at their ends while braces are assumed to be pinned. Panel zones at columns are rigid and beams have rigid end offsets corresponding to the dimensions of the panel zone. Also, braces have rigid end offsets, with the dimension of the gusset plates. Diaphragm constraints are used at each floor, but the top nodes of the braces are not included in the diaphragm. Initial geometric imperfection of L/1000 is introduced to instigate buckling of braces and columns. The seismic mass is assigned in the nodes of beam-column intersection.

3.2. Parameters used in design of D-CBF

The material is steel, elasto-plastic, with Young's modulus *E=210GPa* and Poisson's ratio *v=0.3*. For yield strength it is used expected value obtained by multiplying characteristic value f_y*=355MPa* by $\gamma_{ov} = 1.25$. Linear strain hardening is taken as *0.25%* percentage of the initial elastic modulus.

The design of the reference structures was done using provisions of EN 1993 and EN 1998-1. For modelling is used commercial structural analysis software SAP2000. More details about modelling and design are provided in European pre-qualified steel JOINTS report [9].

3.3. Applied loads

The buildings are intended for residential or office use and values of permanent and imposed loads are given in Table 3.1, and seismic masses per floor are presented inTable 3.2.

Table 3.1 – Design vertical loads

Location	Load [kN/m^2]	
Intermediate Storeys	Permanent	5.8
	Imposed	3.0
Roof	Permanent	5.8
	Imposed	3.0

Table 3.2 – Seismic Masses per Floor

Frame Configuration	Seismic Mass per Floor [tons]	
3-bay, 6m span frames	Intermediate Floors	110.6
	Roof	97.4
3-bay, 8m span frames	Intermediate Floors	196.7
	Roof	173.2
5-bay, 6m span frames	Intermediate Floors	184.4
	Roof	162.4
5-bay, 8m span frames	Intermediate Floors	328.5
	Roof	289.3

3.4. Selected D-CBF

An overview of selected frames is presented in Table 3.3., while section sizes are given in ANNEX 1.

Table 3.3 – Selected dual-concentrically braced frames

Frame Name	Structural Configuration				
D-CBF-6-3-6-MH-a	D-CBF	6-storey	3-bay	6m span	PGA=0.25g
D-CBF-6-3-6-HH-a	D-CBF	6-storey	3-bay	6m span	PGA=0.35g
D-CBF-6-3-8-MH-a	D-CBF	6-storey	3-bay	8m span	PGA=0.25g
D-CBF-6-3-8-HH-a	D-CBF	6-storey	3-bay	8m span	PGA=0.35g
D-CBF-6-5-6-HH-a	D-CBF	6-storey	5-bay	6m span	PGA=0.35g
D-CBF-12-3-6-MH-a	D-CBF	12-storey	3-bay	6m span	PGA=0.25g
D-CBF-12-3-6-HH-a	D-CBF	12-storey	3-bay	6m span	PGA=0.35g
D-CBF-12-3-8-MH-a	D-CBF	12-storey	3-bay	8m span	PGA=0.25g
D-CBF-12-3-8-HH-a	D-CBF	12-storey	3-bay	8m span	PGA=0.35g
D-CBF-12-5-6-HH-a	D-CBF	12-storey	5-bay	6m span	PGA=0.35g

4. FINITE ELEMENT MODELING IN OPENSEES

In order to assess static and dynamic nonlinear behaviour of the structure, numerical models were developed using the software Open System for Earthquake Engineering Simulation (OpenSees). This is a software package for simulating the seismic response of structural and geotechnical systems developed by the Pacific Earthquake Engineering Research Centre, which is located at the University of California, Berkley. OpenSees has been developed as the computational platform for research in performance-based earthquake engineering. As it is primarily created for research purposes it lacks a graphical interface, and it is based on input scripts written in a combination of the TCL programming language and integrated OpenSees commands. This makes creating large and complicated structural models very demanding and time consuming. However, the fact that OpenSees in an open-source software has allowed developers to contribute to improve the software. The user interface is showed in Figure 4.1.

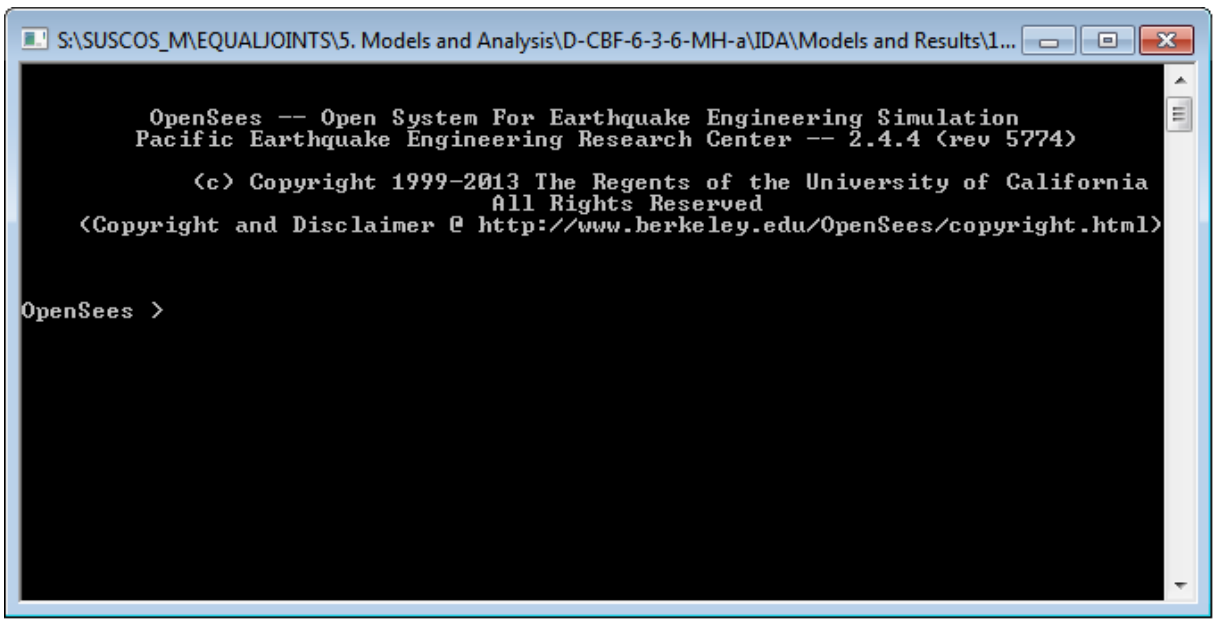

Figure 4.1 – OpenSees user interface

4.1. Model definition

4.1.1. Material properties

The nonlinear analysis of the structures depends on the constitutive stress-strain relation of the material. Steel, when subjected to high stress level, exhibit plastic behaviour and shows yielding and plastic deformation. While tension and compression envelops are enough for definition of the material under monotonic loading, for reversible loading, such as seismic loading, cyclic model has to be defined. The material model that is used in this case study is Giuffre-Monegotto-Pinto model shown in Figure 4.2. [10]

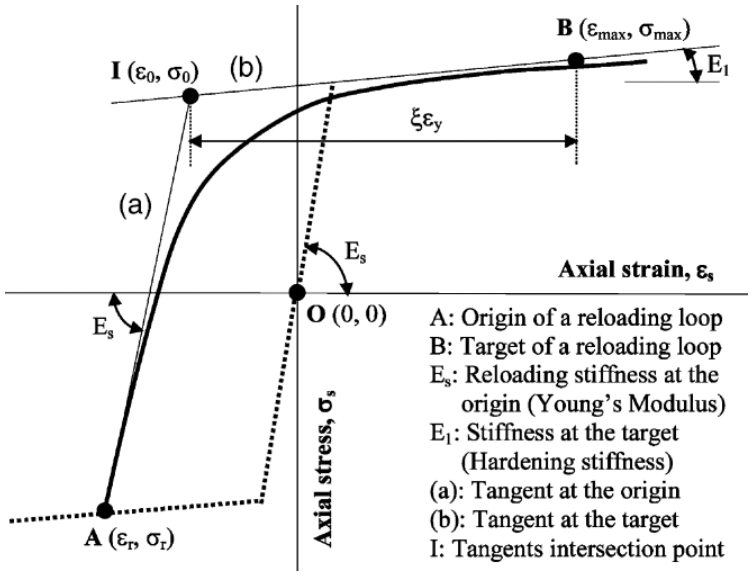

Figure 4.2 – Giuffre-Monegotto-Pinto model for cyclic loop [10]

OpenSees command used to construct a uniaxial Giuffre-Monegotto-Pinto steel material with isotropic hardening is following:

```
set Steel 1;
    set Fy   443.5;      # Steel yield stress
    set E    210000.;    # Steel Young's modulus
    set b    0.0025;     # strain-hardening ratio
    set R0   18;         # controls the transition from elastic to plastic branches
    set cR1 0.925;       # controls the transition from elastic to plastic branches
```

set cR2 0.15; # controls the transition from elastic to plastic branches

uniaxialMaterial Steel02 $Steel $Fy $E $b $R0 $cR1 $cR2

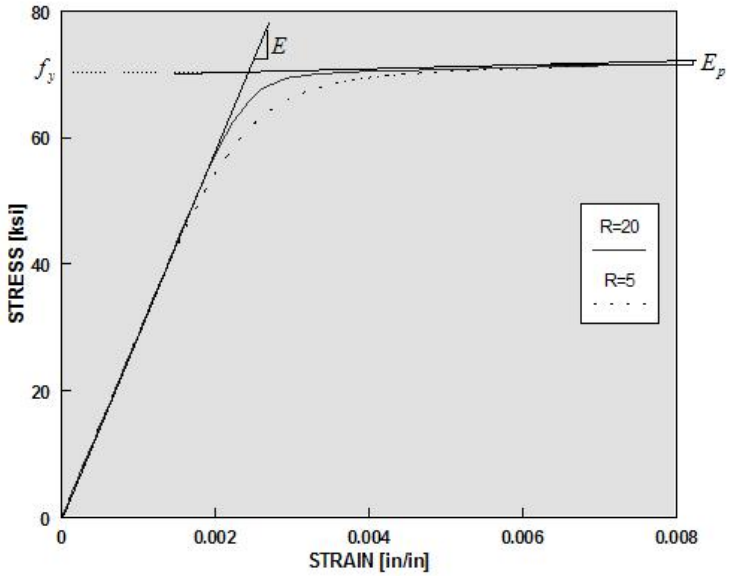

Figure 4.3 – Steel02 Material – Material Parameters of Monotonic Envelope [4]

4.1.2. Elements definition

Element formulation used for beam-column elements in structural seismic analysis can be divided into two categories: elements with distributed plasticity and elements with concentrated plasticity. While elements with concentrated plasticity model allow formation of plastic hinges in the element end, distributed plasticity models permit spread of plasticity along the element allowing yielding to occur at any location along the element. The distributed inelasticity elements are modelled as fiber elements displacement-based (DB) or force-based (FB). The DB formulation is based on displacement shape function, while the FB formulation is based on internal force shape function. As FB elements don't have restrains on their displacement fields they approximate plastic structural response with greater accuracy than DB elements [11]. In this case study "element forceBeamColumn" OpenSees command is used to model the elements, which is based on force-based formulation.

element forceBeamColumn $eleTag $iNode $jNode $numIntgrPts $secTag $transfTag

The programing structure of OpenSees allows independent selection of beam-column element and geometric transformation. The difference between geometric linear and geometric nonlinear analysis lies in the geometric transformation alone, since the elements do not have internal geometric nonlinearity. OpenSees geometric-transformation command "geomTransf" is used to transform beam element stiffness and resisting force from local-coordinate system to the global-coordinate system. Depending on structural element different geometric-transformation types is used in this case study:

Linear Transformation performs a linear geometric transformation of beam stiffness and resisting force from local-coordinate system to the global-coordinate system.

PDelta Transformation performs a linear geometric transformation of beam stiffness and resisting force from local-coordinate system to the global-coordinate system considering second-order P-Delta effects.

Corotational Transformation is used in large displacement-small strain problems [4].

Geometric transformation command additionally enables introducing rigid fields that represents panel zones in columns and rigid end offsets in beams, in the end of the elements using joint offset "jntOffset".

geomTransf $transfType $transfTag <-jntOffset $dXi $dYi $dXj $dYj>

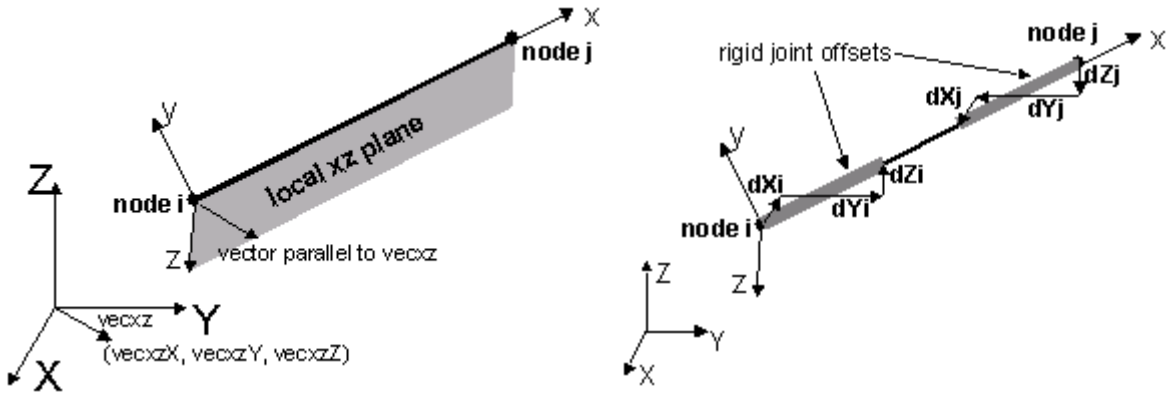

Figure 4.4 – The element coordinate system [4]

Description of each structural element used in nonlinear analysis

Elements are modelled as previously described. Initial geometric imperfection of L/1000 is introduced to instigate buckling of braces and columns, consequently these elements are modelled with two fiber elements. Panel zones at columns are rigid and beams have rigid end offsets corresponding to the dimensions of the panel zone. Also, braces have rigid end offsets, with the dimension of the gusset plates (Figure 4.5).

Columns:

- forceBeamColumn element
- 2 fiber elements
- Initial imperfection $(L_{eff}/1000)$
- 5 integration points
- PDelta geometric transformation (jntOff for panel zone)

Beams:

- forceBeamColumn element
- 1 fiber element
- 5 integration points
- PDelta geometric transformation (jntOff for rigid end offset)

Braces:

- forceBeamColumn element
- 2 fiber elements
- Initial imperfection $(L_{eff}/1000)$
- 5 integration points
- Corotational geometric transformation

Brace rigid elements:

- elasticBeamColumn element
- $EA_{rigid} = 10 \cdot EA_{brace}$
- Linear geometric transformation

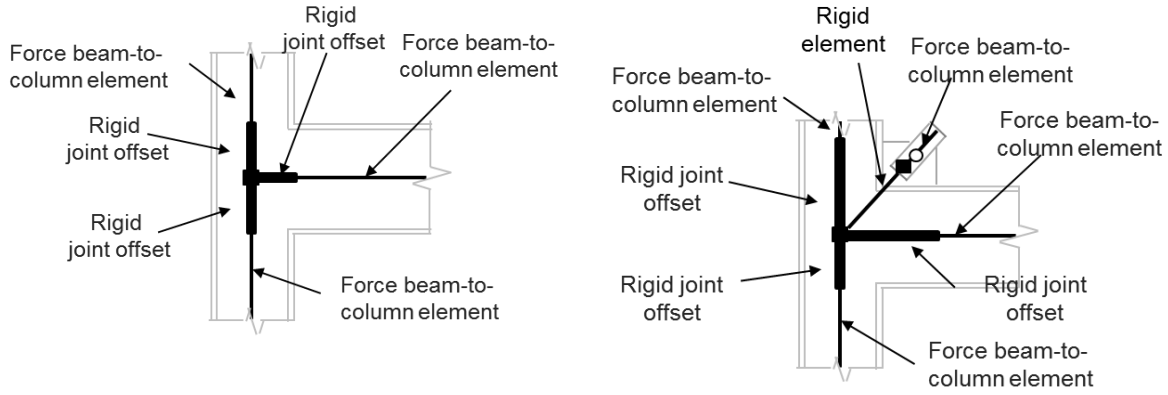

a) beam-columns intersection

b) beam-column-brace intersection

Figure 4.5 – Rigid offsets at elements intersection

Restraints and boundary conditions

The columns of the frames are fixed at their bases. Braces are assumed to be pinned. The pinned connection is simulated in the OpenSees using "equalDOF" command specifying that translation degrees-of-freedom of the beginning of the brace are the same as those at the end of rigid element used for modelling gusset plate. Diaphragm constraints, defined as "equalDOF" for degree-of-freedom 1, are used at each floor, but the top nodes of the braces are not included in the diaphragm.

4.1.3. P-Delta effects

The second order effects are introduced by geometric transformation of the elements as previously defined. Furthermore, in order to take into account the seismic mass that is not tributary to the frame, leaning column was modelled (Figure 4.6).

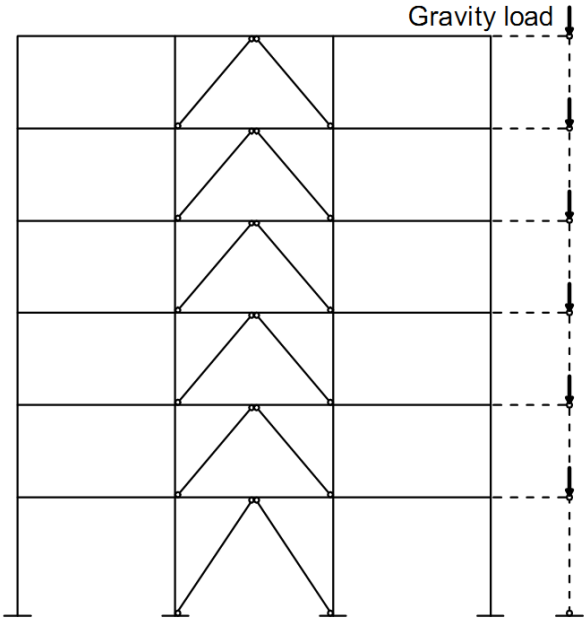

Figure 4.6 – Leaning column

4.2. Definition of Loads and Analysis parameters

In OpenSees loads are applied in three steps:

1. Definition of the loads in a load pattern
2. Definition and of analysis and its features
3. Loads are applied when execute the analysis

1. Load definition

Load are defined using "pattern" command. Currently available patterns are:

Plain Pattern - used to define nodal loads, single-point constrains, element loads

UniformExcitation Pattern – used to define acceleration record to all fixed nodes in specific direction

MultipleSupportPattern – used to define displacement record at specific nodes, in specific direction, or a ground-motion record [12]

2. Analysis definition and its features

In order to perform the analysis in OpenSees, for each analysis following items need to be defined, preferably in this order:

constraints

The OpenSees constraints command is used to construct the ConstraintHandler object. Constraints enforce a relationship between degrees-of-freedom. The ConstraintHandler object determines how the constraint equations are enforced in the analysis.

numberer

The OpenSees numbered command is used to construct the DOF_Numberer object. The DOF_Numberer object determines the mapping between equation numbers and degrees-of-freedom – how degrees-of-freedom are numbered.

system

The OpenSees system command is used to construct the LinearSOE and LinearSOlver objects to store and solve the system of equations in the analysis.

Test

The OpenSees test command is used to construct a Convergance Test object. Certain

SolutionAlgorithm objects require ConverganceTest object to determine if convergence has been achieved at the end of an iteration step.

algorithm

The OpenSees algorithm command is used to construct a SolutionAlgorithm object, which determines the sequence of steps taken to solve the non-linear equation.

Integrator

The OpenSees integrator command is used to construct the Integrator object. The Integrator object determines the meaning of the terms in the system of equation object. The Integrator object is used for the following:

- determine the predictive step for time t+dt
- specify the tangent matrix and residual vector at any iteration
- determine the corrective step based on the displacement increment dU

analysis

The OpenSees analysis command is used to construct the Analysis object. This analysis object is constructed with the component object previously created by the analyst. All available analysis object employ incremental solution strategies [12].

3. Analysis execution

OpenSees “analyze” command executes the analysis in specified number of steps [12].

4.2.1. Modal analysis

Eigen Analysis was performed in order to obtain dynamic characteristics of the structure. To perform Eigen analysis seismic masses are assigned in the nodes of beam-column intersection, but not in the node of beam-brace intersection. Assigned seismic masses are given in Table 3.2. To record eigenvector for modal shapes one step of transient analysis is performed. Tcl scrip to perform Eigen analysis is given in ANNEX 2.

4.2.2. Pushover analysis

Pushover analysis is performed according to EC 8 [2]. Two vertical distribution of lateral loads are considered as described in section 2.4.4. Loads are defined using "Plain Pattern" command.

Following parameters are set up:

constraints	Plain
numberer	RCM
system	BandGeneral
test	EnergyIncr
algorithm	ModifiedNewton
integrator	DisplacementControl
analysis	Static

In case of convergence problems some analysis parameters are changed in order to achieve convergence. Tcl scrip to perform pushover analysis is given in ANNEX 3.

4.2.3. Incremental dynamic analysis

Set of seven ground motions are applied to the structure. For each of the records performance at "design" (D), "near collapse" (NC) and twice NC performance level is analysed. The ratio of the acceleration level and design peak ground acceleration for each of performance levels is given in Table 4.1.

Table 4.1 – Performance levels

Limit state	A/A_d
Design (D)	1.0
Near collapse (NC)	1.73
Twice near collapse (2xNC)	3.46

Rayleigh damping was assigned for all columns, beams and braces in the model as 0.02 damping ratio. Loads are defined using "UniformExcitation" pattern command and for analysis following parameters are set up:

```
set      dt_analysis
wipeAnalysis;
constraints     Transformation
numbered        RCM
system          UmfPack
test            EnergyIncr      1.e-7   10      0
algorithm       ModifiedNewton
integrator      TRBDF2
analysis        VariableTransient       $NumSteps       $dt_analysis    0.00001     $dt_analysis
```

In case of convergence problems algorithm used in analysis was changed. Tcl scrip to perform dynamic analysis is given in ANNEX 4.

5. PARAMETRIC STUDY

The non-linear performance of Dual-Concentrically braced frames are described and discussed. The aim of this chapter is to provide detail results for non-linear procedures previously introduced. The study is focused on evaluation of behaviour and seismic performance of D-CBFs on three previously defined performance levels. The behaviour of the frames is obtained in form of pushover curves and schematic illustration of formed plastic hinges. The seismic performance indicators that have been monitored at each of three performance levels are following: i) peak storey acceleration, ii) peak interstorey drift ratio, iii) residual interstorey drift ratio, iv) beam rotation ratio.

In order to define modal distribution of lateral forces non-linear static pushover analysis, modal analysis was firstly carried out. 1st and 2nd fundamental period of the frames as well as deformed shape are obtained.

5.1. Modal Analysis

Table 5.1 – Fundamental periods [s]

	1st	2nd		1st	2nd
D-CBF-6-3-6-MH-a	0.663	0.236	**D-CBF-12-3-6-MH-a**	1.369	0.441
D-CBF-6-3-6-HH-a	0.566	0.205	**D-CBF-12-3-6-HH-a**	1.247	0.407
D-CBF-6-3-8-MH-a	0.683	0.245	**D-CBF-12-3-8-MH-a**	1.462	0.487
D-CBF-6-3-8-HH-a	0.612	0.222	**D-CBF-12-3-8-HH-a**	1.312	0.431
D-CBF-6-5-6-HH-a	0.650	0.231	**D-CBF-12-5-6-HH-a**	1.387	0.464

Table 5.1 presents 1sr on 2nd fundamental period of the frames. In general, frames with shorter span are stiffer comparing to ones with larger span, while 5-bay frame shows the smallest stiffness. Regarding hazard level, frames designed for HH are stiffer comparing to frames designed for MH.

5.2. Non-linear static pushover analysis

The Figure 5.1. presents pushover curves for the 1st mode and uniform lateral forces distribution. Base shear force is normalized by design base shear V_b. Design base shear force was calculated as explained in 2.3.2.1. In Table 5.2 are given values of calculated designed shear force for examined frames. Presented pushover curves are characteristic for CBFs. It can be clearly seen that after first plastic event, sudden reduction in the lateral resistance of the frame occurs. This behaviour is explained with buckling of brace in compression. Decrease is immediately followed by an increase of lateral stiffness. When comparing frames with different span length, sudden decrease in lateral stiffness influences more frames with larger span, while 5-bay frames are not significantly affected by this behaviour.

Table 5.2 – Base shear force

	V_b [kN]		V_b [kN]
D-CBF-6-3-6-MH-a	1323.5	**D-CBF-12-3-6-MH-a**	1160.5
D-CBF-6-3-6-HH-a	2045.4	**D-CBF-12-3-6-HH-a**	1795.8
D-CBF-6-3-8-MH-a	2313.8	**D-CBF-12-3-8-MH-a**	1981.7
D-CBF-6-3-8-HH-a	3560.3	**D-CBF-12-3-8-HH-a**	3023.0
D-CBF-6-5-6-HH-a	3180.2	**D-CBF-12-5-6-HH-a**	2671.41

Observing V/V_d ratio in case of different building height, it can be noticed that 12 story frames have larger V/V_d ratio then the 6-storey frames. In term of span length V/V_d ratio is slightly higher for frames with shorter span.

Damage distribution in frames is given in Figure 5.2, Figure 5.3 and Figure 5.4.Criteria for formation of shown plastic hinges is analytical defined as:

$$N_{Ed} < N_{pl} = A \cdot f_y \qquad M_{Ed} < M_{pl} = W_{el} \cdot f_y$$

while criteria for buckling of the brace is when axial force reaches $0.3 \cdot N_{pl}$.

In shorter frames damage is mostly located in the braces, while in taller frames plastic hinges occur in high number also in columns. In higher frames damage is located in bottom of the frames. In 5-bay frames plastic hinges in beams are also observed.

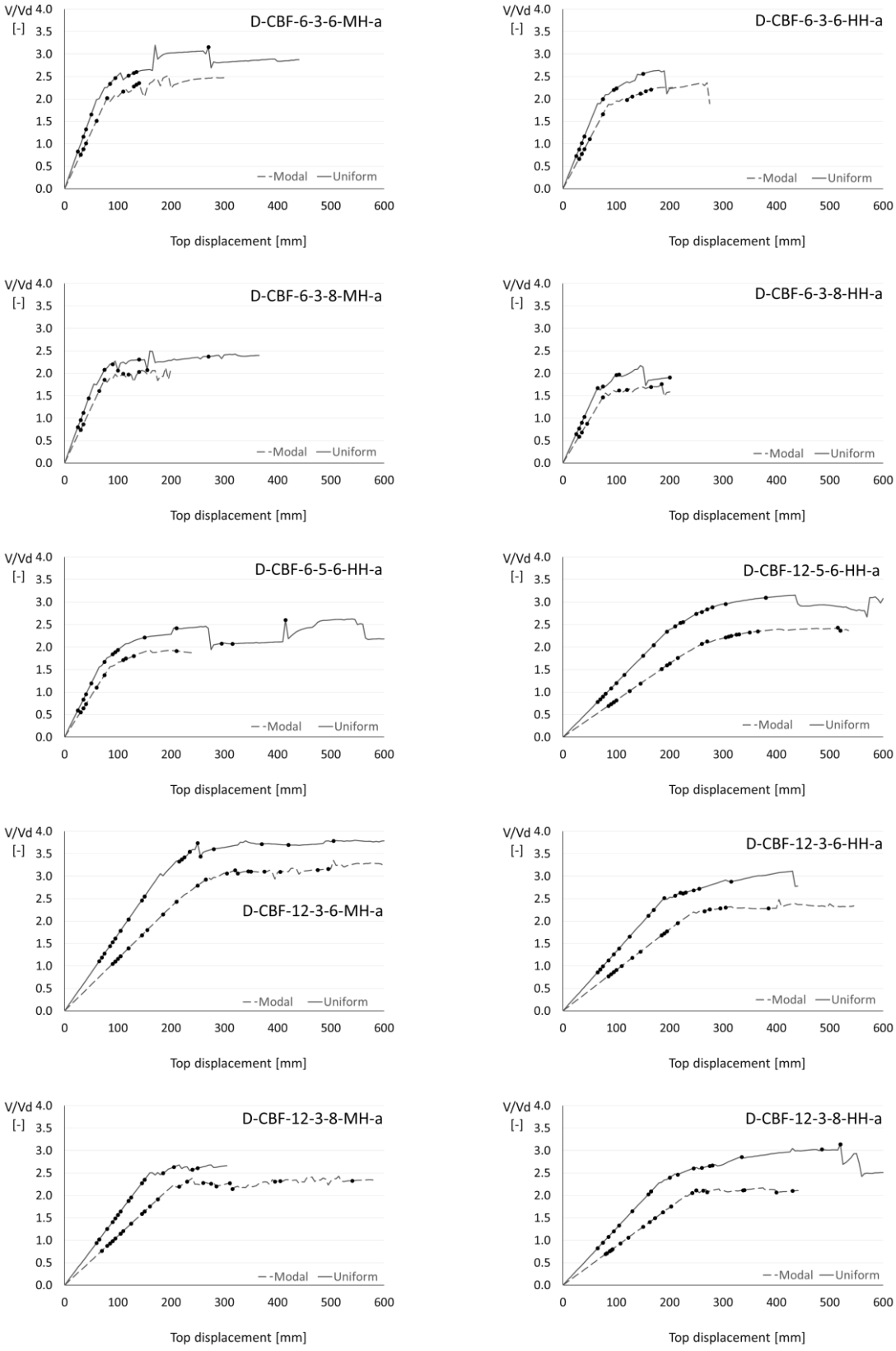

Figure 5.1 – Normalized pushover curves

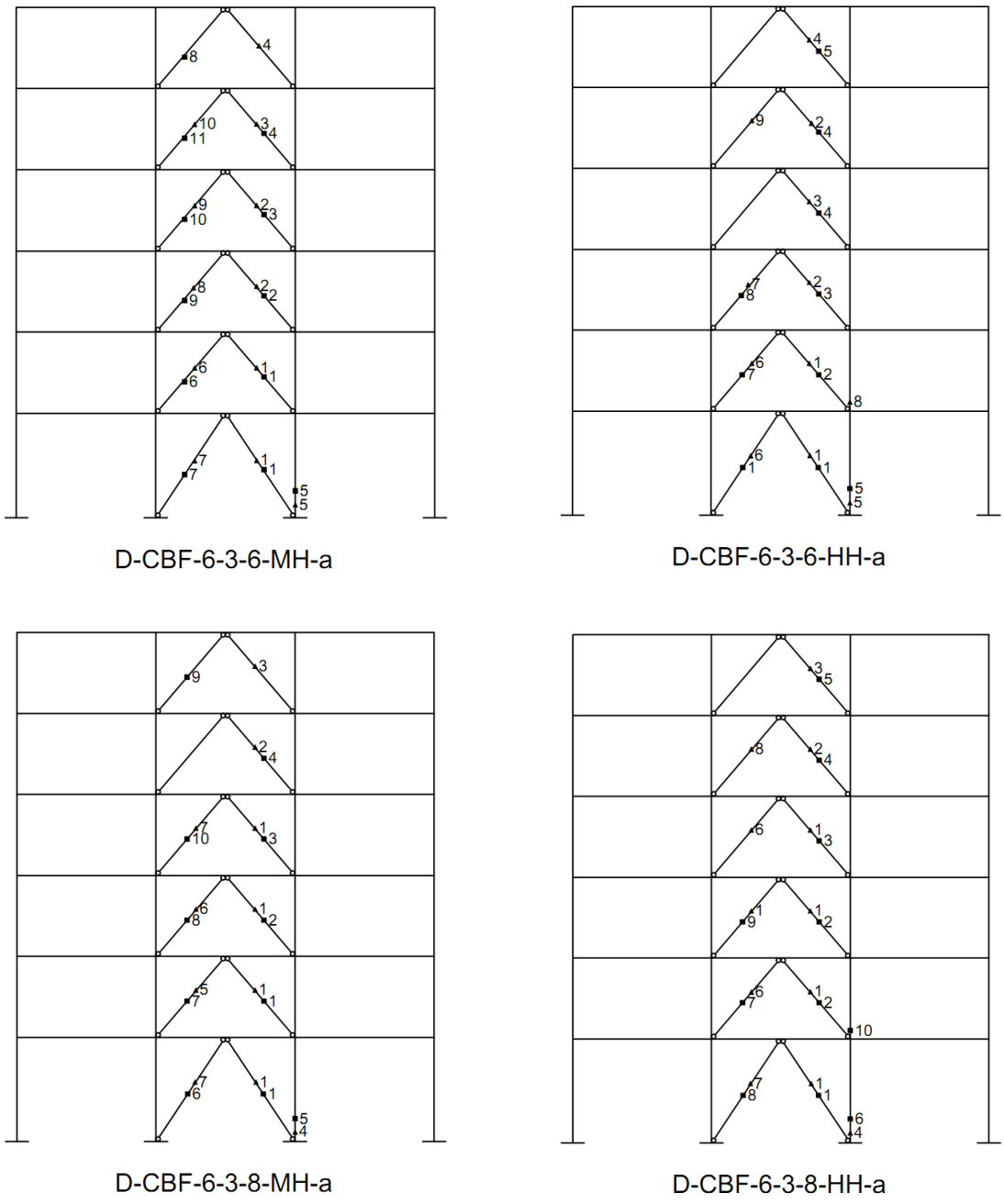

Figure 5.2 – Damage distribution for 6-storey frames

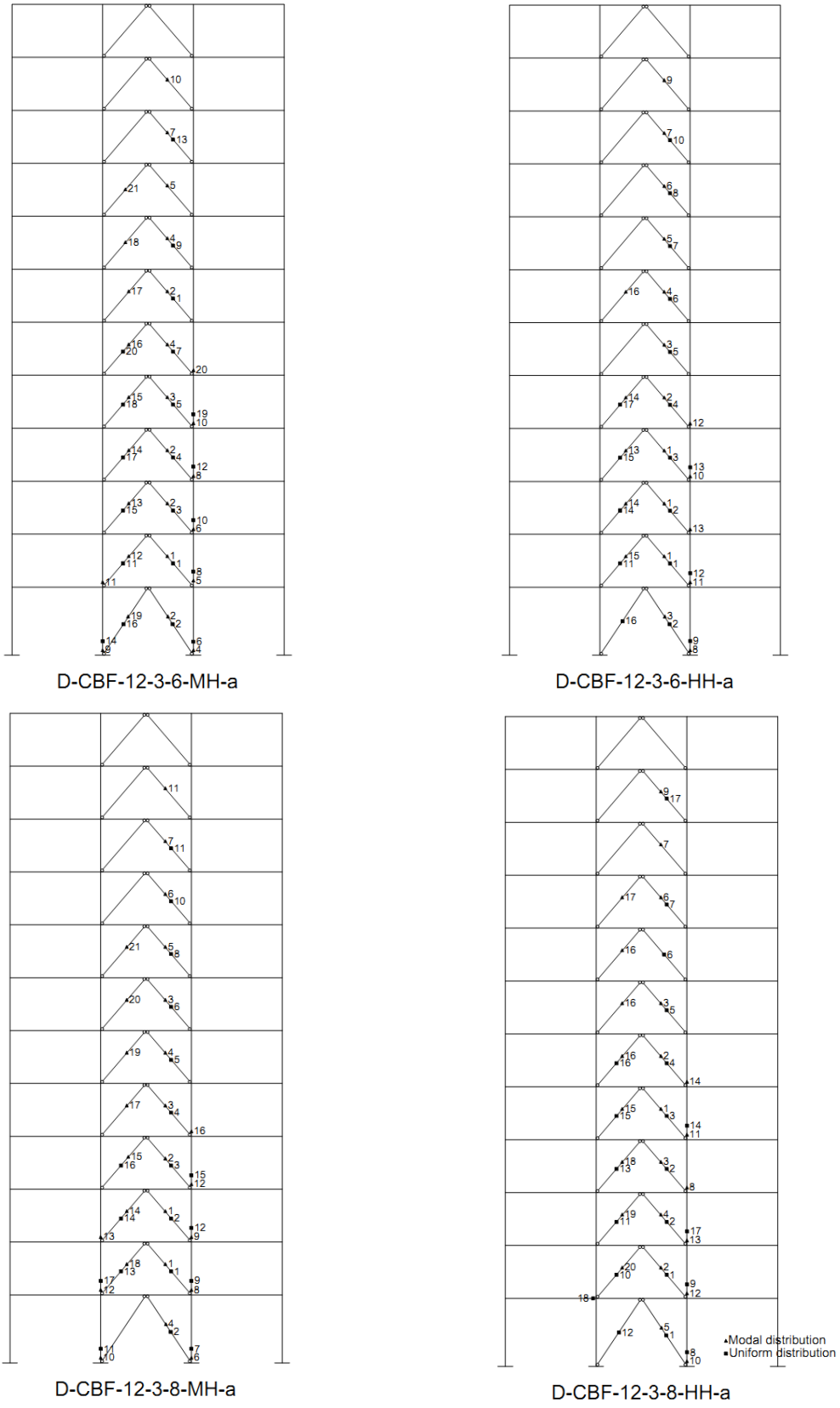

Figure 5.3 – Damage distribution for 12 storey frames

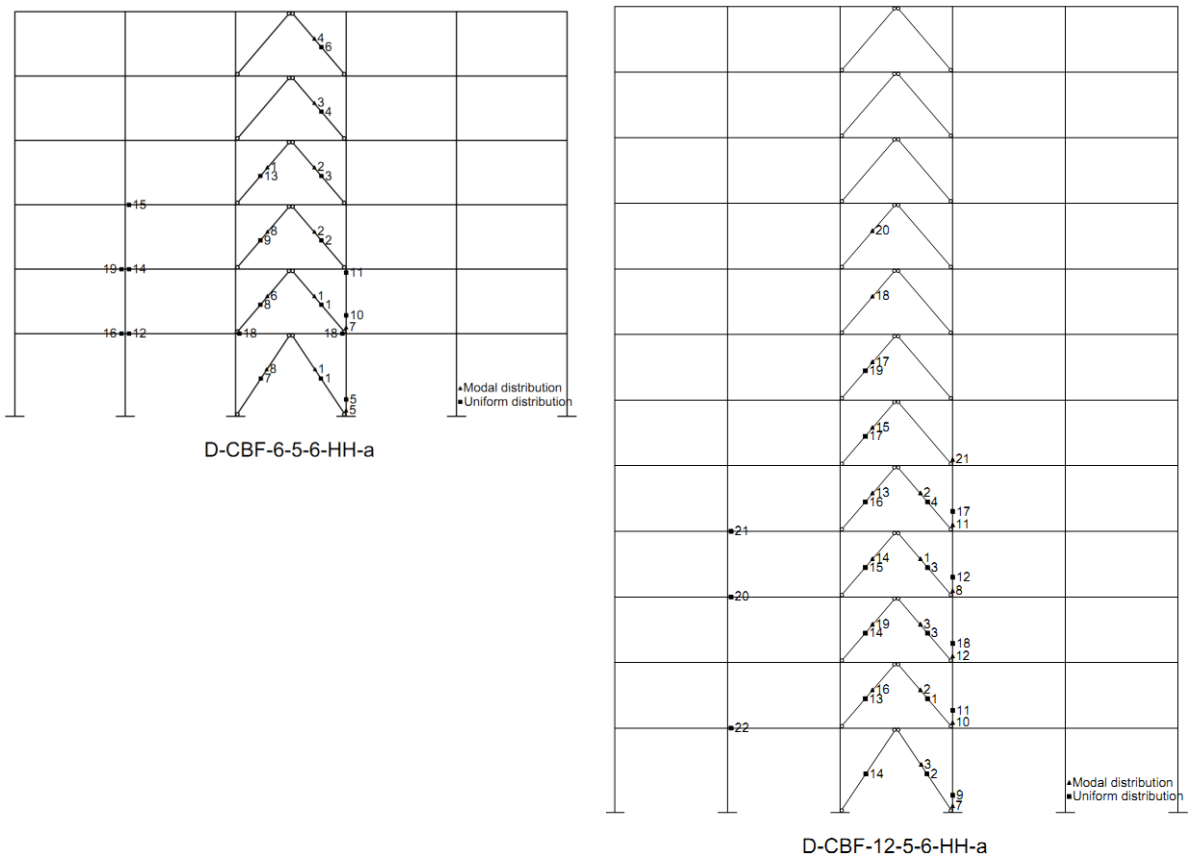

Figure 5.4 – Damage distribution for 5-bay frames

5.2. Incremental dynamic analysis

In addition to static nonlinear pushover analysis, incremental dynamic analysis (IDA) was carried out in order to evaluate inelastic behaviour of examined frames. First, D-CBF-6-3-6-MH-a frame for subjected to increasing PGA in order to check criteria defined for the three limit states. Each record was applied in increments of 0.25 PGA from 0.25 PGA to 4.0 PGA. IDA curves for interstorey drift ratio vs. ground motion intensity level are presented in Figure 5.5. at "near collapse" (NC) performance level (intensity approximately 175%) interstorey drift ratio ranges from 0.8% to 1.5% with a mean value of 1.1%. At twice the NC performance level (intensity approximately 350%), interstorey drift ratio ranges from 1.9% to 3.1% with mean value of 2.6%.

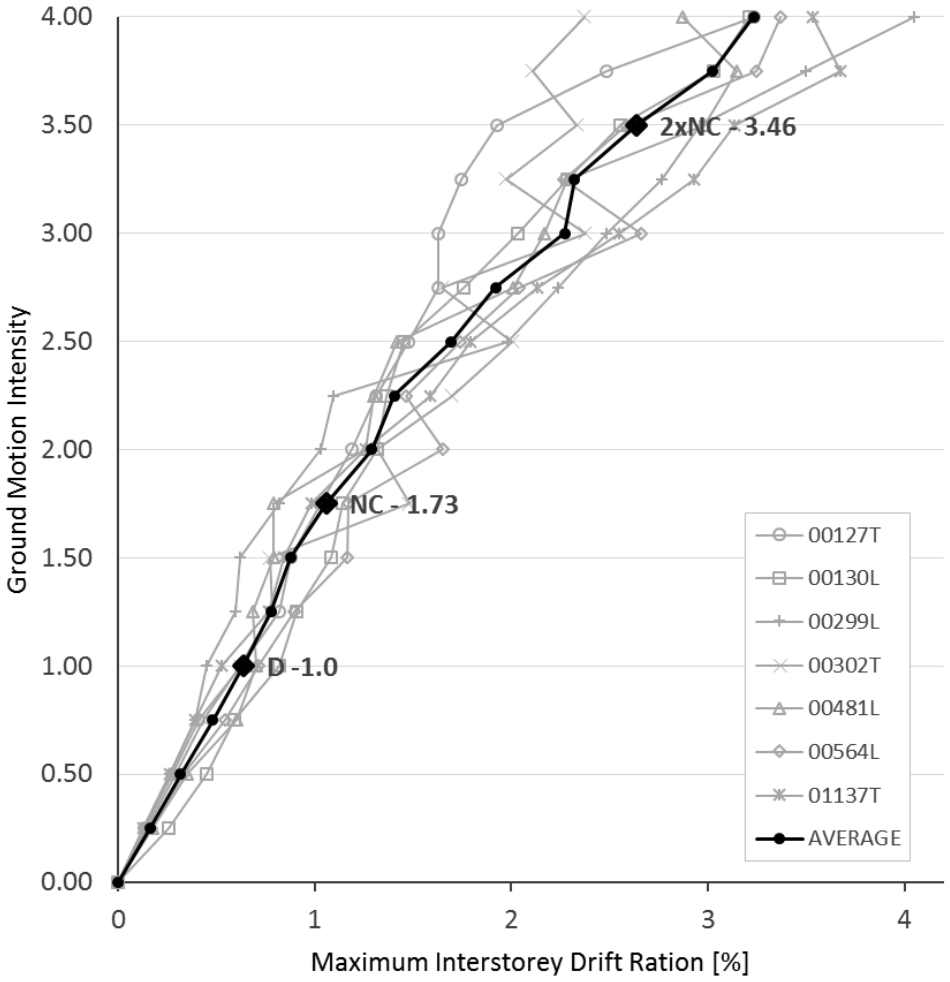

Figure 5.5 – IDA curves in terms of max, interstorey drift ratio for D-CBF-6-3-6-MH-a frame

For all examined frames, dynamic analysis outputs are discussed for three limit states previously defined. The performance of the frames is evaluated in terms of: i) peak storey accelerations, ii) peak interstorey drift ratios, iii) residual interstorey drift ratios and iv) beam rotation ratio.

5.2.1. Peak storey acceleration

Peak storey acceleration (PSA) is usually related to non-structural damage. Intensity of PSA can be used to quantify potential economic loss depending on non-structural building elements.

The plots in Figure 5.6 summarize the mean PSA obtained from seven previously defined records at three performance levels. The results are divided in two groups according to building height. Parameters varied within the groups are hazard level, span length and number of spans. The results are presented in form of PSA along the building height. More detailed results showing PSA for each record as well as mean PSA are given in ANNEX 5.

In general, PSA is constant along the height for shorter frames (6-storey), while for taller frames (12-storey) the higher PSA values are found at the ground floor. In case of 12-storey frames PSA is decreasing along the height up to 7^{th} floor and from 7^{th} to 12^{th} floor is constant. Considering number of spans, frames with more spans show lower PSA.

In general, high values of PSA indicate that severe damage in non-structural elements can be expected.

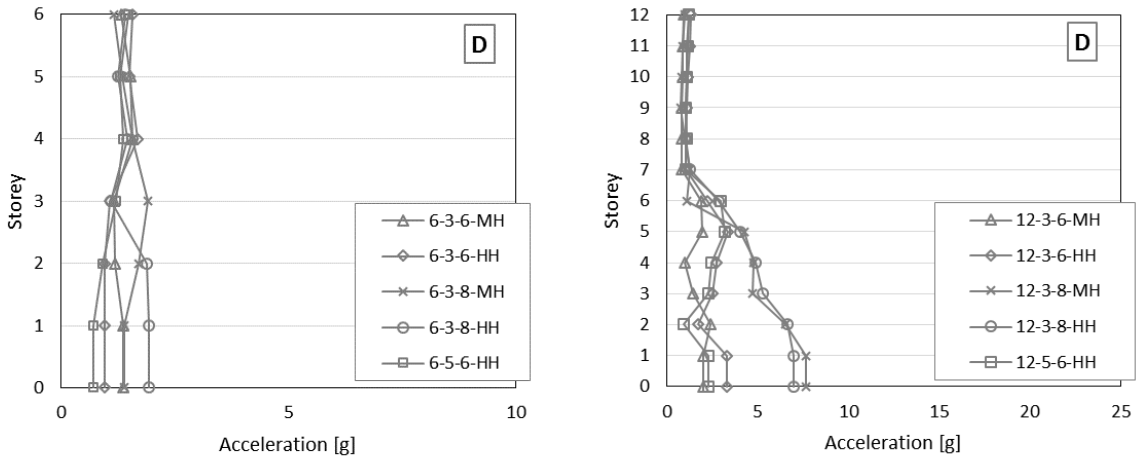

a) D – Design Performance Level

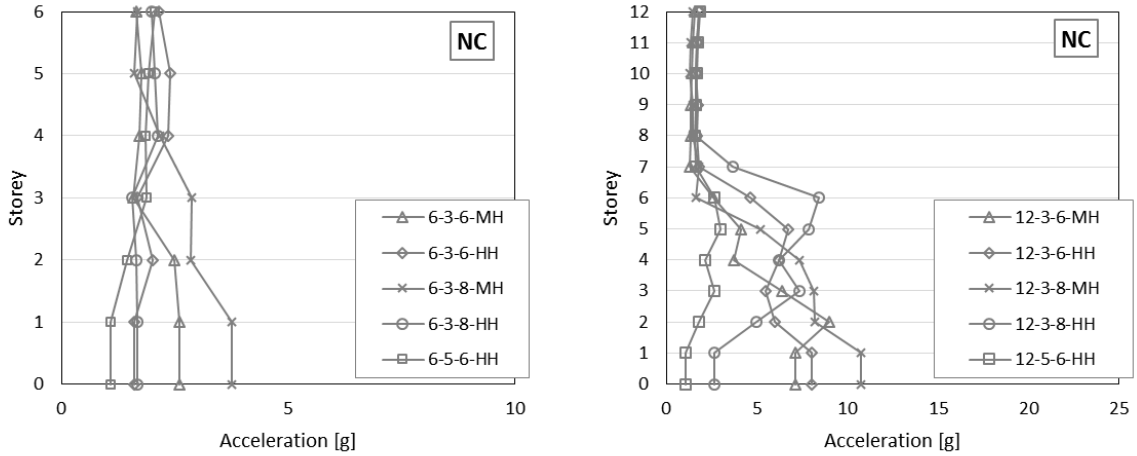

b) NC – Near Collapse Performance Level

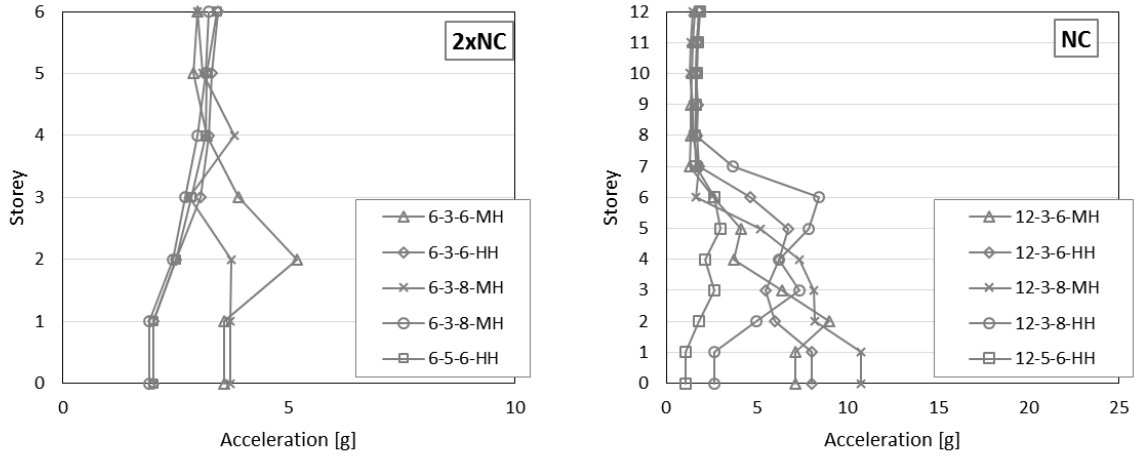

c) 2xNC – Two times Near Collapse Performance Level

Figure 5.6 – Mean peak storey acceleration for the three performance levels

5.2.2. Interstorey drift ratio

The plots in Figure 5.7 summarize the mean interstorey drift ratio at three performance levels. More detailed results showing interstorey drift ratio for each record as well as mean interstorey drift ratio are given in ANNEX 5.

The 6-storey frames have lower interstorey drift ratio comparing to 12-storey frames, this is justified by higher initial stiffness of shorter frames, as can be observed in pushover curves. The maximum drifts are constant along the height with small decrease in the value at the top of the frame, while taller show maximum drifts around mid-height. Higher values of maximum drifts in case of 12-storey frames are in mid-height for frames designed for HH, while at the bottom and top of the frame maximum drift is the same. 12-storey frames designed for MH show uniform pattern along the height.

Focusing on the hazard level, frames subjected to high hazard level suffer larger interstorey drift comparing to the frames subjected to medium hazard level. This difference is caused by higher mass of frames designed for high hazard, which induces larger inertial forces in the frames.

5.2.3. Residual interstorey drift ratio

The residual interstorey dift ratio is important parameter to describe level of damage caused by seismic event. Its importance is significant in building rehabilitation assessment.
The plots in Figure 5.8 summarize median residual drift ratio for the three performance levels. More detailed results showing residual interstorey drift ratio for each record as well as mean residual interstorey drift ratio are given in ANNEX 5.

Comparing the residual interstorey drift radio depending on height of the frame, 6-storey frames suffer larger residual drift in the bottom of the fame, while 12-storey frames have larger value of residual interstorey drift ratio in mid-high of the frame.

In term of hazard level, higher values are observed in frames subjected to high hazard.

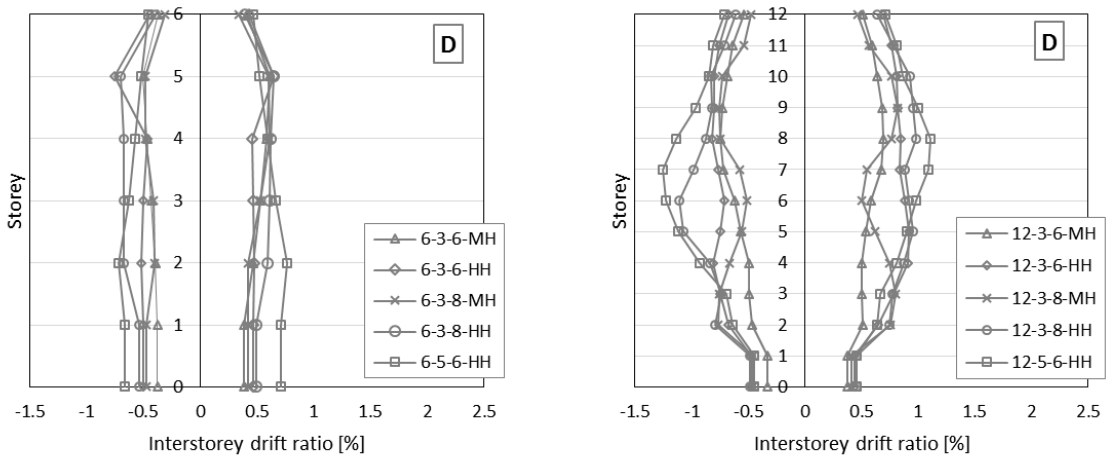

a) D – Design Performance Level

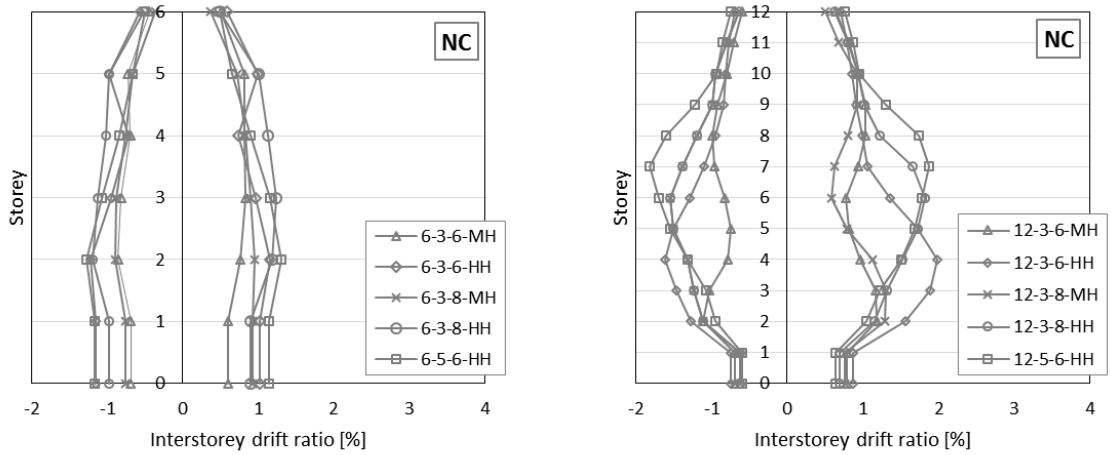

b) NC – Near Collapse Performance Level

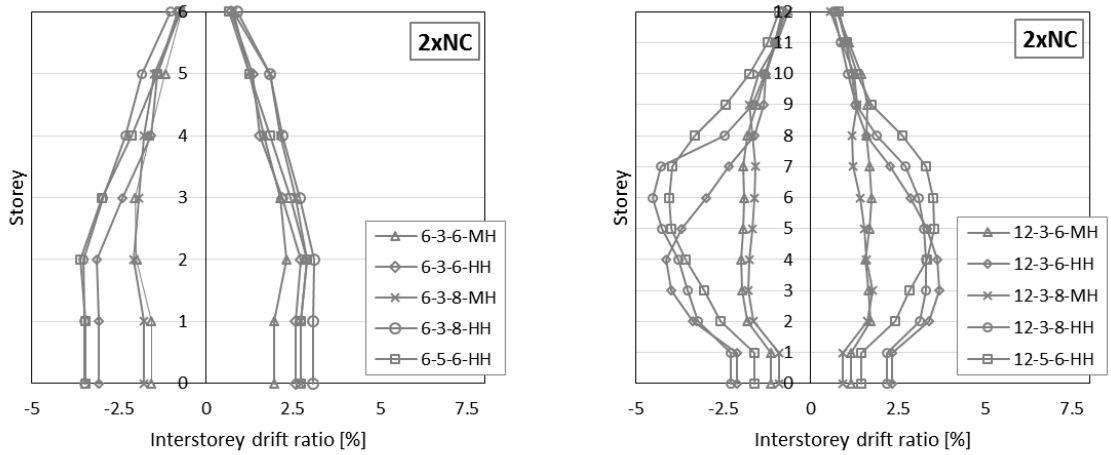

c) 2xNC – Two times Near Collapse Performance Level

Figure 5.7 – Median peak interstorey drift ratio for the three performance levels

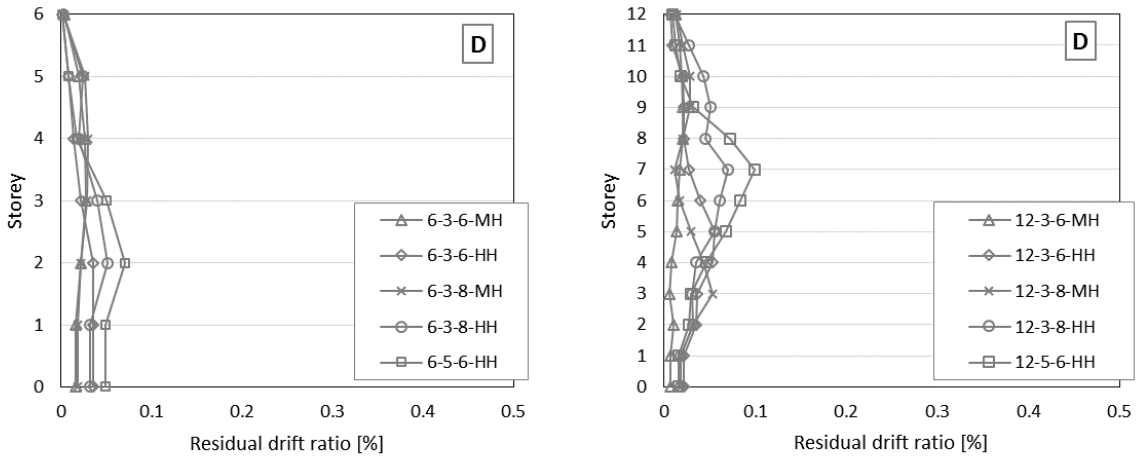

a) D – Design Performance Level

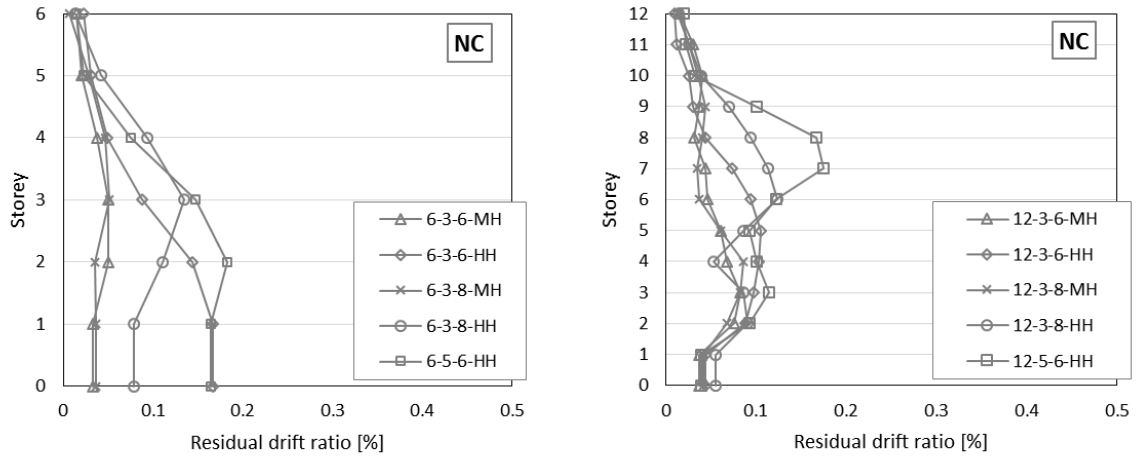

b) NC – Near Collapse Performance Level

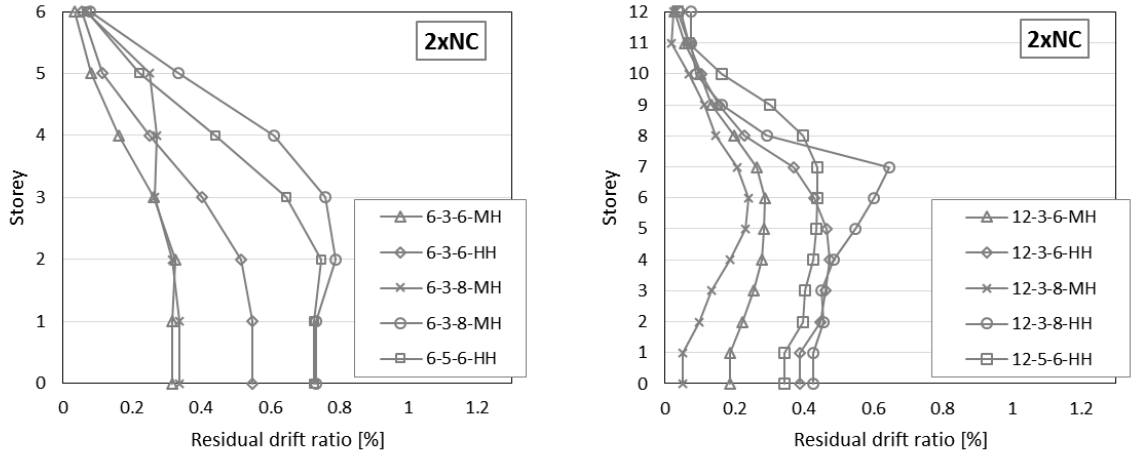

c) 2xNC – Two times Near Collapse Performance Level

Figure 5.8 – Median residual drift ratio for the three performance levels

5.2.4. Beam rotation ratio

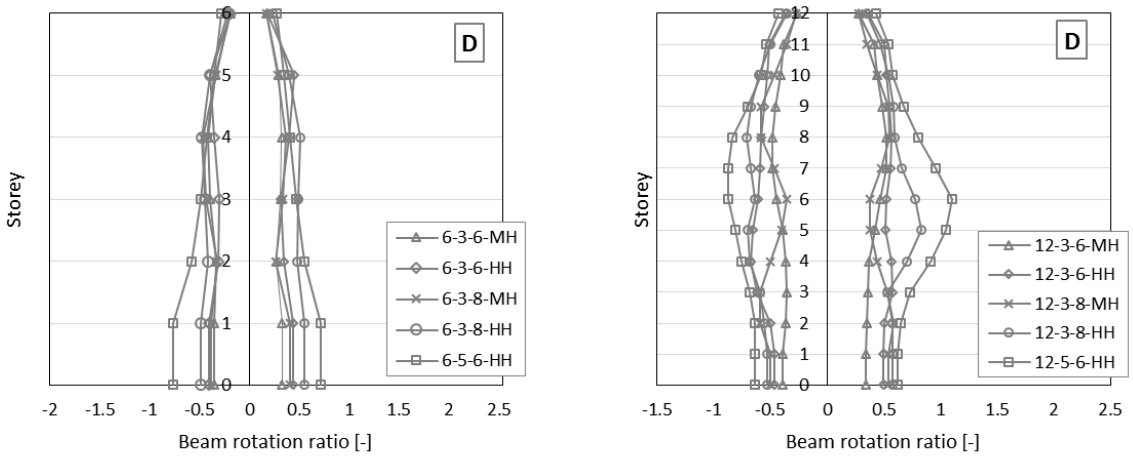

a) D – Design Performance Level

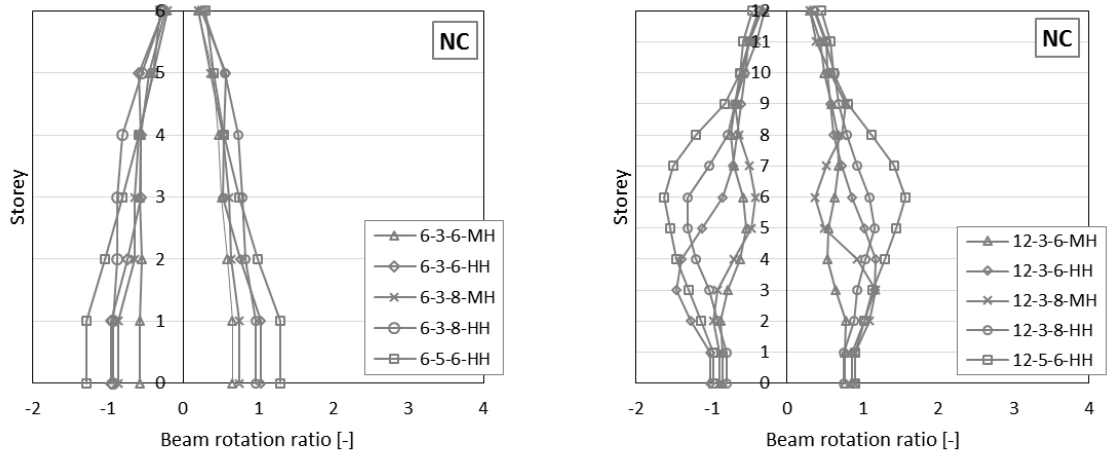

b) NC – Near Collapse Performance Level

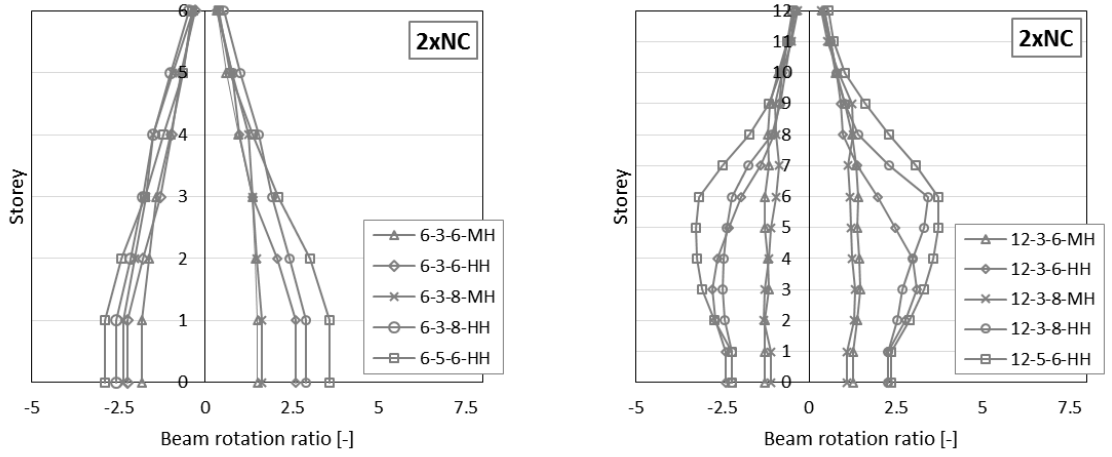

c) 2xNC – Two times Near Collapse Performance Level

Figure 5.9 – Median beam to yield beam rotation ratio for the three performance levels

The plots in Figure 5.9 summarize median beam to yield beam rotation ratio for the three performance levels and more detailed results showing beam rotation ratio for each record as well as mean beam rotation ratio are given in ANNEX 5. In order to estimate the seismic demand at the exterior, one-side beam-to-column joints in the frames, which are to be designed and tested, ductility demand is expressed in terms of beam rotation in the connection to yield beam rotation ratio.

As well as in the case of interstorey drift ration, 12-storey frames experience higher beam rotation comparing to 6-storey frames. Also the highest ratio in case of 6-storey frames is in the bottom of the building, while in case of 12-storey frames is located at mid-height.

At design performance level, rotation capacity of most of the frames is in elastic range.

6. CONCLUSIONS AND FUTURE WORK

In this thesis parametric study was carried out in order to address frame behaviour and seismic demand on beam-column connection of typical frame typologies. Focus was on Dual-Concentrically Braced Frames. Parameters that was chosen are level of seismic hazard, building height, span length and number of bays.

Frame behaviour was obtained carrying out modal and pushover analysis. The results are presented in form of pushover curves and schematic illustration of formed plastic hinges. Seismic performance and dynamic response were evaluated carrying out non-linear time history analysis (incremental dynamic analysis) at three performance levels: design (D), near collapse (NC) and twice near collapse (2xNC). The performance variables are defined as: (i) maximum interstorey drift ratio, (ii) residual interstorey drift ratio, (iii) maximum floor acceleration, and (iv) maximum beam rotation (at the exterior, one-side beam-column joints).

The main observation obtained from pushover analysis is sudden reduction in the lateral resistance when brace in compression buckles. This decrease is immediately followed by an increase of lateral stiffness. The mean V/V_d ratio is around 2.5. As this value is higher than 1.0 there is a space for future optimization of the structure.

The non-linear time history analysis shows that 12-storey frames have higher seismic demand comparing to 6-storey frames. Also frames designed for HH show higher seismic demand comparing to those designed for MH. MH frames have uniform pattern along height in term of seismic design, while HH in case of 6-storey frames seismic demand is decreasing from bottom to the top of the frame and in case of 12-storey frames highest seismic demand is in mid-height of the frame.

Future work will be focused on calibration of analysis parameters for pushover analysis in order to avoid numerical problems that occur when brace in compression buckles. This problems are manifested as deviation from pushover curve trend with sudden significant drops or increases.

Regarding seismic demand interstorey drift response histories will be extracted from available results at 2xNC performance level. The drift response histories will be post-processed and presented in term of series of cycles. This is the first step in order to define loading protocol [13].

From the point of view of the research project in the scope of which this thesis has been developed, the response of the frames at beam-column connection level will allow the definition of a new load protocol to be used in the experimental tests to be performed in connections.

REFERENCES

[1] EN 1993-1-8, *Eurocode 3: Design of steel structures - Part 1-8: Design of joints,* Brussels: CEN, 2004.

[2] EN 1998-1, *Eurocode 8: Design of structures for earthquake resistance - Part 1L General rules, seismic actions and rules for buildings,* Brussels: CEN, 2004.

[3] R. LANDOLFO , *EQUALJOINTS - European pre-QUALified steel JOINTS - Proposal Description,* Belgium: RFCS-Research fund for coal and steel, European commission.

[4] OpenSees, "Open System for Earthquake Engineering Simulation," [Online]. Available: http://opensees.berkeley.edu/.

[5] J. J. Bommer and R. Pinho, "Adapting earthquake actions in Eurocode 8 for performance-based seismic design," *Wiley InterScience,* 2005.

[6] T. Irvine, "http://www.vibrationdata.com/tutorials/ModalMass.pdf," 28 March 2013. [Online].

[7] D. Vamvatsikos and C. Cornell, "Incremental Dynamic ANalysis," 2002.

[8] "FEMA 356," in *5.5.2.2.2 Nonlinear Static Procedure* , November 2000 .

[9] A. Tsitos and A. Elghazouli, “Provisional Design of Prototype Buildings & Selection of Strong Motion Records,” Imperial College, London, 2014.

[10] R. P. Dhakal and K. Maekawa, “Path-dependent cyclic stress-strain relationship of reinforcing bar including nuskling,” *Engineering Structures,* no. 24, pp. 1383-1396, 2002.

[11] A. Gharakhanloo, “Distributed and Concentrated Inelasticity Beam-Column Elements used in Earthquake Engineering,” Norwegian University of Science and Technology, 2014.

[12] “ Open System for Earthquake Engineering Simulation software manual,” [Online]. Available: http://opensees.berkeley.edu/wiki/index.php/Getting_Started_with_OpenSees_--_Loads_and_Analysis.

[13] P. W. Richards and C.-M. Uang, “Testing Protocol for Short Links in Eccentrically Braced Frames,” *ASCE,* pp. 1183-1191, 2006.

[14] A. Tsitos and A. Elghazouil, “Recommendations for Modelling & Non-Linear Analysis,” Imperial College, London, 2014.

ANNEX 1

In this annex designed frame sections for examined frames are given

Table A 1 – **D-CBF-6-3-6-MH-a:** D-CBF, 6-storey, 3-bay, 6m span, PGA=0.25g

Storey	Ext.Column	Br. Column	Beam	Braced Beam	Brace
6	HE300B	HE300B	IPE360	HE360A	SHHF100x100x5
5	HE300B	HE300B	IPE360	HE400A	SHHF120x120x6.3
4	HE360B	HE360B	IPE360	HE450A	SHHF140x140x6.3
3	HE360B	HE360B	IPE360	HE450A	SHHF140x140x8
2	HE400B	HE400M	IPE360	HE500A	SHHF140x140x8
1	HE400B	HE400M	IPE360	HE500A	SHHF160x160x8

Table A 2 – **D-CBF-6-3-6-HH-a:** D-CBF, 6-storey, 3-bay, 6m span, PGA=0.35g

Storey	Ext.Column	Br. Column	Beam	Braced Beam	Brace
6	HE300B	HE300B	IPE360	HE400A	SHHF120x120x5
5	HE300B	HE300B	IPE360	HE450A	SHHF140x140x6.3
4	HE360B	HE360M	IPE360	HE550A	SHHF140x140x10
3	HE360B	HE360M	IPE360	HE550A	SHHF150x150x10
2	HE400B	H400x347	IPE360	HE600A	SHHF160x160x10
1	HE400B	H400x347	IPE360	HE600A	SHHF180x180x10

Table A 3 – **D-CBF-6-3-8-MH-a:** D-CBF, 6-storey, 3-bay, 8m span, PGA=0.25g

Storey	Ext.Column	Br. Column	Beam	Braced Beam	Brace
6	HE360B	HE360B	IPE360	HE450A	SHHF120x120x8
5	HE360B	HE360B	IPE360	HE500A	SHHF140x140x8
4	HE450B	HE450B	IPE360	HE550A	SHHF160x160x8
3	HE450B	HE450B	IPE360	HE550B	SHHF160x160x10
2	HE500B	H400x340	IPE360	HE600B	SHHF180x180x10
1	HE500B	H400x340	IPE360	HE600B	SHHF180x180x10

Table A 4 – **D-CBF-6-3-8-HH-a:** D-CBF, 6-storey, 3-bay, 8m span, PGA=0.35g

Storey	Ext.Column	Br. Column	Beam	Braced Beam	Brace
6	HE360B	HE360B	IPE360	HE450A	SHHF140x140x6
5	HE360B	HE360B	IPE360	HE500B	SHHF160x160x8
4	HE450B	HE450M	IPE360	HE500M	SHHF180x180x8
3	HE450B	HE450M	IPE360	HE550M	SHHF180x180x10
2	HE500B	H400x422	IPE360	HE600M	SHHF180x180x12.5
1	HE500B	H400x422	IPE360	HE600M	SHHF200x200x12.5

Table A 5 – **D-CBF-6-5-6-HH-a:** D-CBF, 6-storey, 5-bay, 6m span, PGA=0.35g

Storey	Ext./Int. Col.	Br. Column	Beam	Braced Beam	Brace
6	HE360B	HE360B	IPE360	HE400A	SHHF120x120x6
5	HE360B	HE360B	IPE360	HE500A	SHHF140x140x10
4	HE450B	HE400M	IPE400	HE550A	SHHF150x150x10
3	HE450B	HE400M	IPE400	HE550A	SHHF180x180x10
2	HE500B	H400x383	IPE450	HE600A	SHHF180x180x10
1	HE500B	H400x383	IPE450	HE600A	SHHF200x200x10

Table A 6 – **D-CBF-12-3-6-MH-a:** D-CBF, 12-storey, 3-bay, 6m span, PGA=0.25g

Storey	Ext.Column.	Br. Column	Beam	Braced Beam	Brace
12	HE360B	HE450B	IPE360	HE360A	SHHF100x100x5
11	HE360B	HE450B	IPE360	HE360A	SHHF100x100x8
10	HE360B	HE450B	IPE360	HE400A	SHHF120x120x8
9	HE400B	HE500B	IPE360	HE400A	SHHF120x120x8
8	HE400B	HE500B	IPE360	HE400A	SHHF140x140x8
7	HE400B	HE500B	IPE360	HE400A	SHHF140x140x8
6	HE450B	HE550M	IPE360	HE450A	SHHF140x140x10
5	HE450B	HE550M	IPE360	HE450A	SHHF140x140x10
4	HE450B	HE550M	IPE360	HE500A	SHHF150x150x10
3	HE500B	H400x463	IPE360	HE500A	SHHF150x150x10
2	HE500B	H400x463	IPE360	HE500A	SHHF150x150x10
1	HE500B	H400x463	IPE360	HE500B	SHHF160x160x10

Table A 7 – **D-CBF-12-3-6-HH-a:** D-CBF, 12-storey, 3-bay, 6m span, PGA=0.35g

Storey	Ext.Column.	Br. Column	Beam	Braced Beam	Brace
12	HE360B	HE450B	IPE360	HE360A	SHHF100x100x5
11	HE360B	HE450B	IPE360	HE400A	SHHF120x120x8
10	HE360B	HE450B	IPE360	HE400A	SHHF120x120x10
9	HE400B	HE500B	IPE360	HE450A	SHHF140x140x10
8	HE400B	HE500B	IPE360	HE450A	SHHF140x140x10
7	HE400B	HE500B	IPE360	HE500A	SHHF150x150x10
6	HE450B	H400x383	IPE360	HE500A	SHHF150x150x10
5	HE450B	H400x383	IPE360	HE500A	SHHF160x160x10
4	HE450B	H400x383	IPE360	HE500A	SHHF160x160x10
3	HE500B	H400x634	IPE360	HE500A	SHHF160x160x10
2	HE500B	H400x634	IPE360	HE500B	SHHF180x180x10
1	HE500B	H400x634	IPE360	HE500B	SHHF180x180x10

Table A 8 – **D-CBF-12-3-8-MH-a:** D-CBF, 12-storey, 3-bay, 8m span, PGA=0.25g

Storey	Ext.Column.	Br. Column	Beam	Braced Beam	Brace
12	HE360B	HE400B	IPE360	HE360B	SHHF120x120x6.3
11	HE360B	HE400B	IPE360	HE400B	SHHF140x140x8
10	HE360B	HE400B	IPE360	HE400B	SHHF140x140x8
9	HE400B	H400x237	IPE360	HE450B	SHHF140x140x10
8	HE400B	H400x237	IPE360	HE450B	SHHF150x150x10
7	HE400B	H400x237	IPE360	HE500B	SHHF160x160x10
6	HE450B	H400x393	IPE360	HE500B	SHHF180x180x10
5	HE450B	H400x393	IPE360	HE500B	SHHF180x180x10
4	HE450B	H400x393	IPE360	HE500B	SHHF180x180x10
3	HE500B	H400x593	IPE360	HE500B	SHHF180x180x10
2	HE500B	H400x593	IPE360	HE500B	SHHF180x180x10
1	HE500B	H400x593	IPE360	HE600B	SHHF180x180x12.5

Table A 9 – **D-CBF-12-3-8-HH-a:** D-CBF, 12-storey, 3-bay, 8m span, PGA=0.35g

Storey	Ext.Column.	Br. Column	Beam	Braced Beam	Brace
12	HE360B	HE400B	IPE360	HE450B	SHHF120x120x10
11	HE360B	HE400B	IPE360	HE500B	SHHF140x140x10
10	HE360B	HE400B	IPE360	HE500B	SHHF160x160x10
9	HE400B	H400x237	IPE360	HE550B	SHHF180x180x10
8	HE400B	H400x237	IPE360	HE550B	SHHF180x180x10
7	HE400B	H400x237	IPE360	HE600B	SHHF200x200x10
6	HE450B	H400x422	IPE360	HE600B	SHHF200x200x10
5	HE450B	H400x422	IPE360	HE600B	SHHF200x200x10
4	HE450B	H400x422	IPE360	HE600M	SHHF200x200x12.5
3	HE550B	H400x634	IPE360	HE600M	SHHF200x200x12.5
2	HE550B	H400x634	IPE360	HE600M	SHHF200x200x12.5
1	HE550B	H400x818	IPE360	HE600M	SHHF250x250x10

Table A 10 – **D-CBF-12-5-6-HH-a:** D-CBF, 12-storey, 5-bay, 6m span, PGA=0.35g

Storey	Ext./Int. Col.	Br. Column	Beam	Braced Beam	Brace
12	HE360B	HE450B	IPE360	HE360A	SHHF100x100x8
11	HE360B	HE450B	IPE360	HE450A	SHHF120x120x10
10	HE360B	HE450B	IPE360	HE450A	SHHF140x140x10
9	HE400B	HE500B	IPE400	HE500A	SHHF140x140x10
8	HE400B	HE500B	IPE400	HE500A	SHHF150x150x10
7	HE400B	HE500B	IPE400	HE500A	SHHF160x160x10
6	HE450B	H400x422	IPE450	HE500A	SHHF160x160x10
5	HE450B	H400x422	IPE450	HE500B	SHHF180x180x10
4	HE450B	H400x422	IPE450	HE500B	SHHF180x180x10
3	HE550M	H400x678	IPE500	HE500B	SHHF180x180x10
2	HE550M	H400x678	IPE500	HE550B	SHHF200x200x10
1	HE550M	H400x678	IPE500	HE550B	SHHF200x200x10

ANNEX 2

```
################################################################################
#                                EIGENVALUE  ANALYSIS
################################################################################
set nEigenI 1;                                  # mode i = 1
set nEigenJ 2;                                  # mode j = 2
set lambdaN [eigen [expr $nEigenJ]];            # eigenvalue analysis for nEigenJ modes
set lambdaI [lindex $lambdaN [expr 0]];         # eigenvalue mode i = 1
set lambdaJ [lindex $lambdaN [expr $nEigenJ-1]]; # eigenvalue mode j = 2
set pi   [expr 2.0*asin(1.0)];                  # Definition of pi
set w1 [expr pow($lambdaI,0.5)];                # w1 (1st mode circular frequency)
set w2 [expr pow($lambdaJ,0.5)];                # w2 (2nd mode circular frequency)
set T1  [expr 2.0*$pi/$w1];                     # 1st mode period of the structure
set T2  [expr 2.0*$pi/$w2];                     # 2nd mode period of the structure

# Create a recorder to monitor eigen modes
recorder Node -file Eigen/eigen1.out -node 1010 1020 1030 1040 1050 1060 -dof 1 "eigen 1"
recorder Node -file Eigen/eigen2.out -node 1010 1020 1030 1040 1050 1060 -dof 1 "eigen 2"

# Do 1 step of transient analysis for recorders to work
set tol 1e-7
set maxNumIter 10
set testtype NormDispIncr
test $testtype $tol $maxNumIter 1;
system BandGeneral
constraints Transformation
numberer Plain
algorithm Newton
integrator Newmark 0.5 0.25
analysis Transient
analyze 1 0.1

puts "T1 = $T1 s"
puts "T2 = $T2 s"

# create display  for mode shapes
# command: recorder display $windowTitle $xLoc $yLoc $xPixels $yPixels
```

```
set h 0;
recorder display "Mode Shape 1"   10    510    400     400  -wipe
prp $h $h 1;
vup  0  1 0;
vpn  0  0 1;
display -1 1 20000;

recorder display "Mode Shape 2"  610         10         400       400   -wipe
prp $h $h 1;
vup  0  1 0;
vpn  0  0 1;
display -2 1 20000;

wipe all
```

ANNEX 3

```
#########################################################################
#                          STATIC PUSHOVER ANALYSIS
#########################################################################
If {$analysisType == "pushover"} {
        puts "Running Pushover..."
# create load pattern for lateral pushover load
set Hload $MIntFloors;                  # define the lateral load as a proportion of
                                          the weight so that the pseudo time equals
                                          the lateral-load coefficient when using linear
                                          load pattern
pattern Plain 200 Linear {;             # define load pattern -- generalized
        load    1010    [expr 0.073*$Hload] 0.0     0.0;
        load    1020    [expr 0.161*$Hload] 0.0     0.0;
        load    1030    [expr 0.262*$Hload] 0.0     0.0;
        load    1040    [expr 0.371*$Hload] 0.0     0.0;
        load    1050    [expr 0.479*$Hload] 0.0     0.0;
        load    1060    [expr 0.500*$Hload] 0.0     0.0;
}

# parameters that are particular to the model
set     IDctrlNode      1060;           # node where displacement is read for
                                          displacement control
set     IDctrlDOF       1;              # degree of freedom of displacement
                                          read for displacement control
set     Dmax    [expr   0.1*$HBuilding]; # maximum displacement of pushover
set     Dincr   5;                      # displacement increment for pushover

# analysis parameters
constraints     Plain;
numberer        RCM;
system BandGeneral
set     Tol     1.e-9;                  # Convergence Test: tolerance
set     maxNumIter  6;                  # Convergence Test: maximum number of
                                          iterations that will be performed before
                                          "failure to converge" is returned
```

```
set     printFlag       0;                      # Convergence Test: flag used to print
                                                  information on convergence (optional)
set     TestType        EnergyIncr      ;       # Convergence Test type
test    $TestType       $Tol    $maxNumIter $printFlag;
set     algorithmType           ModifiedNewton
algorithm       $algorithmType;
integrator      DisplacementControl             $IDctrlNode     $IDctrlDOF      $Dincr

analysis        Static

# perform static pushover analysis
set     Nsteps [expr    int($Dmax/$Dincr)];
set     ok      [analyze        $Nsteps];       # will return 0 if no convergence problems

# in case of convergence problems
if      {$ok    !=      0}      {
# change some analysis parameters to achieve convergence
# performance is slower inside this loop
        set     ok      0;
        set     controlDisp     0.0;    # start from zero
        set     D0      0.0;            # start from zero
        set     Dstep   [expr   ($controlDisp-$D0)/($Dmax-$D0)]
        while   {$Dstep         <       1.0     &&      $ok     ==      0}      {
                set     controlDisp     [nodeDisp       $IDctrlNode     $IDctrlDOF      ]
                set     Dstep   [expr   ($controlDisp-$D0)/($Dmax-$D0)]
                set     ok      [analyze        1       ]
                if      {$ok    !=      0}      {
                        puts    "TryingNewton with Initial Tangent .."
                        test    NormDispIncr $Tol       2000    5
                        algorithm       Newton          -initial
                        set     ok      [analyze        1       ]
                        test    $TestType       $Tol    $maxNumIter             0
                        algorithm       $algorithmType
                }
                if      {$ok    !=      0}      {
                        puts    "TryingBroyden          .."
                        algorithm       Broyden         8
                        set     ok      [analyze        1       ]
                        algorithm       $algorithmType
                }
                if      {$ok    !=      0}      {
                        puts    "TryingNewtonWithLineSearch         .."
                        algorithm       NewtonLineSearch        .8

                        set     ok      [analyze        1       ]
```

```
                    algorithm       $algorithmType
                }
        }
        };                                  # end if ok !0

puts    "DonePushover"
}

wipe    all;
```

ANNEX 4

```
################################################################################
#                                    TIME  HISTORY  ANALYSIS
################################################################################
if {$analysisType == "dynamic"} {
        puts "Running dynamic analysis..."
# RAYLEIGH damping parameters
        set xDamp 0.02; # damping ratio
        set betaKcomm [expr 2.*$xDamp*$T1/(2.*$pi)];
#assign tangent stifness proportional damping to columns, beams, braces and gusset plate of a braced frame
# columns
region  1 -ele 110101 110102 110201 110202 110301 110302 110401 110402 110501 110502 110601 110602 -rayleigh 0. 0. 0. $betaKcomm;
region  2 -ele 120101 120102 120201 120202 120301 120302 120401 120402 120501 120502 120601 120602 -rayleigh 0. 0. 0. $betaKcomm;
region  3 -ele 130101 130102 130201 130202 130301 130302 130401 130402 130501 130502 130601 130602 -rayleigh 0. 0. 0. $betaKcomm;
region  4 -ele 140101 140102 140201 140202 140301 140302 140401 140402 140501 140502 140601 140602 -rayleigh 0. 0. 0. $betaKcomm;
# bemas
region  5 -ele 20101 20102 20103 20104 -rayleigh 0. 0. 0. $betaKcomm;
region  6 -ele 20201 20202 20203 20204 -rayleigh 0. 0. 0. $betaKcomm;
region  7 -ele 20301 20302 20303 20304 -rayleigh 0. 0. 0. $betaKcomm;
region  8 -ele 20401 20402 20403 20404 -rayleigh 0. 0. 0. $betaKcomm;
region  9 -ele 20501 20502 20503 20504 -rayleigh 0. 0. 0. $betaKcomm;
region 10 -ele 20601 20602 20603 20604 -rayleigh 0. 0. 0. $betaKcomm;
# braces
region 11 -ele 30102 30103 30106 30107  -rayleigh 0. 0. 0. $betaKcomm;
region 12 -ele 30202 30203 30206 30207  -rayleigh 0. 0. 0. $betaKcomm;
region 13 -ele 30302 30303 30306 30307  -rayleigh 0. 0. 0. $betaKcomm;
region 14 -ele 30402 30403 30406 30407  -rayleigh 0. 0. 0. $betaKcomm;
region 15 -ele 30502 30503 30506 30507  -rayleigh 0. 0. 0. $betaKcomm;
region 16 -ele 30602 30603 30606 30607  -rayleigh 0. 0. 0. $betaKcomm;
# define ground motion parameters
        set patternID 1;
```

```
	set GMdirection 1;
	set GMfile "R-00127T.tcl";
	set dt 0.005;
	set Scalefact [expr 1.0*7.5509];
	set TotalNumberOfSteps 7769;
	set GMtime [expr $dt*$TotalNumberOfSteps + 20.0];
# define the acceleration series for the ground motion
	set accelSeries "Series -dt $dt -filePath $GMfile -factor [expr $Scalefact*$g]";
# create load pattern: apply acceleration to all fixed nodes with UniformExcitation
	pattern UniformExcitation $patternID $GMdirection -accel $accelSeries;
# define dynamic analysis parameters
	set dt_analysis 0.005;
	wipeAnalysis;
	set NumSteps [expr round(($GMtime + 0.0)/$dt_analysis)];
# dynamic-analysis parameters
	constraints	Transformation;
	numbered	RCM;
	system		UmfPack;
	variable	TolDynamic 1.e-7;
	variable	 maxNumIterDynamic 10;
	variable	printFlagDynamic 0;
	variable	testTypeDynamic EnergyIncr;
	test	$testTypeDynamic $TolDynamic $maxNumIterDynamic $printFlagDynamic;
	# for improved-convergence procedure:
	variable	maxNumIterConvergeDynamic 200;
	variable	printFlagConvergeDynamic 0;
	variable	 algorithmTypeDynamic ModifiedNewton
	algorithm	$algorithmTypeDynamic;
	integrator	TRBDF2
	analysis	VariableTransient  $NumSteps  $dt_analysis 0.00001 $dt_analysis
# perform the dynamic analysis and display whether analysis was successful
	set ok [analyze $NumSteps $dt_analysis];    # ok = 0 if analysis was completed
	if {$ok == 0} {
		puts "Dynamic analysis complete";
	} else {
		puts "Dynamic analysis did not converge";
	}
# ---------------------------------------------------------------------------------------------------------------------
# change some analysis parameters to achieve convergence
# performance is slower inside this loop
# Time-controlled analysis
set ok 0;
set controlTime [getTime];
while {$controlTime < $GMtime && $ok == 0} {
set controlTime [getTime]
set ok [analyze 1 $dt_analysis]
```

```
if {$ok != 0} {
puts "Trying Newton with Initial Tangent .."
test NormDispIncr $TolDynamic 1000 0
algorithm Newton -initial
set ok [analyze 1 $dt_analysis]
test $testTypeDynamic $TolDynamic $maxNumIterDynamic 0
algorithm $algorithmTypeDynamic
}
if {$ok != 0} {
puts "Trying Broyden .."
algorithm Broyden 8
set ok [analyze 1 $dt_analysis]
algorithm $algorithmTypeDynamic
}
if {$ok != 0} {
puts "Trying NewtonWithLineSearch .."
algorithm NewtonLineSearch .6
set ok [analyze 1 $dt_analysis]
algorithm $algorithmTypeDynamic
}
if {$ok != 0} {
puts "Trying ModifiedNewton .."
algorithm ModifiedNewton
set ok [analyze 1 $dt_analysis]
algorithm $algorithmTypeDynamic
}
if {$ok != 0} {
puts "Trying BFGS.."
algorithm BFGS
set ok [analyze 1 $dt_analysis]
algorithm $algorithmTypeDynamic
}
}
}; # end if ok !0

set currentTime [getTime];    # get current analysis time     (after dynamic analysis)
puts "The current time is: $currentTime";
if {$currentTime >= $GMtime}         {
          puts "Dynamic analysis complete";
} else {
          puts "Dynamic analysis did not converge";
}
wipe all;
```

ANNEX 5

In this annex are given graph that show seismic demand at each performance level for all 7 applied accelerograms, as well as mean value.

Peak storey acceleration

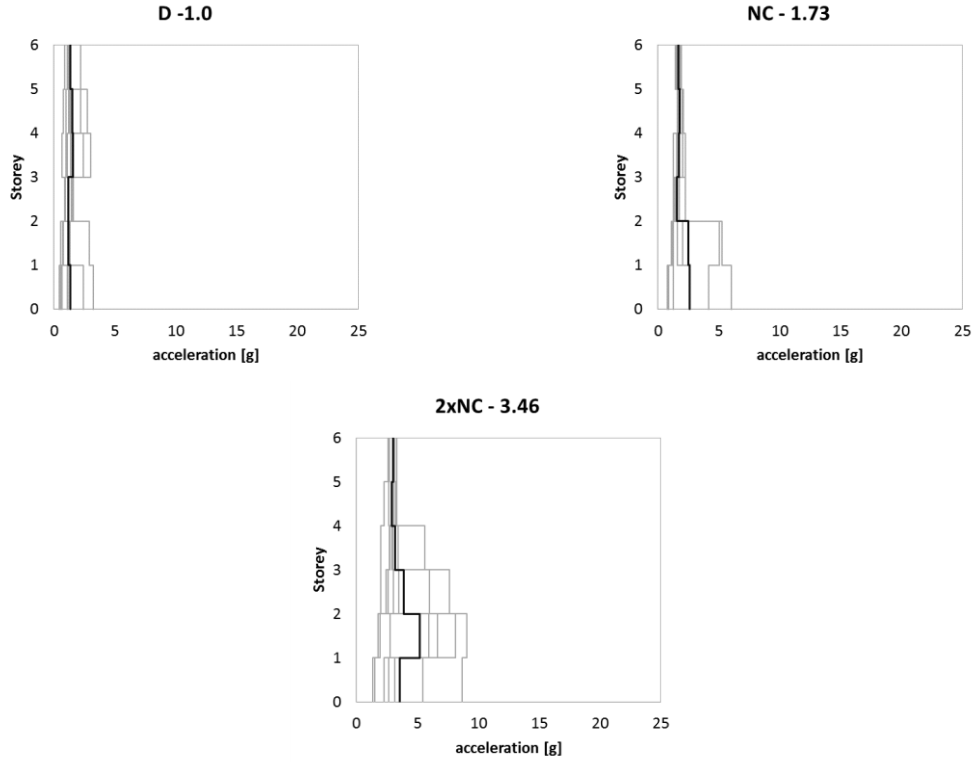

Figure A 1 – Peak storey acceleration for **D-CBF-6-3-6-MH-a**

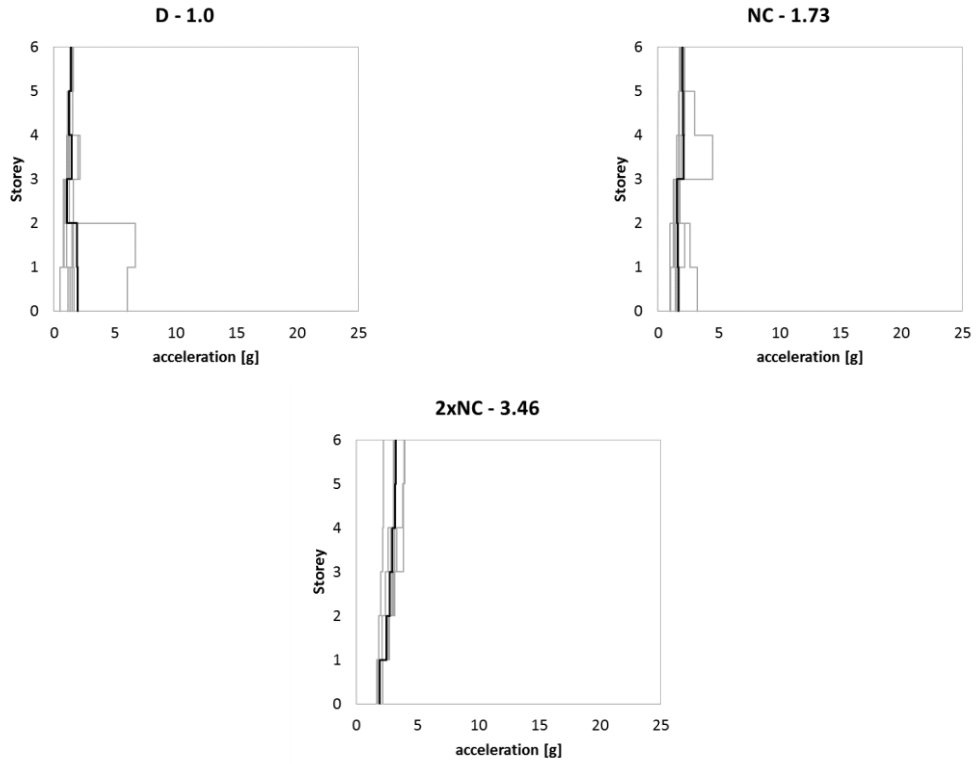

Figure A 2 – Peak storey acceleration for **D-CBF-6-3-6-HH-a**

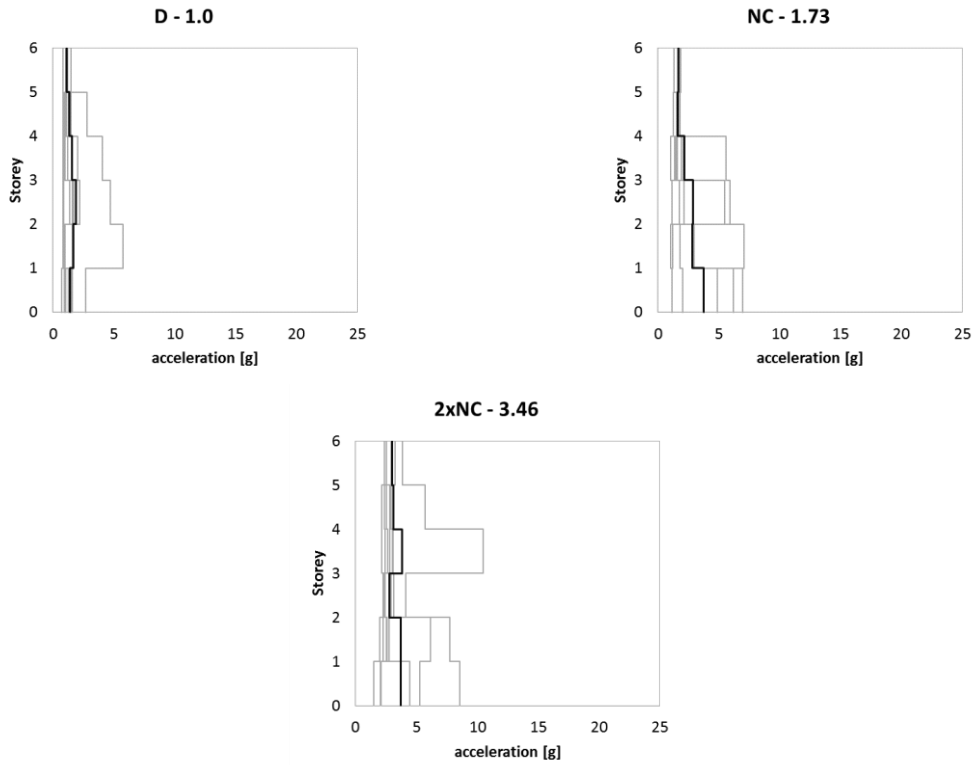

Figure A 3 – Peak storey acceleration for **D-CBF-6-3-8-MH-a**

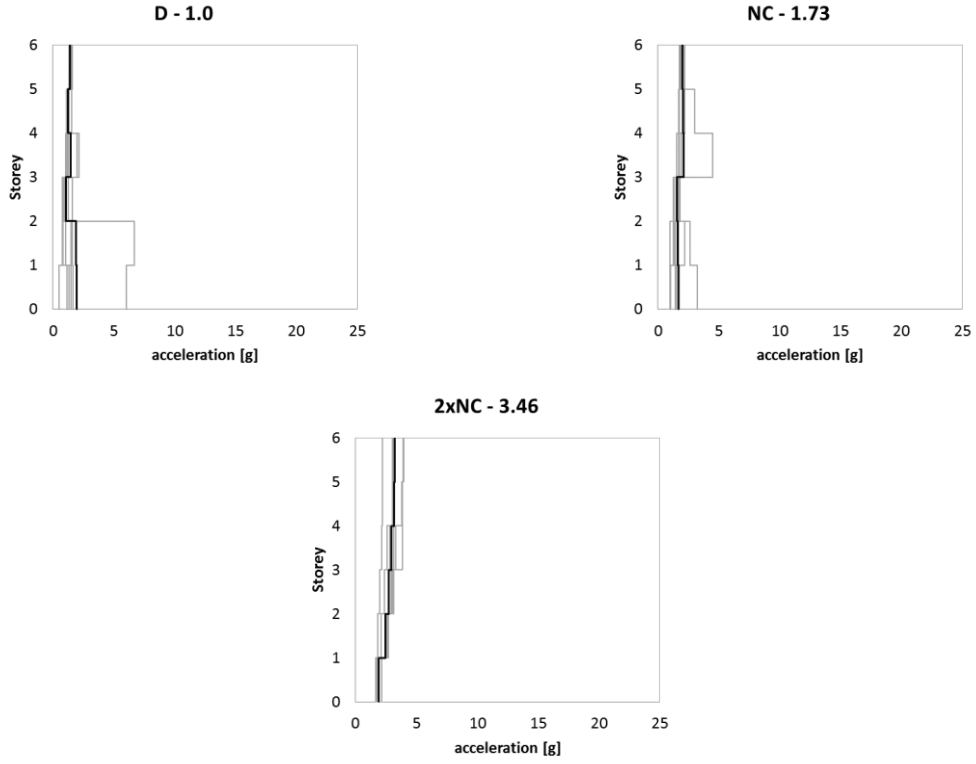

Figure A 4 – Peak storey acceleration for **D-CBF-6-3-8-HH-a**

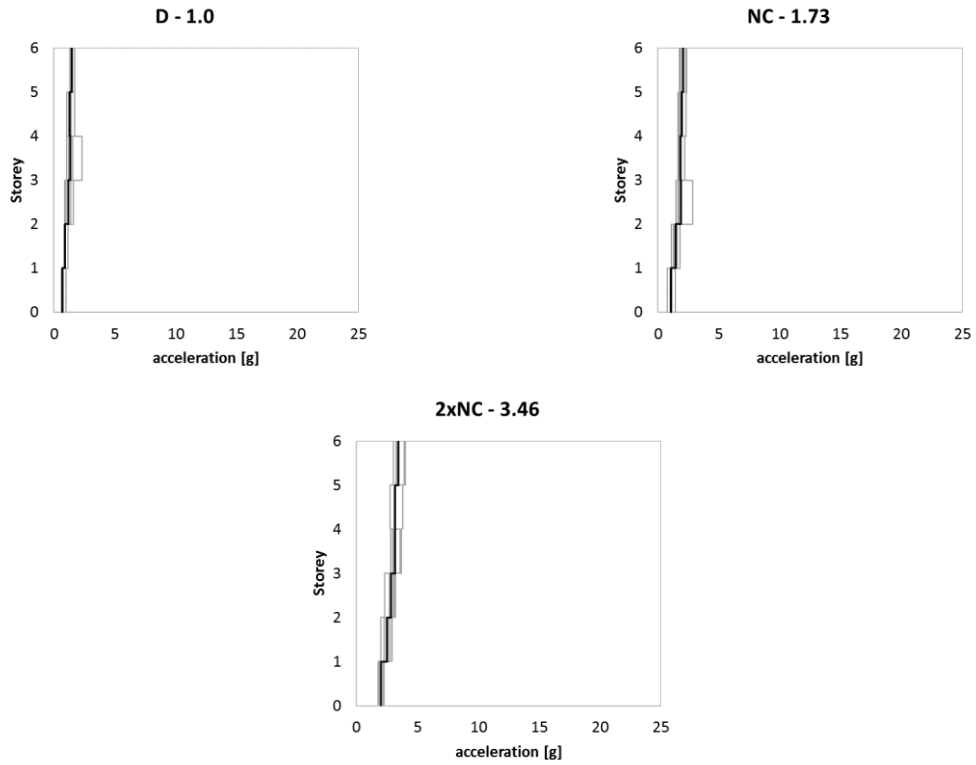

Figure A 5 – Peak storey acceleration for **D-CBF-6-5-6-HH-a**

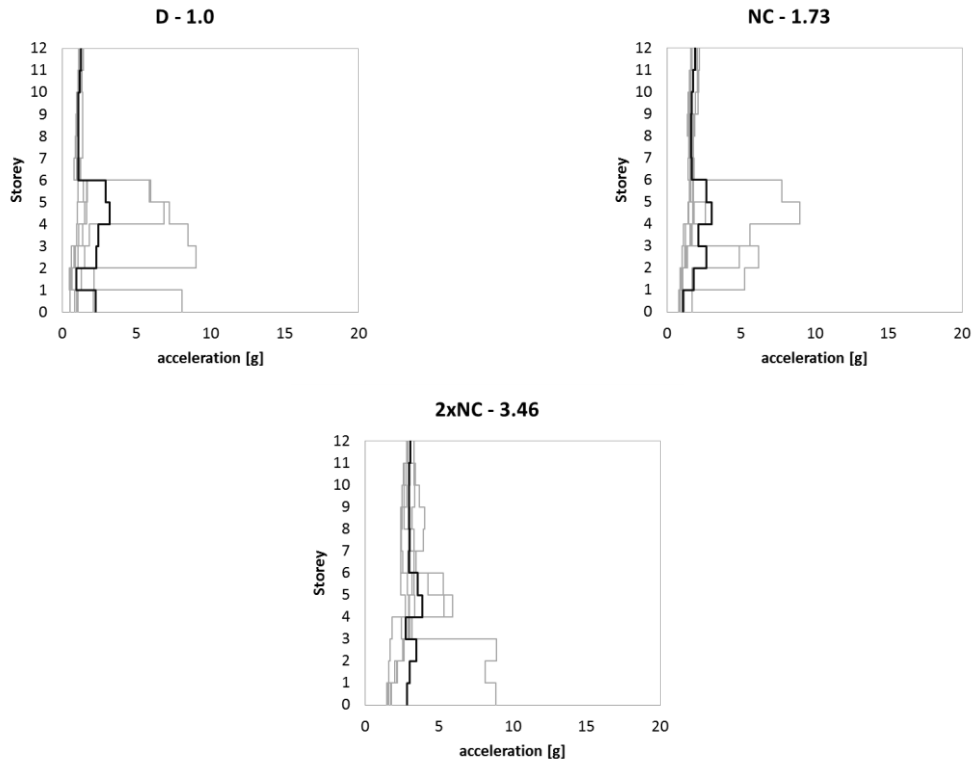

Figure A 6 – Peak storey acceleration for **D-CBF-12-5-6-HH-a**

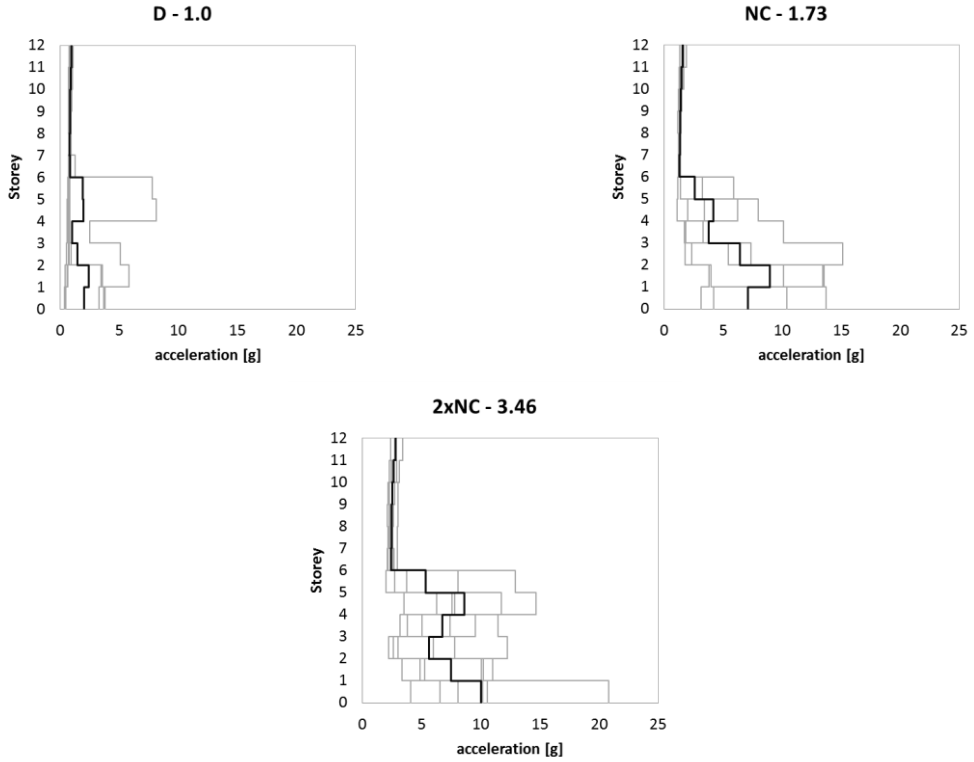

Figure A 7 – Peak storey acceleration for **D-CBF-12-3-6-MH-a**

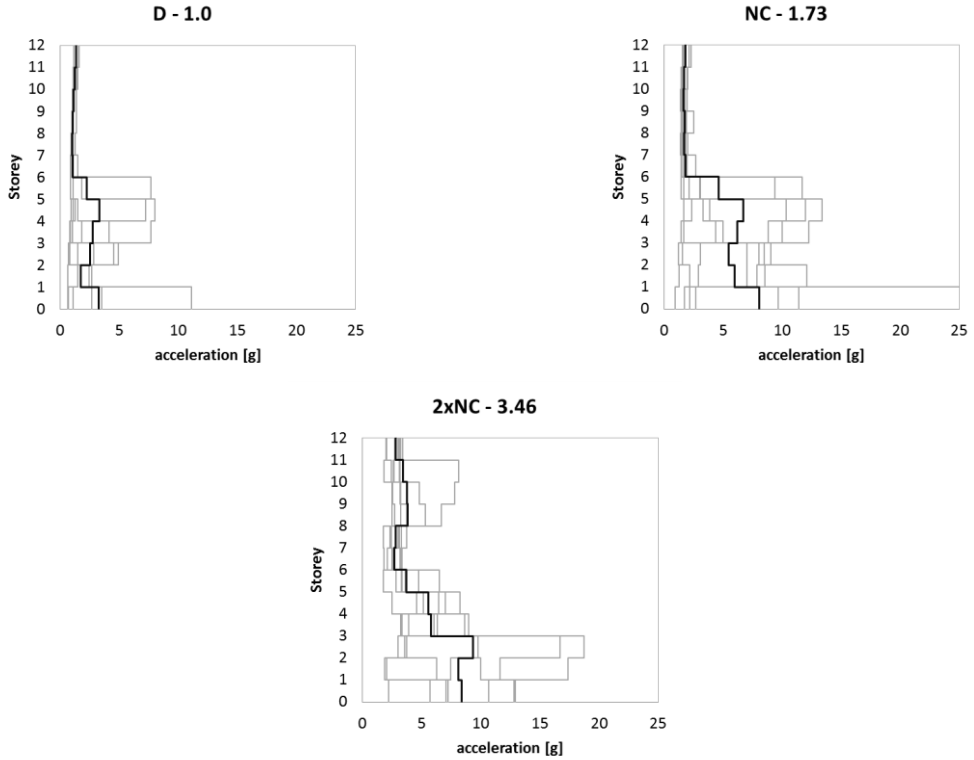

Figure A 8 – Peak storey acceleration for **D-CBF-12-3-6-HH-a**

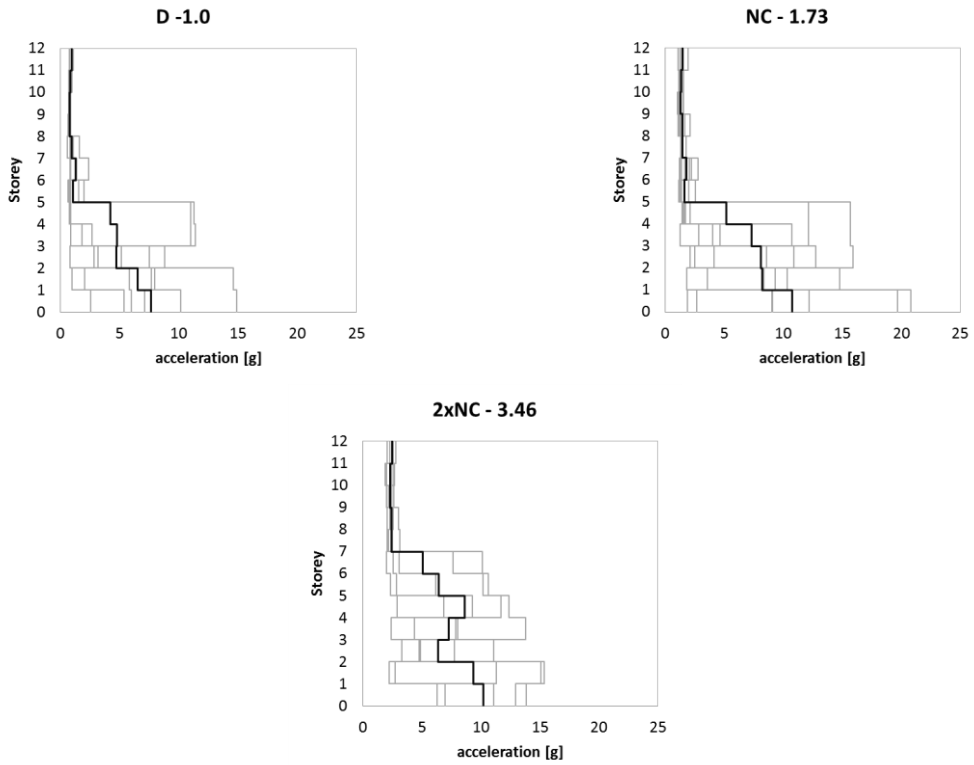

Figure A 9 – Peak storey acceleration for **D-CBF-12-3-8-MH-a**

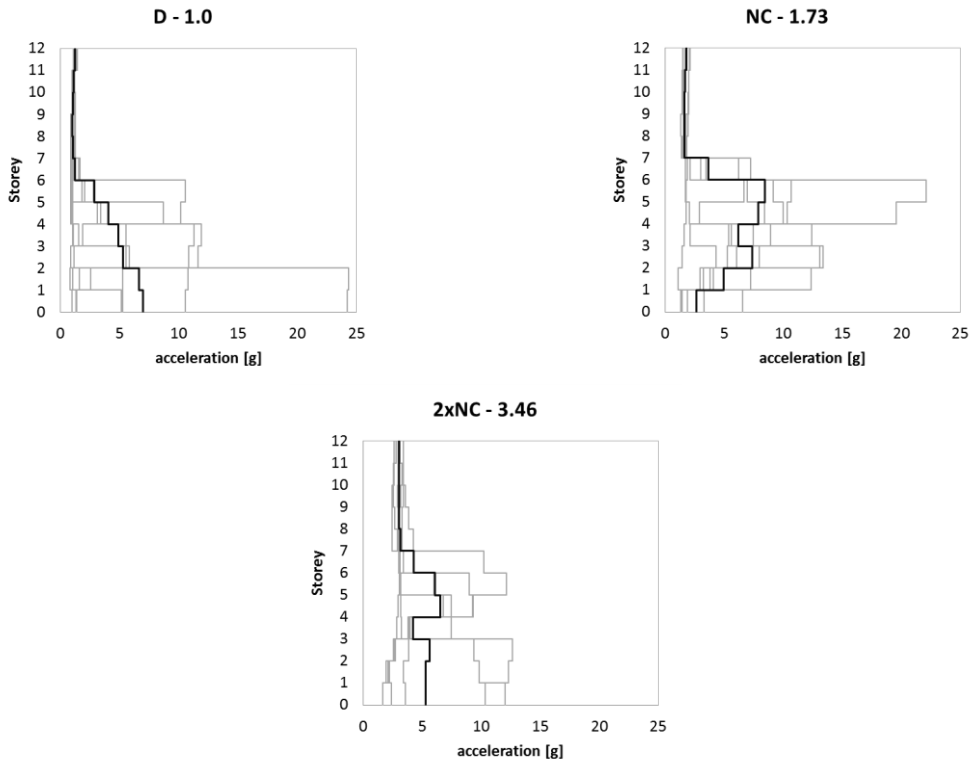

Figure A 10 – Peak storey acceleration for **D-CBF-12-3-8-HH-a**

Peak interstorey drift ratio

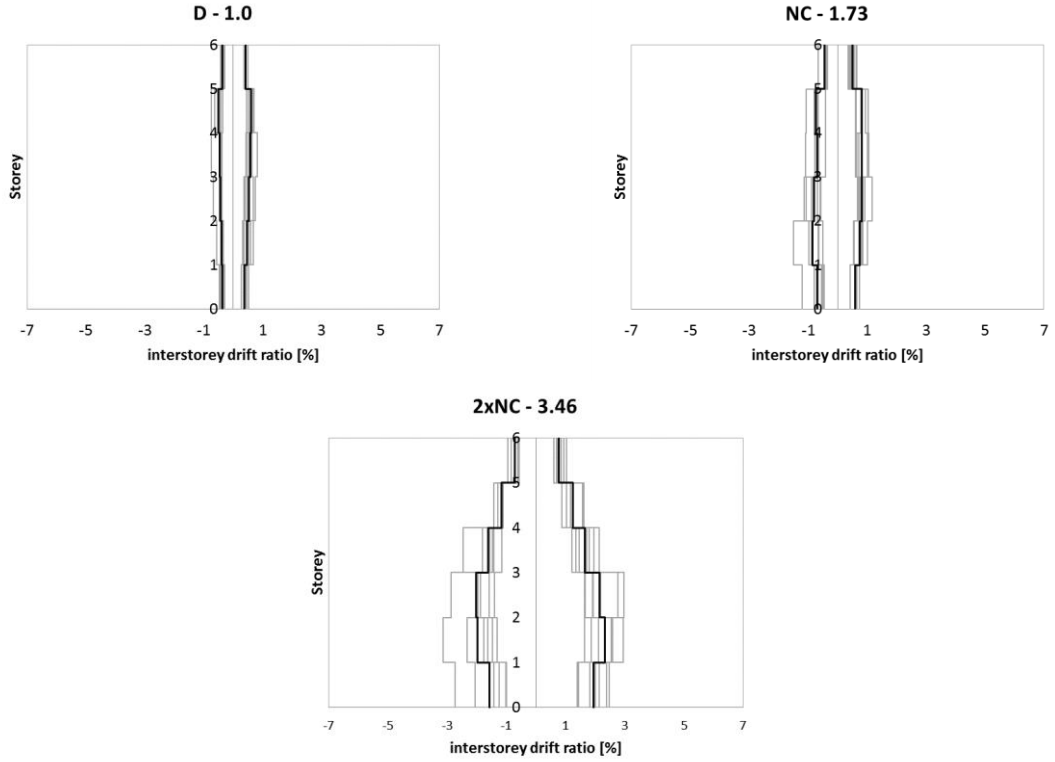

Figure A 11 – Peak interstorey drift ratio for **D-CBF-6-3-6-MH-a**

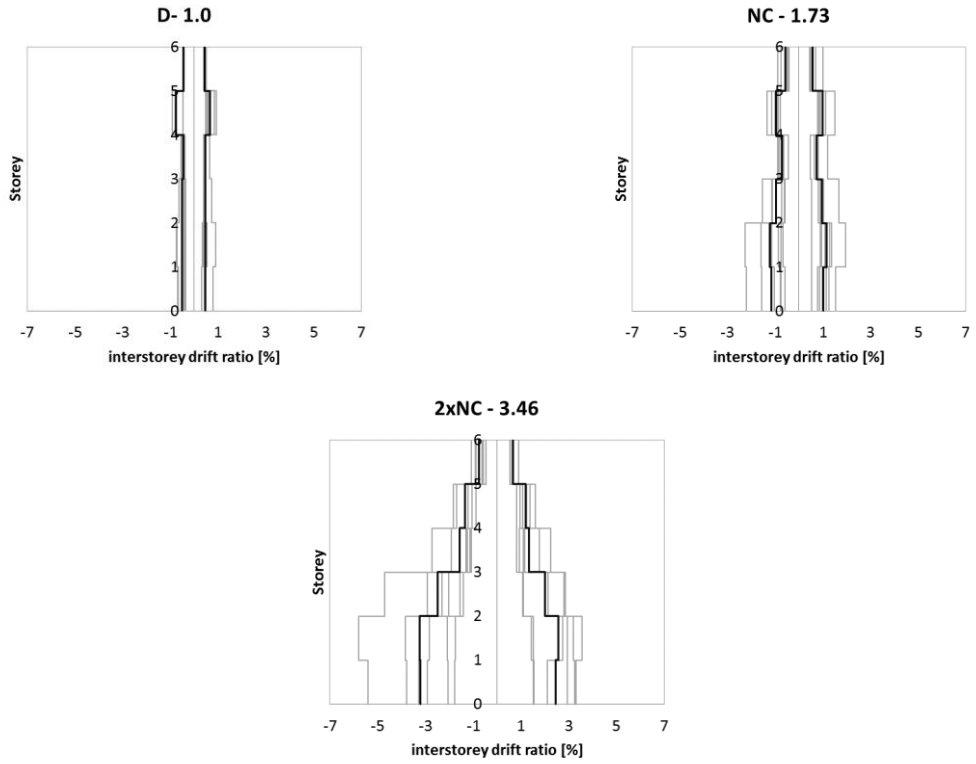

Figure A 12 – Peak interstorey drift ratio for **D-CBF-6-3-6-HH-a**

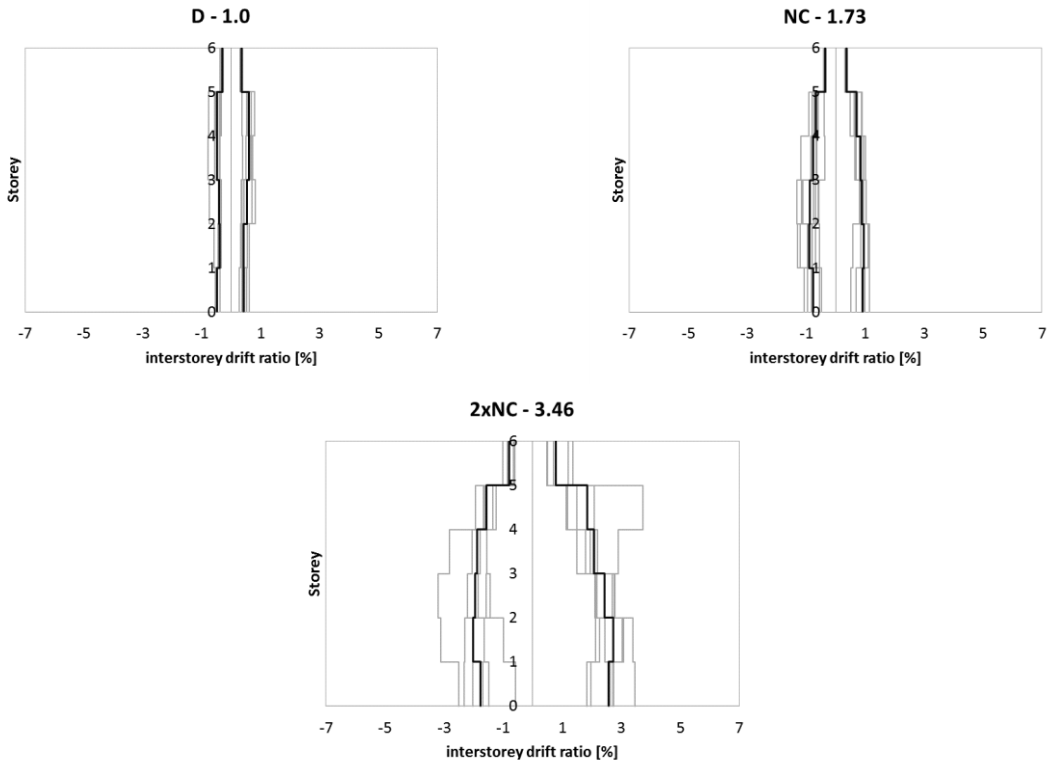

Figure A 13 – Peak interstorey drift ratio for **D-CBF-6-3-8-MH-a**

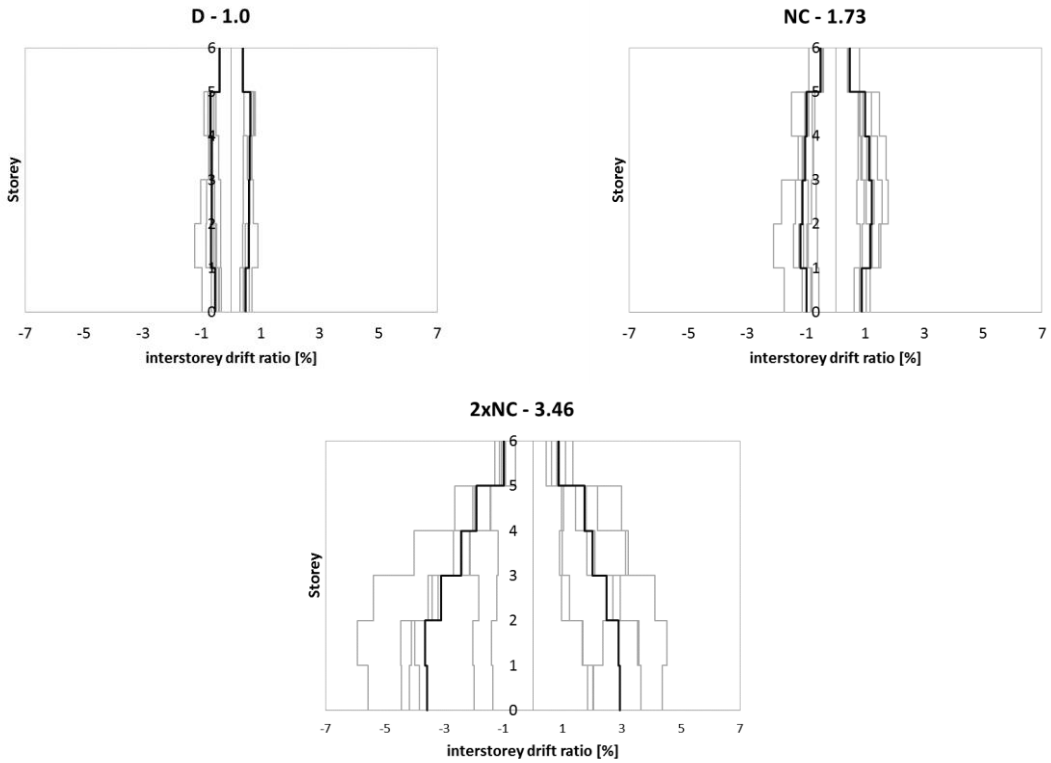

Figure A 14 – Peak interstorey drift ratio for **D-CBF-6-3-8-HH-a**

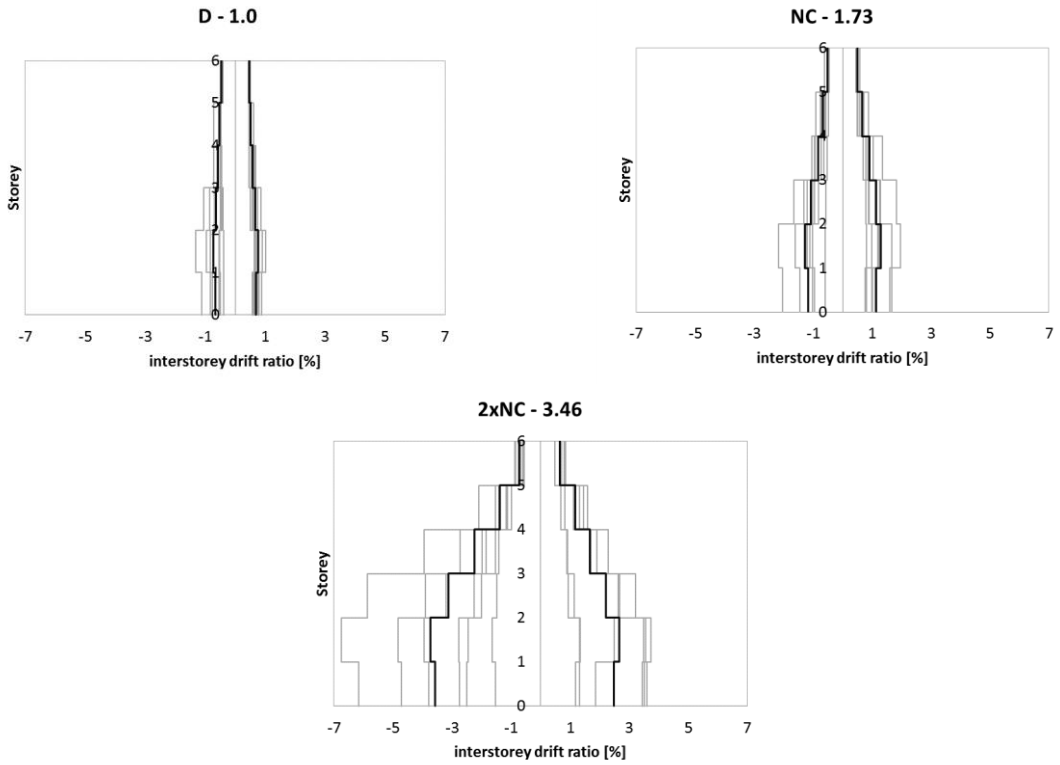

Figure A 15 – Peak interstorey drift ratio for **D-CBF-6-5-6-HH-a**

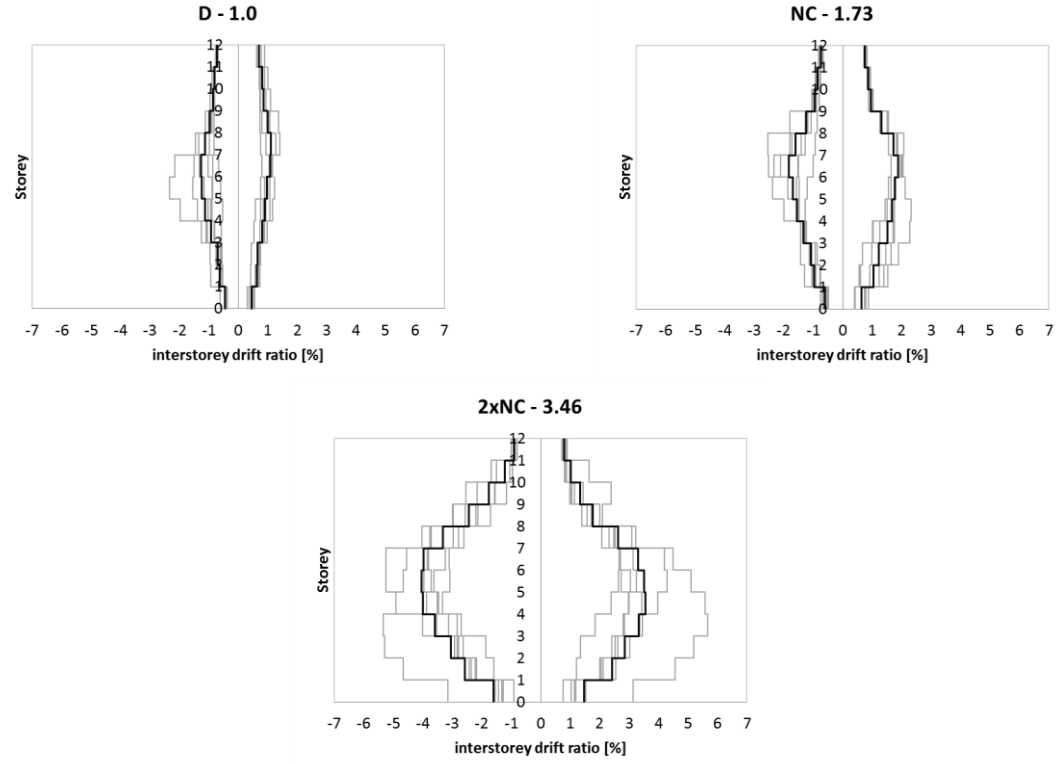

Figure A 16 – Peak interstorey drift ratio for **D-CBF-12-5-6-HH-a**

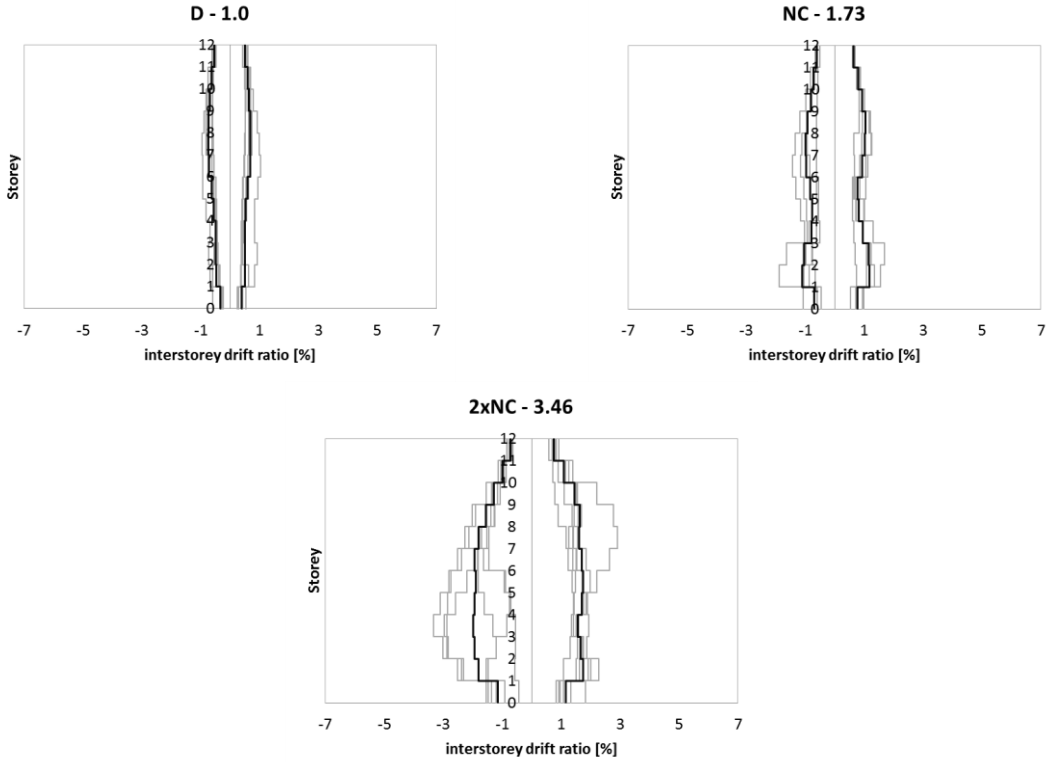

Figure A 17 – Peak interstorey drift ratio for **D-CBF-12-3-6-MH-a**

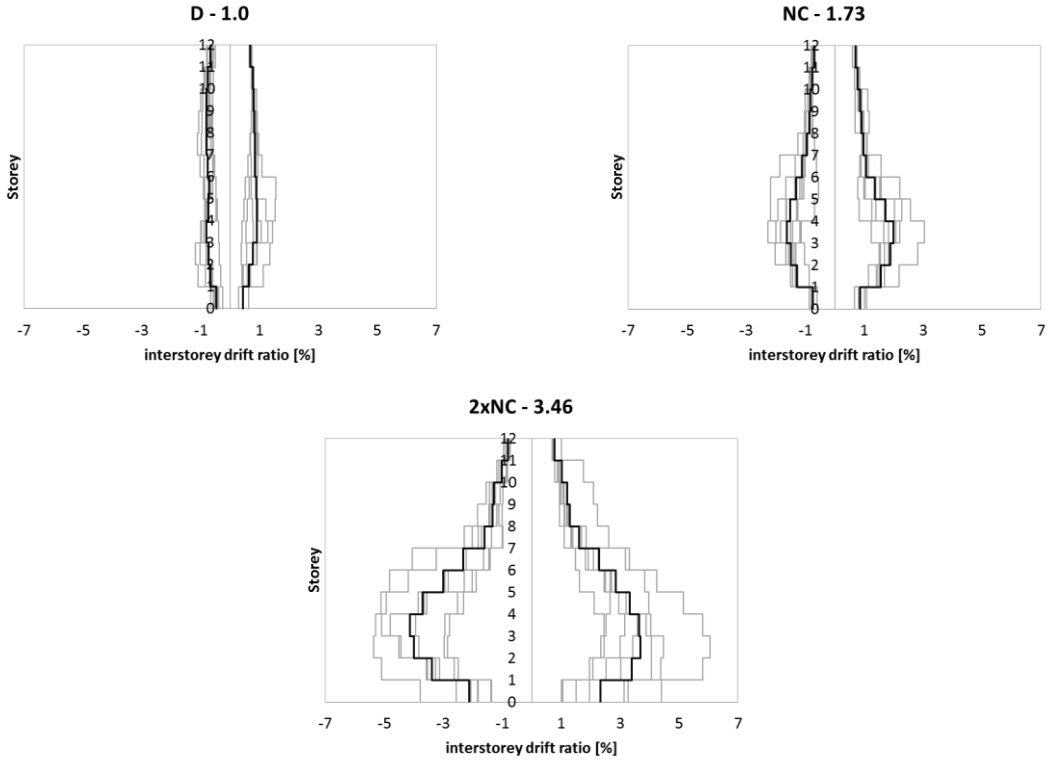

Figure A 18 – Peak interstorey drift ratio for **D-CBF-12-3-6-HH-a**

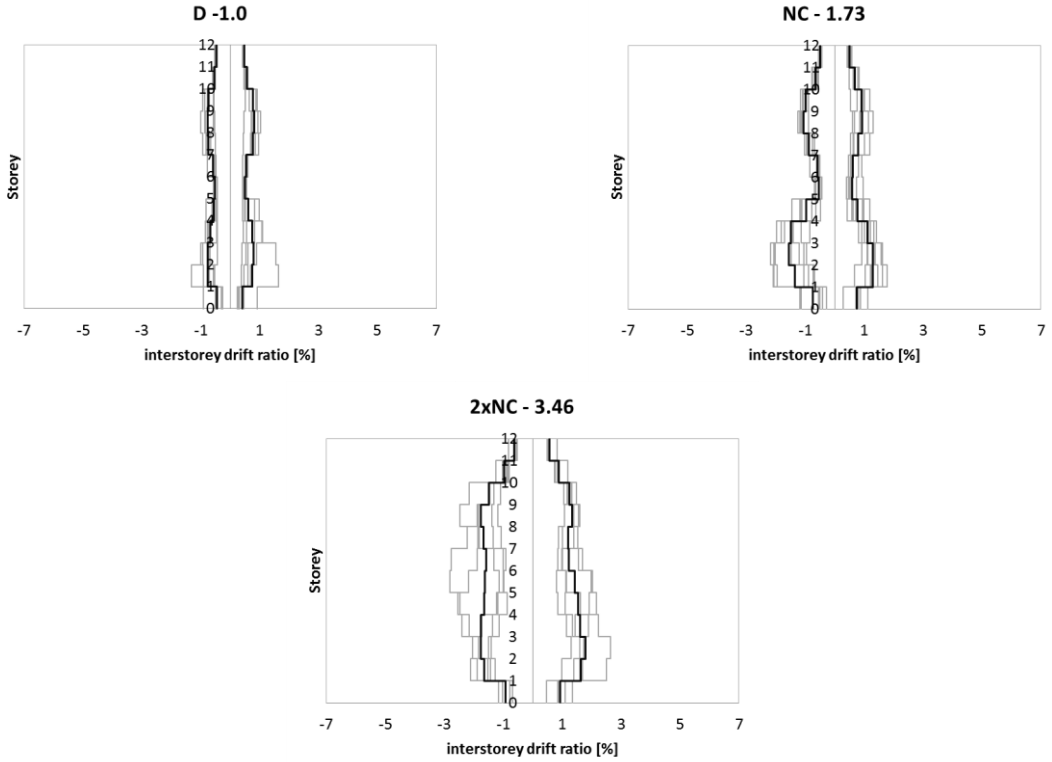

Figure A 19 – Peak interstorey drift ratio for **D-CBF-12-3-8-MH-a**

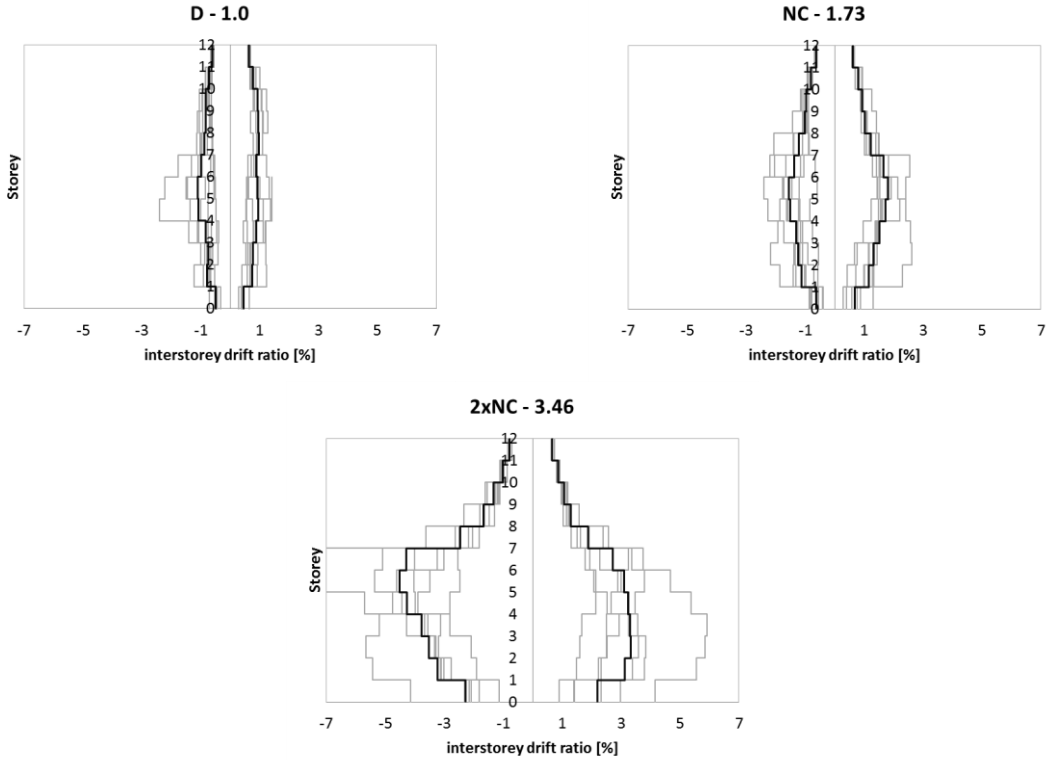

Figure A 20 – Peak interstorey drift ratio for **D-CBF-12-3-8-HH-a**

Residual interstorey drift ratio

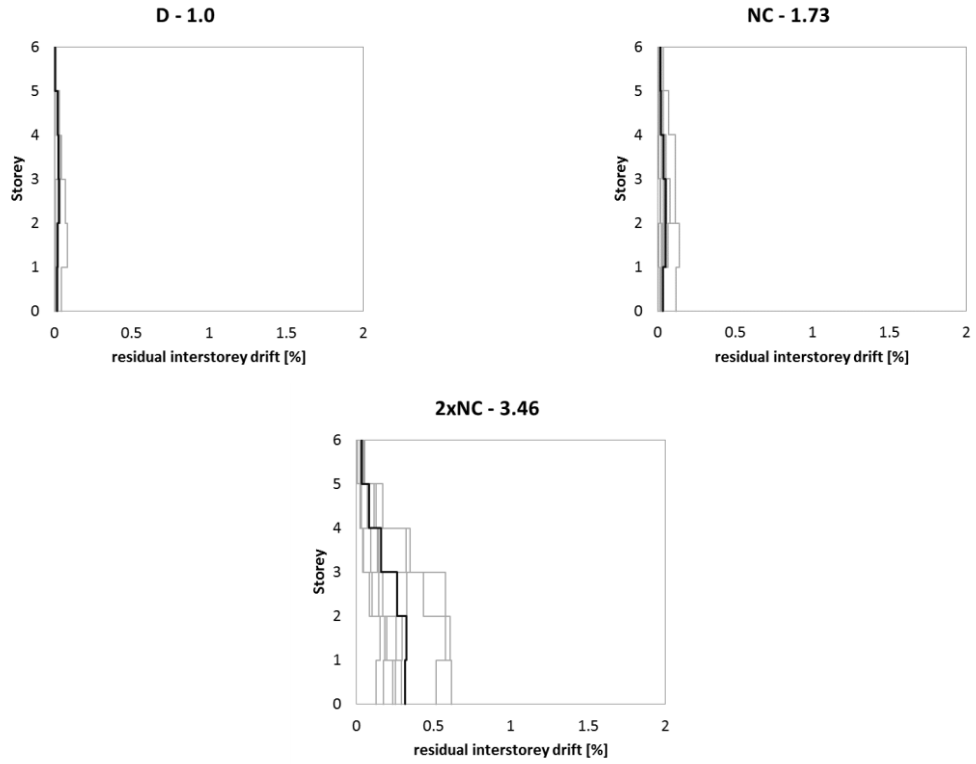

Figure A 21 – Residual interstorey drift ratio for **D-CBF-6-3-6-MH-a**

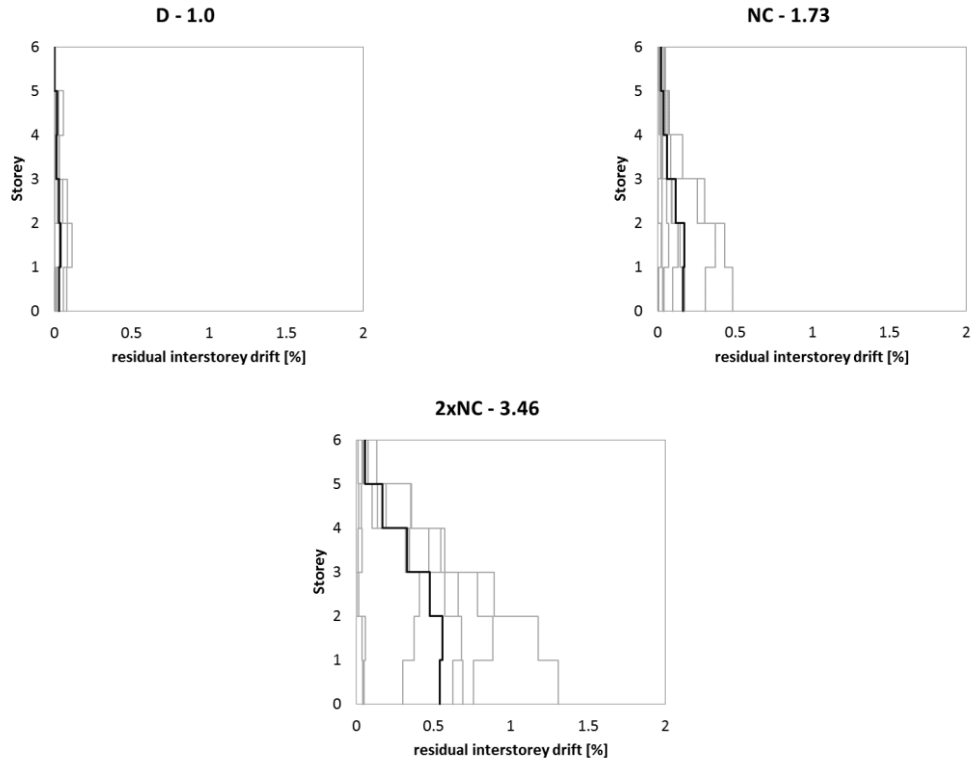

Figure A 22 – Residual interstorey drift ratio for **D-CBF-6-3-6-HH-a**

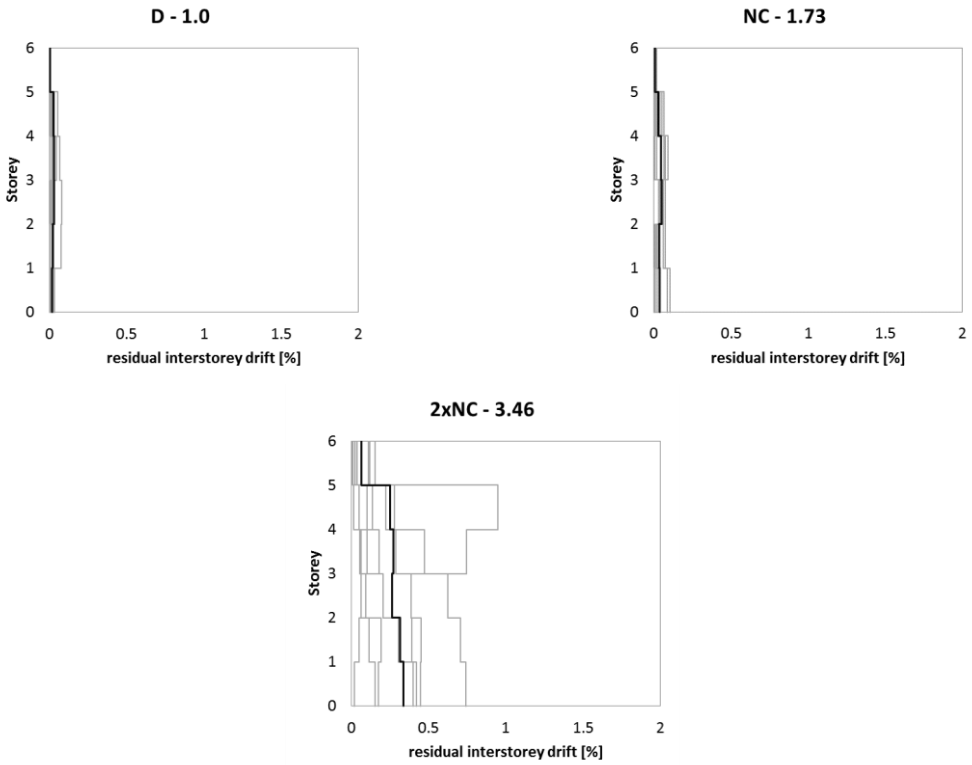

Figure A 23 – Residual interstorey drift ratio for **D-CBF-6-3-8-MH-a**

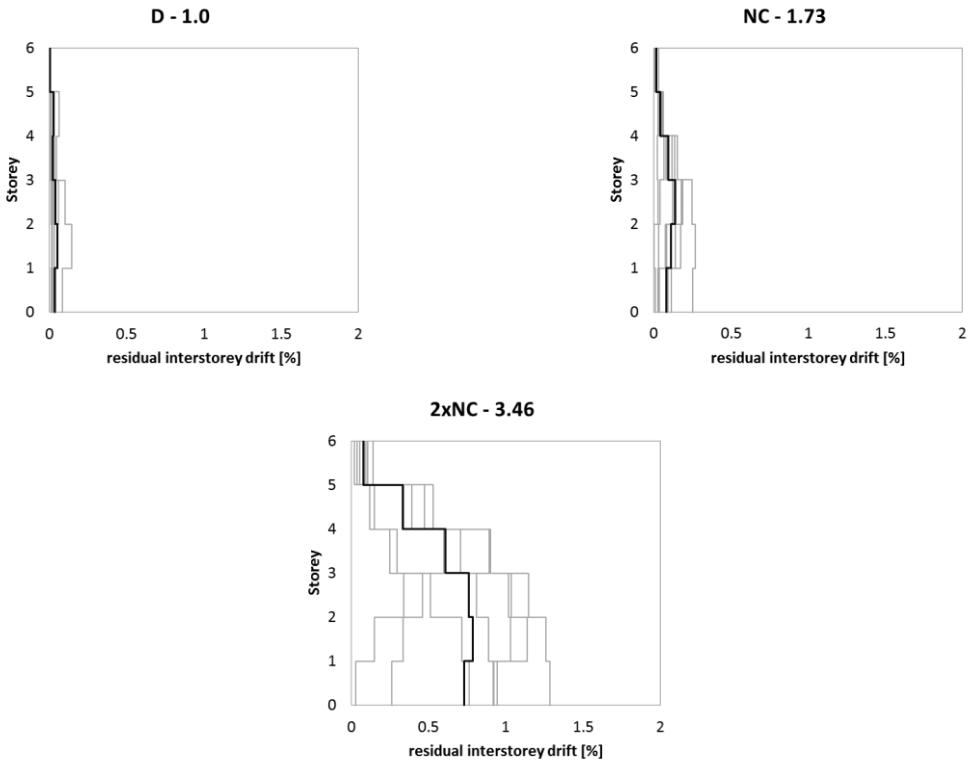

Figure A 24 – Residual interstorey drift ratio for **D-CBF-6-3-8-HH-a**

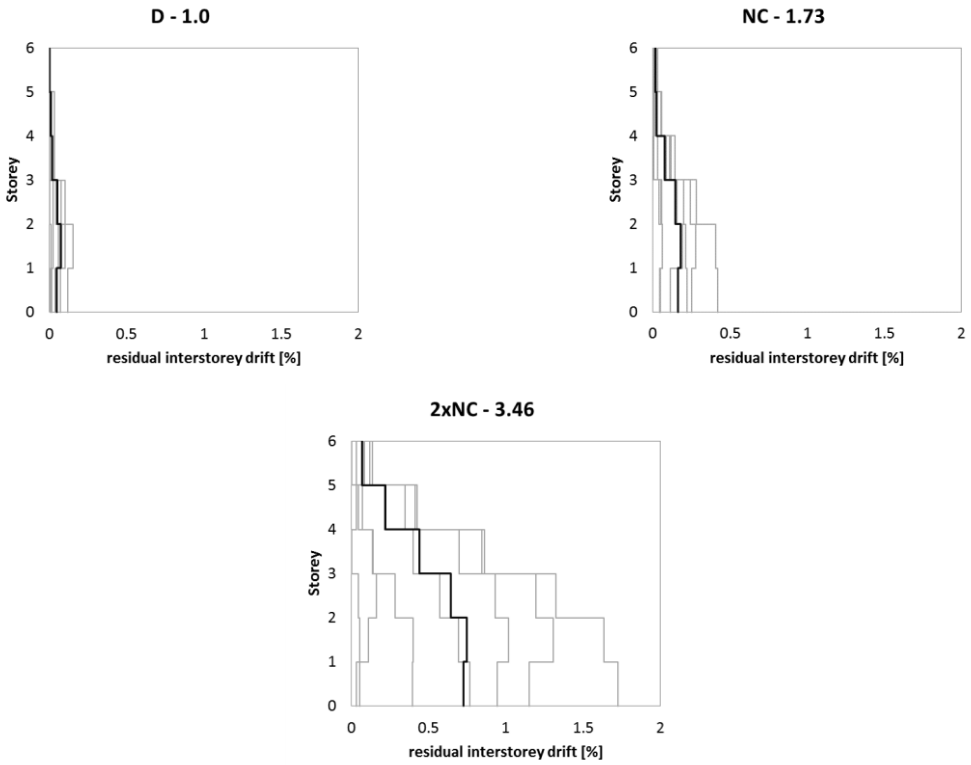

Figure A 25 – Residual interstorey drift ratio for **D-CBF-6-5-5-HH-a**

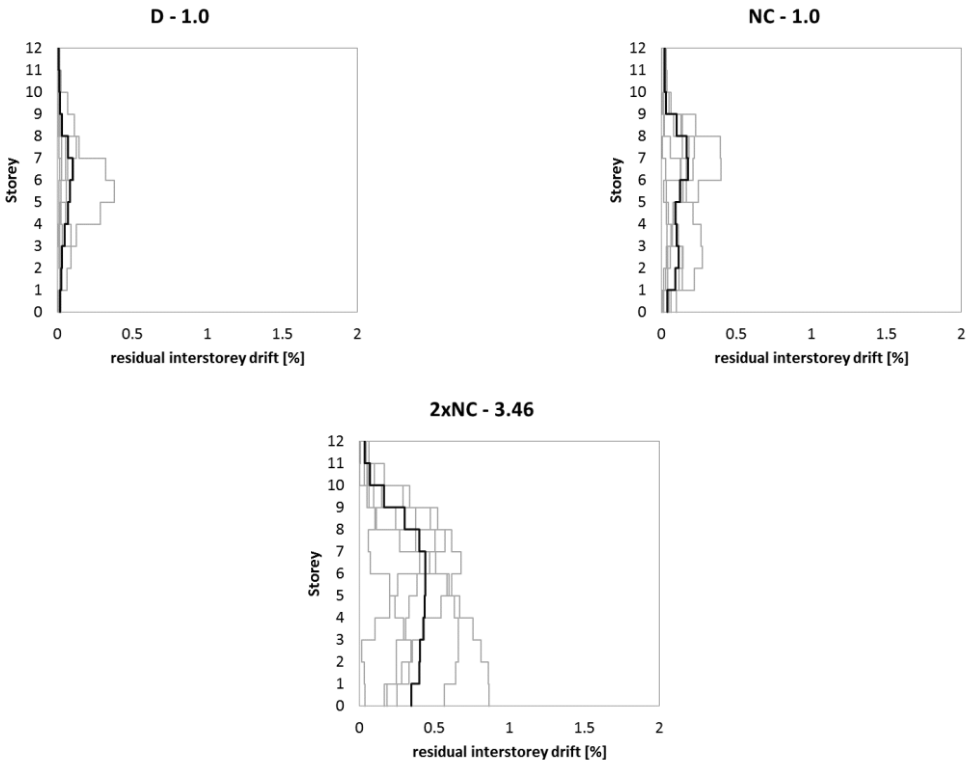

Figure A 26 – Residual interstorey drift ratio for **D-CBF-12-5-6-HH-a**

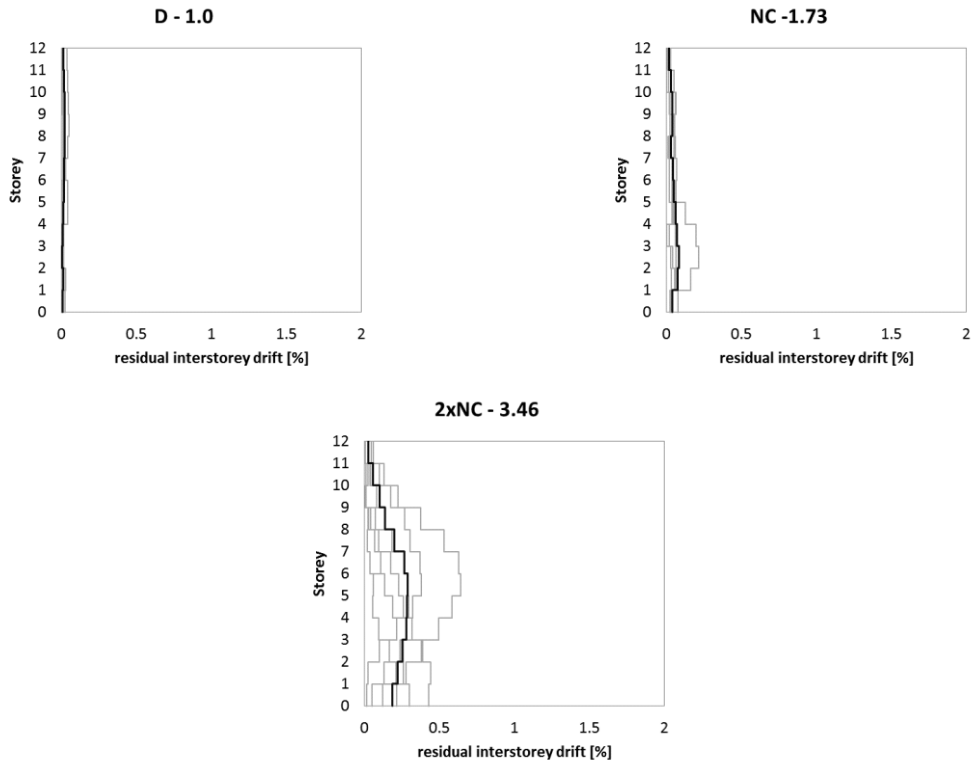

Figure A 27 – Residual interstorey drift ratio for **D-CBF-12-3-6-MH-a**

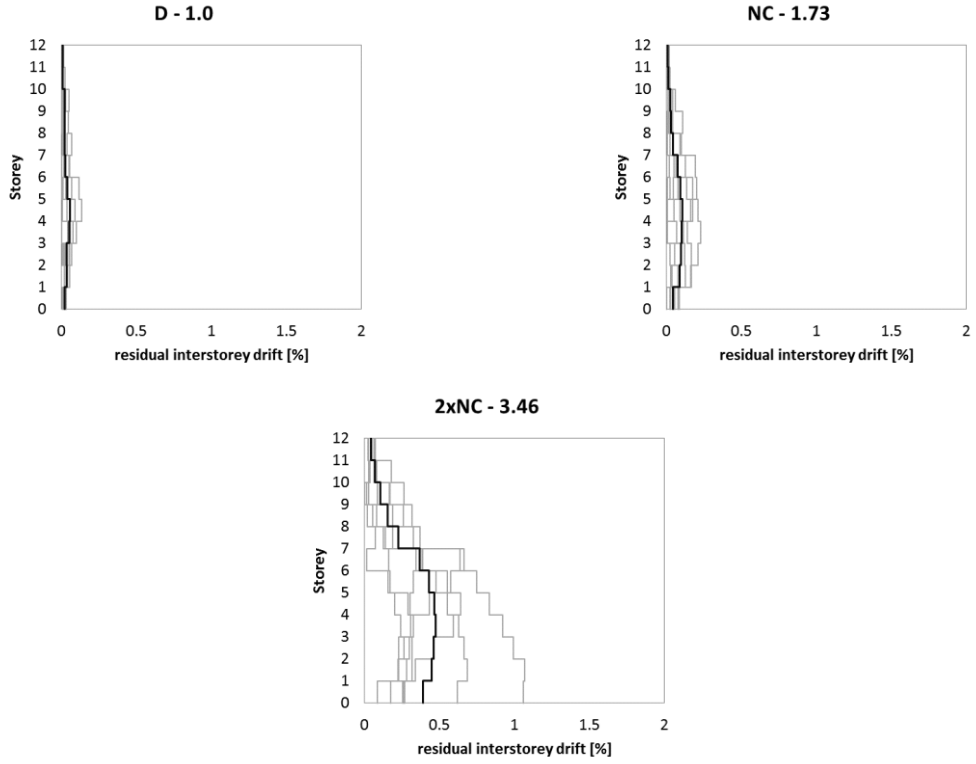

Figure A 28 – Residual interstorey drift ratio for **D-CBF-12-3-6-HH-a**

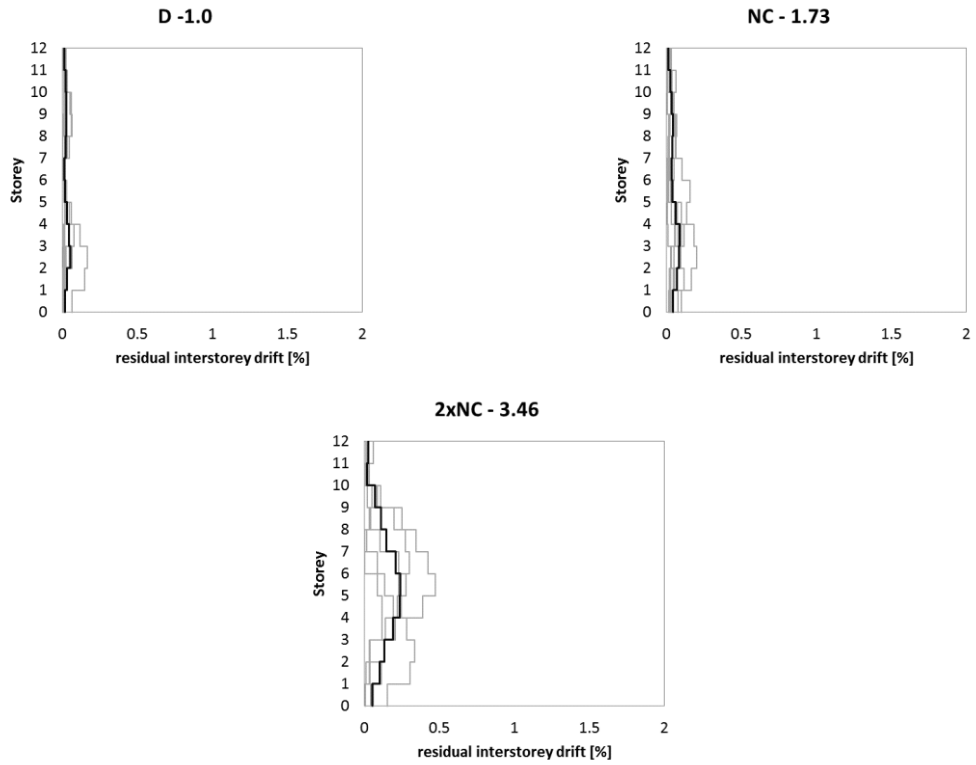

Figure A 29 – Residual interstorey drift ratio for **D-CBF-12-3-8-MH-a**

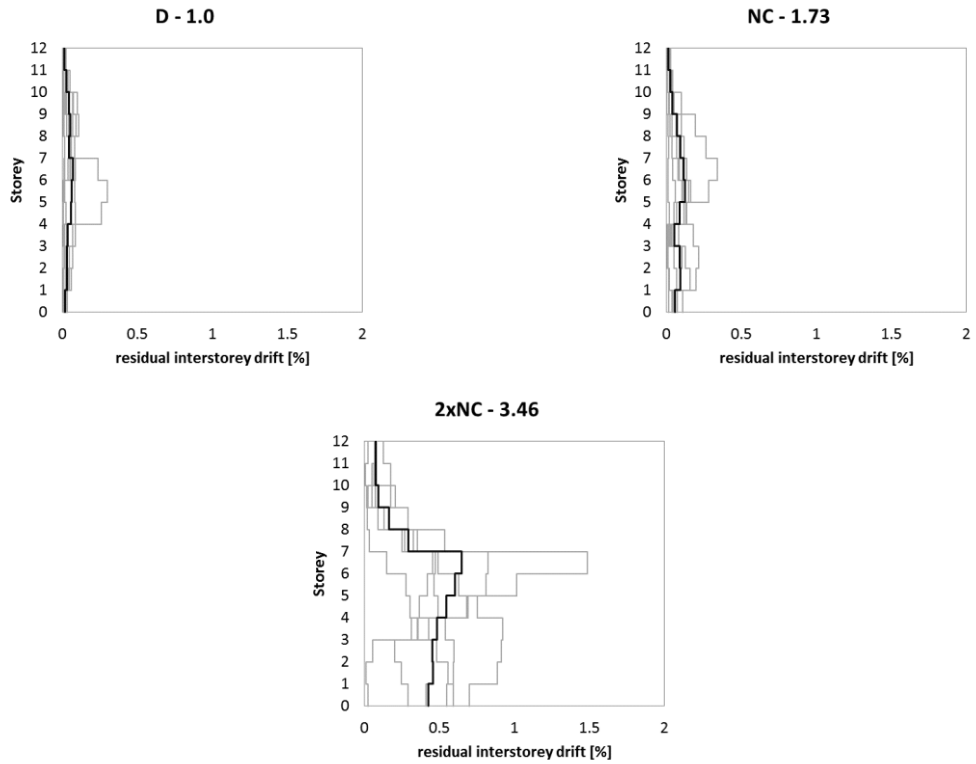

Figure A 30 – Residual interstorey drift ratio for **D-CBF-12-3-8-HH-a**

Beam rotation ratio

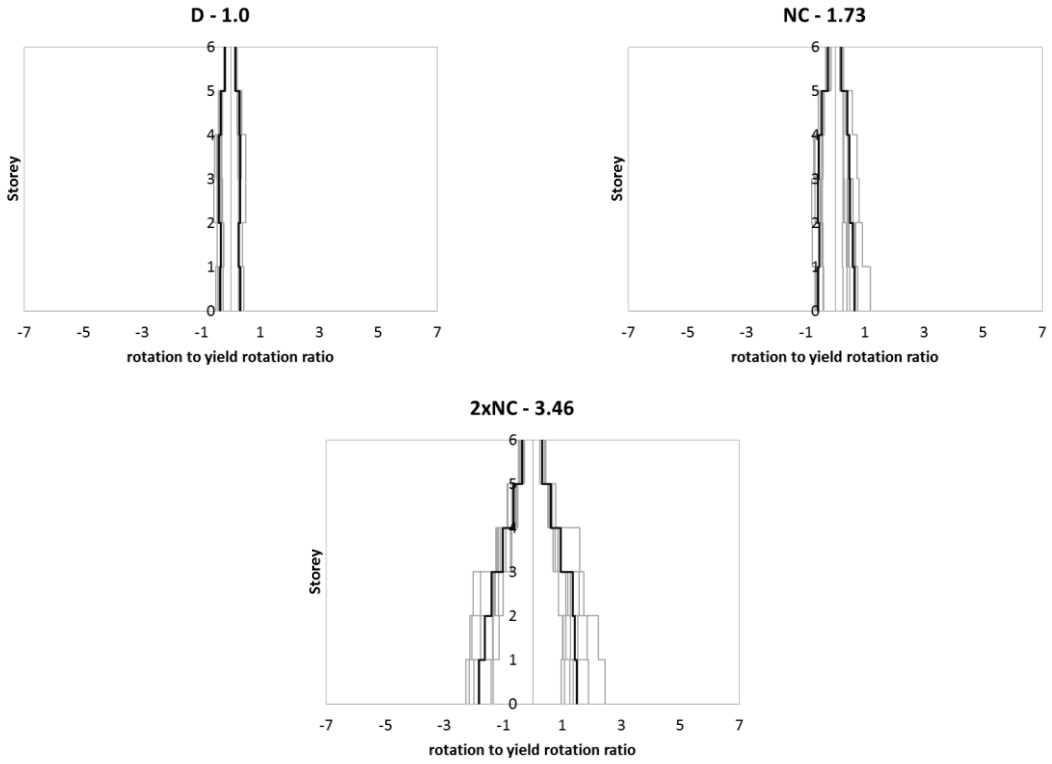

Figure A 31 – Beam to yield beam rotation ratio for **D-CBF-6-3-6-MH-a**

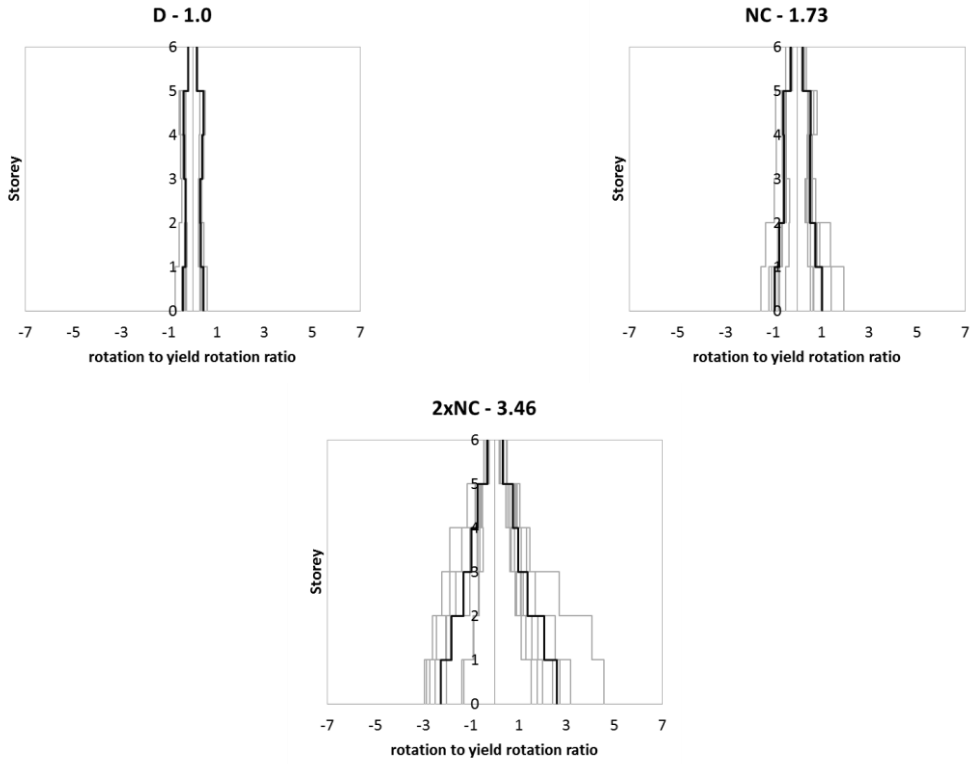

Figure A 32 – Beam to yield beam rotation ratio for **D-CBF-6-3-6-HH-a**

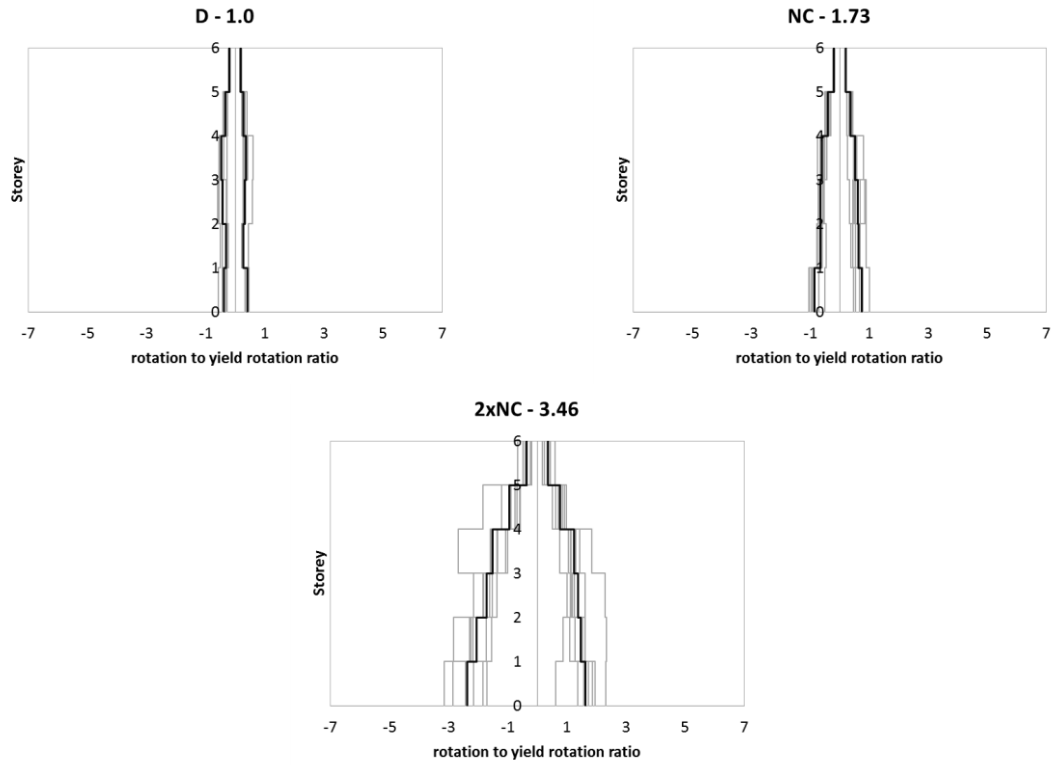

Figure A 33 – Beam to yield beam rotation ratio for **D-CBF-6-3-8-MH-a**

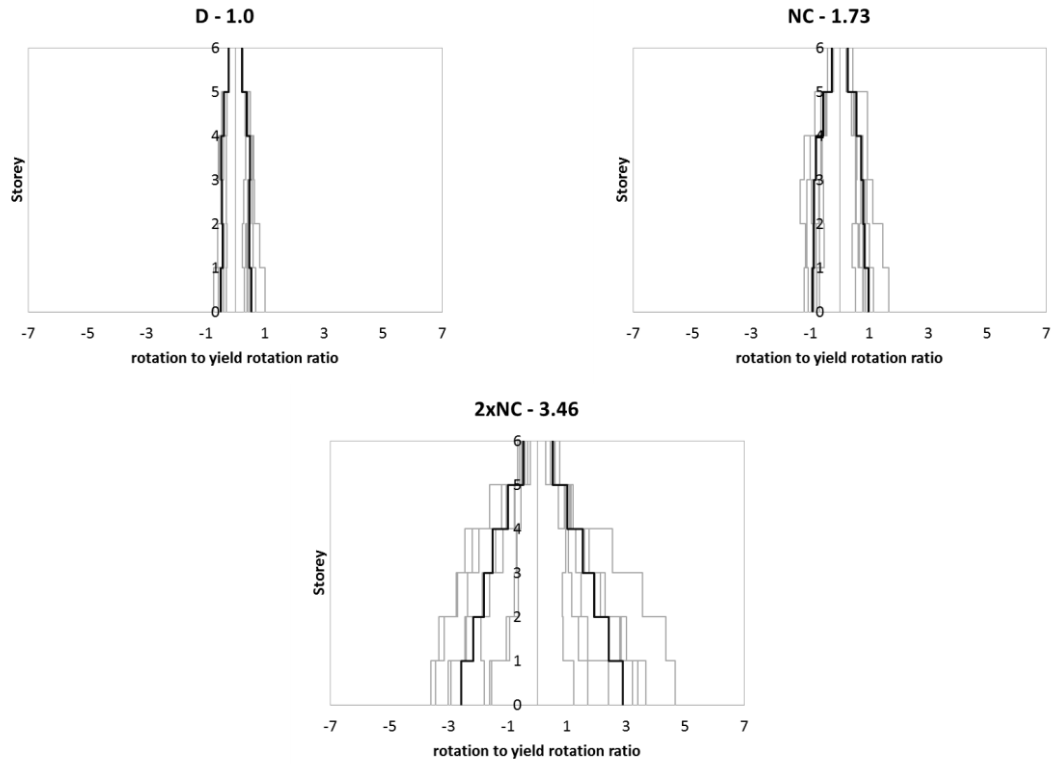

Figure A 34 – Beam to yield beam rotation ratio for **D-CBF-6-3-8-HH-a**

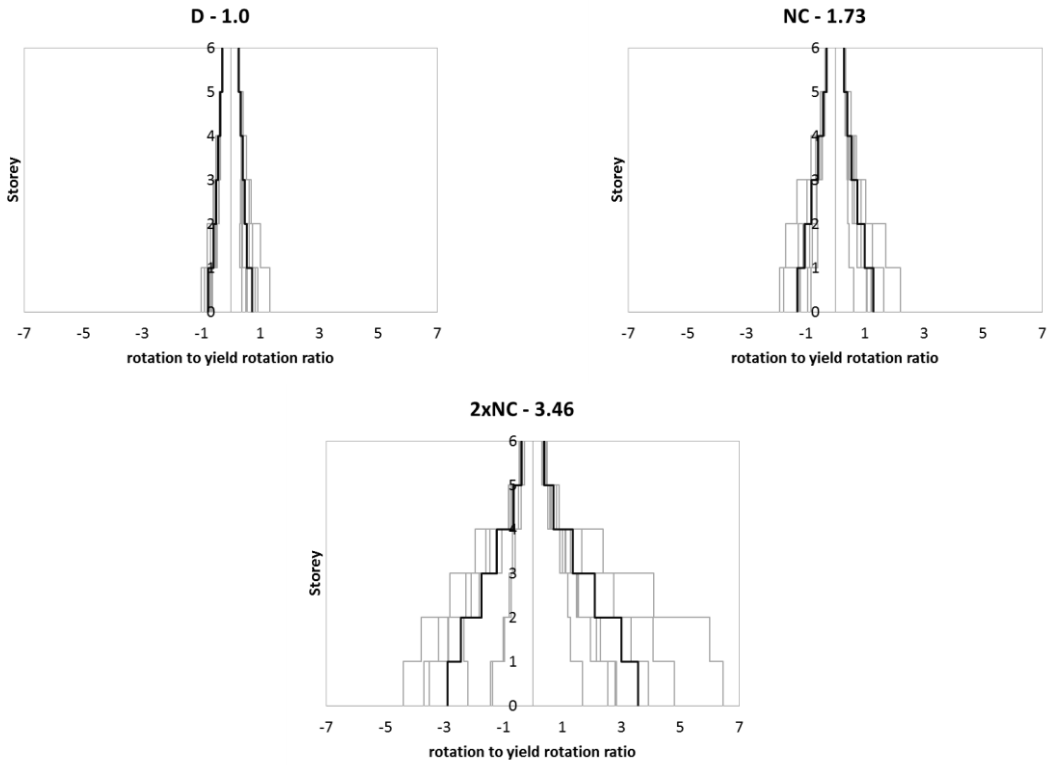

Figure A 35 – Beam to yield beam rotation ratio for **D-CBF-6-5-6-HH-a**

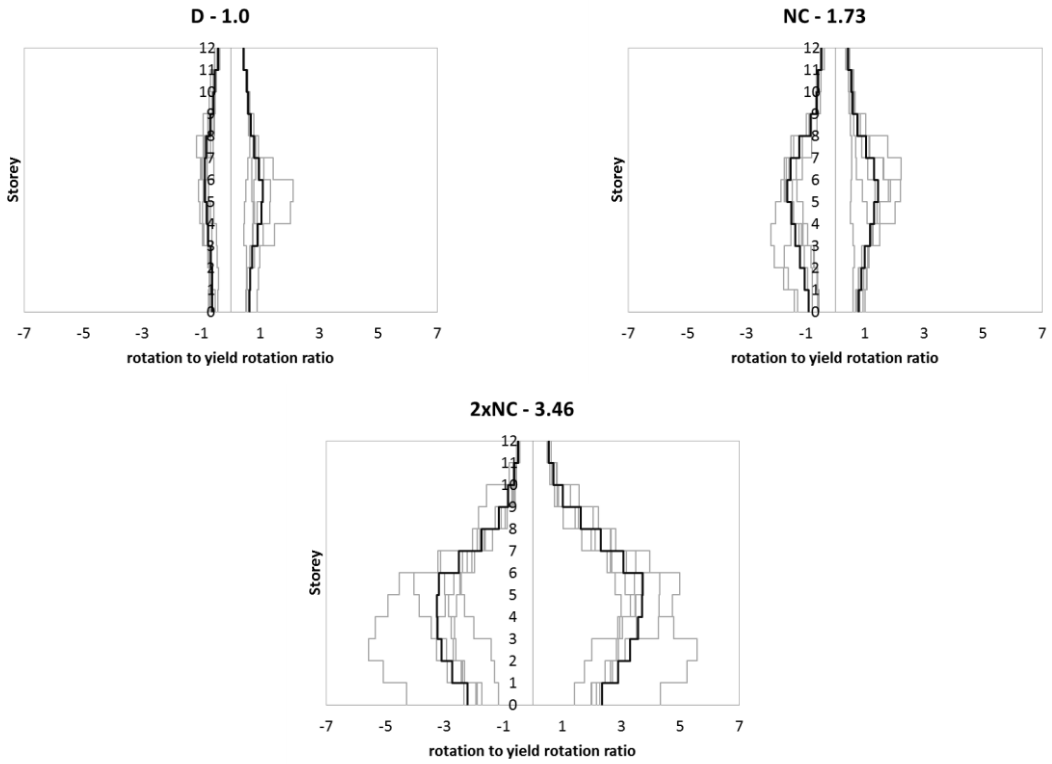

Figure A 36 – Beam to yield beam rotation ratio for **D-CBF-12-5-6-HH-a**

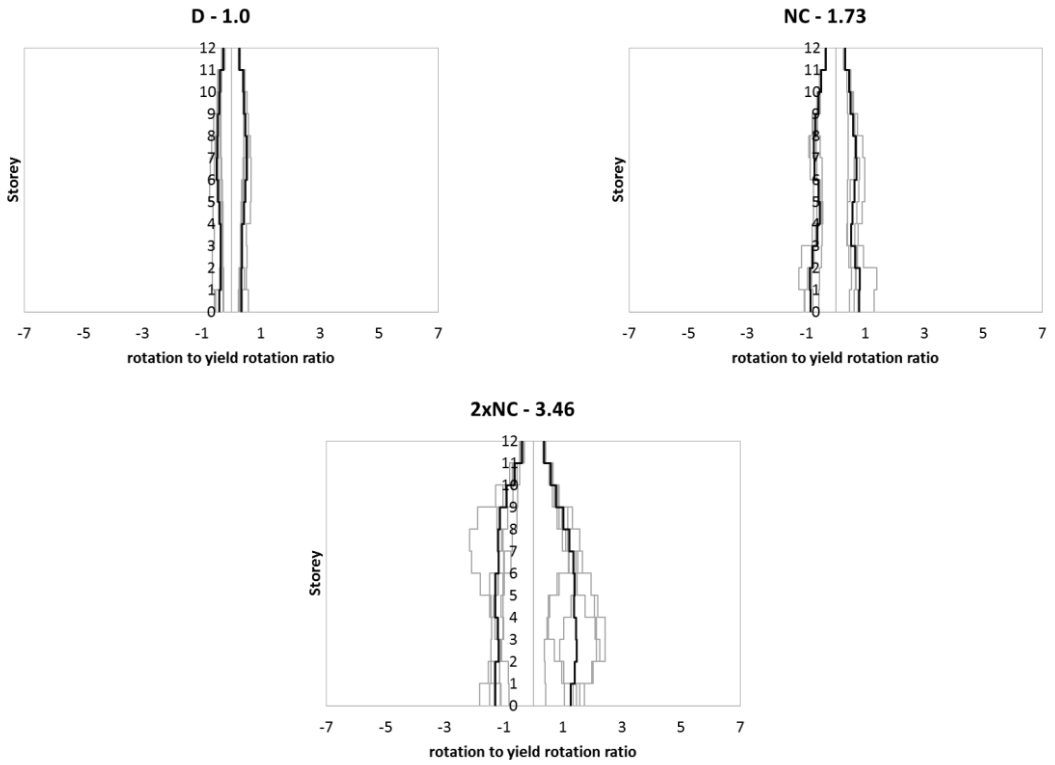

Figure A 37 – Beam to yield beam rotation ratio for **D-CBF-12-3-6-MH-a**

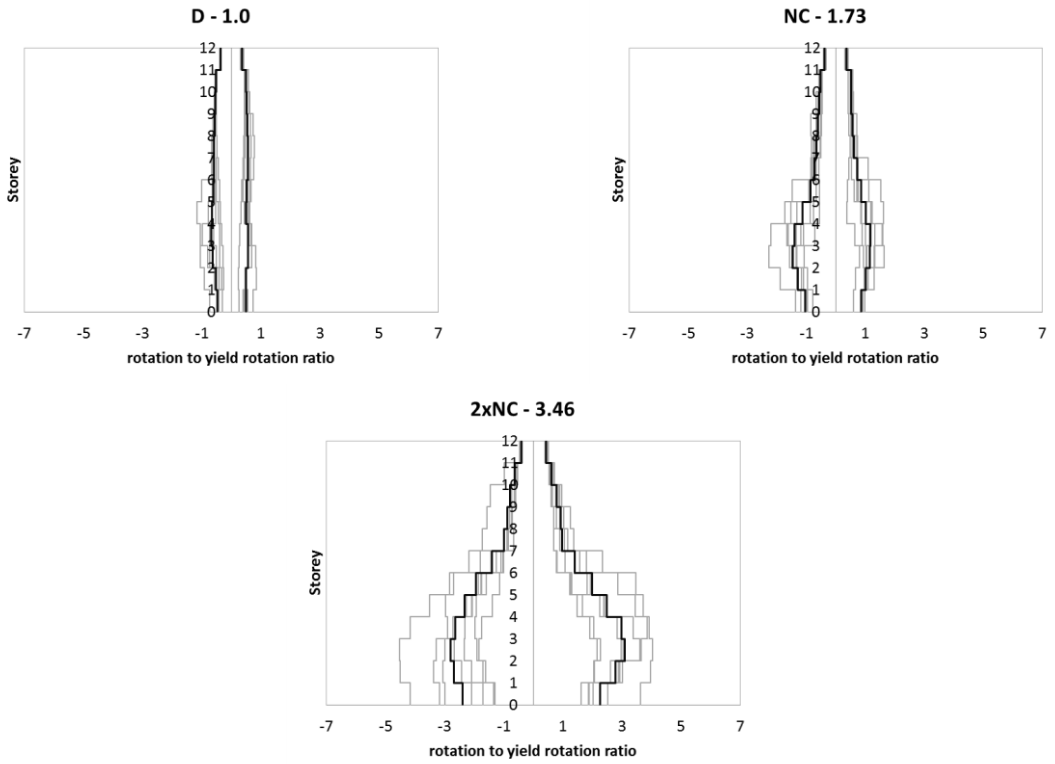

Figure A 38 – Beam to yield beam rotation ratio for **D-CBF-12-3-6-HH-a**

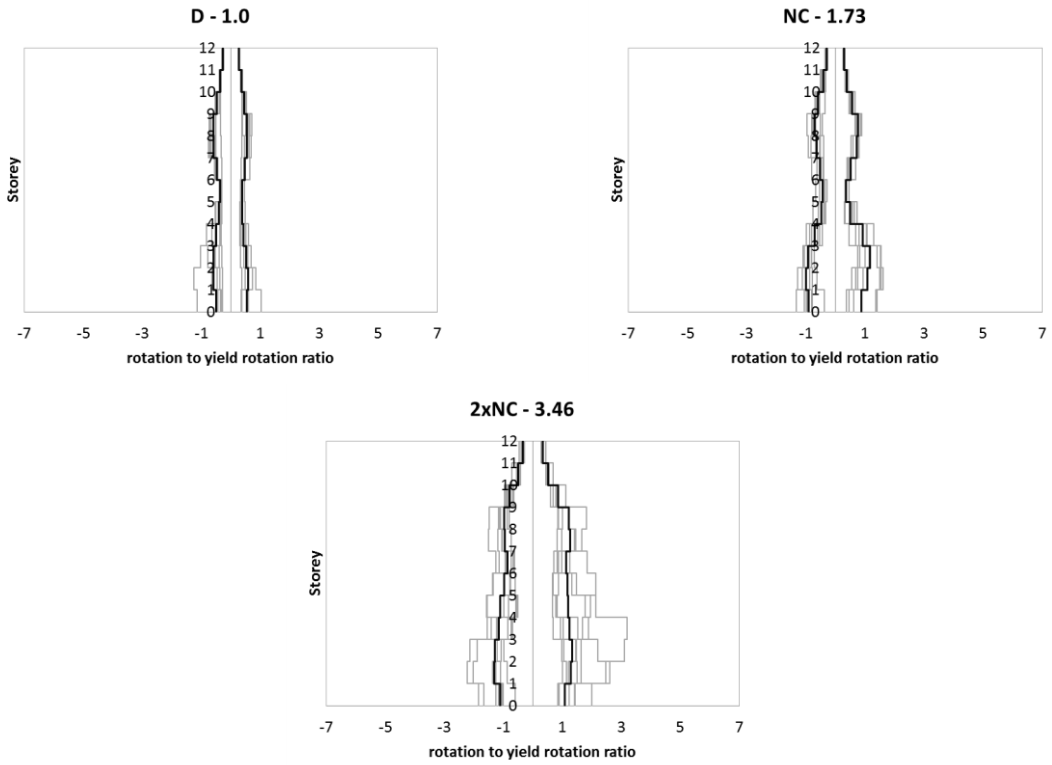

Figure A 39 – Beam to yield beam rotation ratio for **D-CBF-12-3-8-MH-a**

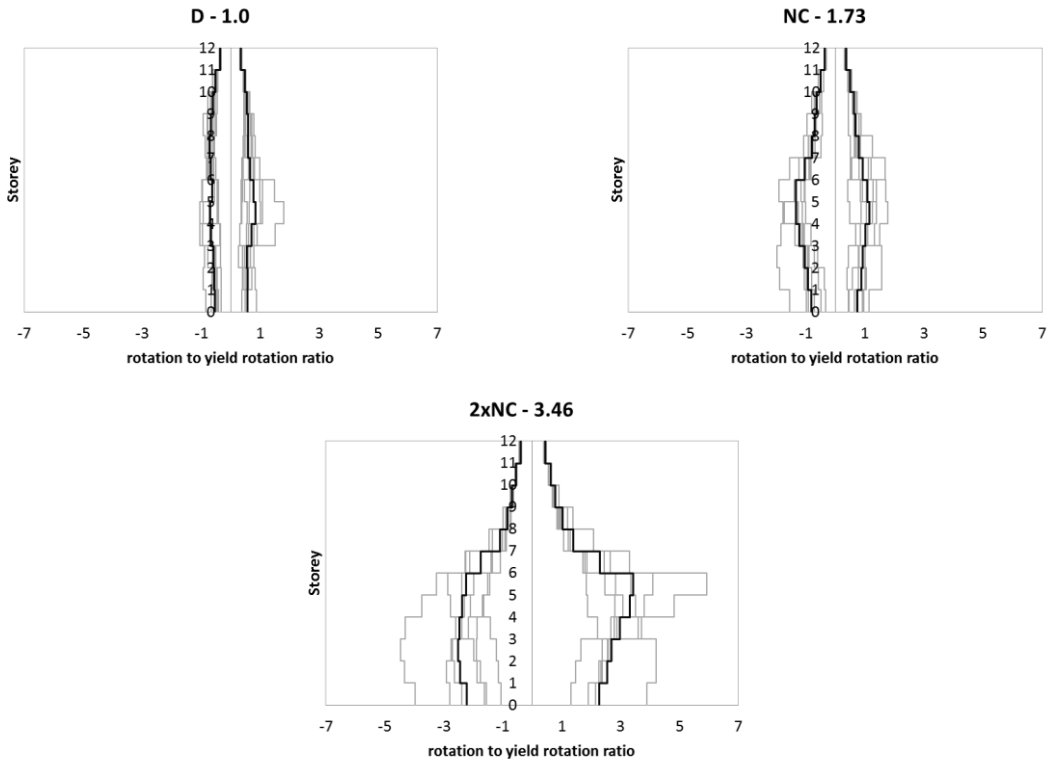

Figure A 40 – Beam to yield beam rotation ratio for **D-CBF-12-3-8-HH-a**